

- 1 -

REACTIVITY OF SOME ALUMINOSILICATE MINERALS

IN THE WATER-SODIUM HYDROXIDE-LIME

SYSTEM

A Thesis Submitted for the Degree of Ph.D.

in

The University of London

by

Sadi Badawi Mujahed

B.Sc. M.Sc.

Department of Mining and Mineral Technology,  
Royal School of Mines,  
Imperial College.

August, 1970.

ABSTRACT

The reactivities of a number of aluminosilicate minerals of different types and compositions in the system  $\text{Na}_2\text{O}-\text{CaO}-\text{H}_2\text{O}$  have been investigated under the conditions of the hydrochemical alkaline process for the purpose of recovering alumina from these minerals. The influence of some important factors on the alumina recovery has been examined and the optimum leaching conditions determined. The chemical and physical nature of the products was determined by chemical analysis, optical microscopy, X-ray powder diffraction and by thermo-analytical methods.

The different aluminosilicate minerals examined, with the exception of kyanite, were decomposed completely and their alumina extracted into solution when treated under the optimum conditions. No significant differences in the reactivities of most of the minerals were noticed under these conditions and sodium calcium hydrosilicate was formed as the solid product in the process. However, the differences in the mineral reactivities became pronounced at lower temperatures.

The changes which took place on the surface of the different minerals during the different stages of the leaching process were followed by scanning electron microscopy, electron-probe microanalysis and X-ray powder diffraction. A product layer was formed on the surface of most of the minerals during the leaching process. Its formation and composition depended upon the reactivity of the mineral in the leaching solution.

A mechanism for the leaching process and for the formation of the solid products under the different leaching conditions is proposed and the role of calcium hydroxide with its favourable effect on the rate and the degree of mineral decomposition and on the alumina recovery is discussed.

TABLE OF CONTENTS

	Page
<u>INTRODUCTION</u>	9
<u>CHAPTER 1. THEORETICAL CONSIDERATIONS</u>	25
1.1 Factors Affecting the Hydrochemical Process	26
1.1.1 Sodium Hydroxide Concentration	27
1.1.2 The Caustic Ratio	30
1.1.3 Effect of Lime	32
1.1.4 Behaviour of Potassium Hydroxide	34
1.2 Thermodynamic Assessment	35
1.2.1 Estimation of Thermodynamic Data	37
1.2.2 Thermodynamic Feasibility of the Reactions	41
1.2.2.1 Reactions at Room Temperature	41
1.2.2.2 Reactions at Higher Temperatures	43
1.3 Kinetics of the Process	50
1.3.1 Rate of Mineral Dissolution	51
1.3.1.1 Temperature	51
1.3.1.2 Sodium Hydroxide Concentration	51
1.3.1.3 Particle Size	51
1.3.1.4 Factors Related to the Mineral	52
1.3.1.5 Impurities	52
1.3.2 Transport of Solute Species	52
1.3.2.1 Solubility of Calcium Hydroxide	53

	Page
<u>CHAPTER 2.    <u>EXPERIMENTAL MATERIALS AND TECHNIQUES</u></u>	55
2.1 Experimental Methods and Techniques	56
2.1.1 Autoclave Leaching Experiments	56
2.1.1.1 Apparatus	56
2.1.1.2 Experimental Procedure	57
2.1.2 Chemical Methods of Analysis	58
2.1.2.1 Determination of Silicon	59
2.1.2.2 Determination of Aluminium	59
2.1.2.3 Determination of Sodium	61
2.1.2.4 Determination of Calcium	61
2.1.2.5 Determination of Iron	63
2.1.3 Thermo-analytical Methods	63
2.1.3.1 Differential Thermal Analysis	63
2.1.3.2 Thermogravimetric Analysis	64
2.1.4 X-ray Powder Diffractometry	64
2.1.5 Electron-Probe X-ray Microanalysis	65
2.1.6 Scanning Electron Microscopy	66
2.1.7 Optical Microscopy	66
2.2 Experimental Materials	66
2.2.1 Natural Minerals	66
2.2.1.1 Albite	67
2.2.1.2 Oligoclase	68
2.2.1.3 Andesine	71
2.2.1.4 Labradorite	71

	Page
2.2.1.5 Anorthosite	72
2.2.1.6 Microcline	75
2.2.1.7 Muscovite Mica	75
2.2.1.8 Kyanite	76
2.2.1.9 Clays	77
2.2.1.10 Quartz	81
2.2.2 Synthetic Minerals	81
2.2.3 Other Materials	82
<u>CHAPTER 3 PRELIMINARY STUDIES</u>	83
3.1 Preliminary Leaching Studies	84
3.1.1 Effect of Particle Size	85
3.1.2 Effect of Leaching Time	86
3.1.3 Effect of Leaching Temperature	87
3.1.4 Effect of Sodium Hydroxide Concentration	89
3.1.5 Effect of Addition of Calcium Oxide	90
3.1.6 Leaching Residues	91
3.2 Sodium Calcium Hydrosilicate	96
3.2.1 Synthesis of the Pure Compound	97
3.2.2 Some Properties of Sodium Calcium Hydrosilicate	97
<u>CHAPTER 4 THE REACTIVITY OF SOME ALUMINOSILICATE MINERALS</u>	104
4.1 Detailed Study of the Reactivities of Feldspars	105
4.1.1 Effect of Calcium Oxide Addition	107
4.1.2 Effect of Leaching Temperature	112
4.1.3 Effect of Alumina in the Initial Leaching Solution	114

	Page
4.1.4 Effect of Calculated Final Caustic Ratio	117
4.2 The Reactivities of Quartz and Some Aluminosilicates Other than Feldspars	123
4.2.1 Reactivities at 280°C	124
4.2.2 Reactivities at Temperature Below 280°C	127
4.2.2.1 Treatment of Muscovite	127
4.2.2.2 Treatment of Kyanite	128
4.2.2.3 Treatment of Clays	128
4.2.2.4 Treatment of Quartz	129
4.2.3 Treatment of Kyanite Under More Severe Conditions	130
4.3 Discussion of Results	132
<u>CHAPTER 5 MECHANISM OF SOLID FORMATION DURING THE LEACHING PROCESS</u>	134
5.1 Experimental Results	135
5.1.1 Results Obtained During the Heating Period	135
5.1.1.1 Lumps Heated to 160°C	136
5.1.1.2 Lumps Heated to 190°C	139
5.1.1.3 Lumps Heated to 220°C	144
5.1.1.4 Lumps Heated to 250°C	145
5.1.2 Effect of Alumina in the Leaching Solutions	148
5.1.2.1 Results of Treatment at 160°C	148
5.1.2.2 Results of Treatment at 220°C	152
5.1.3 Results of Treatment at 280°C for Two Hours	155
5.1.3.1 Anorthosite	156
5.1.3.2 Muscovite	156
5.1.3.3 Kyanite	156

	Page
5.1.3.4 Feldspars Other than Anorthosite	158
5.1.4 Kyanite Treatment at 300°C	162
5.1.5 Reactivity of Quartz in the Leaching Solutions	163
5.1.6 Treatment of Some Calcium Silicate Minerals	168
5.1.6.1 Results of Treatment of Wollastonite	168
5.1.6.2 Results of Treatment of Pectolite	170
5.1.7 Treatment of Coarsely Ground Mineral Samples	170
5.2 Discussion and Conclusions	173
5.2.1 Role of Calcium Hydroxide in the Leaching Process	175
5.2.2 Mechanism of Solid Formation during the Leaching Process	177
<u>SUMMARY</u>	182
<u>ACKNOWLEDGEMENTS</u>	187
<u>REFERENCES</u>	188



I N T R O D U C T I O N

The light metal aluminium is a comparative newcomer to the industrial field compared to the heavier metals copper, lead and zinc. The metal was first discovered by Davy in 1807 and first isolated by Oersted in 1825<sup>(1)</sup>. The introduction of the Hall-Heroult electrolytic process in 1886 for the reduction of fused alumina to aluminium metal brought the price of aluminium down to economic level. Aluminium soon found its way into numerous applications. In 1900 world output of virgin metal was about 7,000 tons. In 1952 aluminium measured by volume of production ranked second only to iron and by weight (2,247,000 tons) next to copper<sup>(2)</sup>. The output has been steadily increasing since 1920 at the average rate of about 8.5% per year<sup>(3)</sup>. The huge expansion in the aluminium industry can be explained only by the wide range of usage based on the diversity of its properties. In addition to its lightness, other related qualities are high electric and thermal conductivities, resistance to corrosive environments including industrial and marine atmospheres, ease of fabrication and readiness to form with other metals alloys possessing high tensile strength. Another important fact in its wide usage is its abundance. Aluminium in the form of various compounds, notably the complex silicates, is widely distributed and it is a constituent of many rocks particularly clay, shale, slate, schists and granite, and occurs fairly commonly in the form of hydrated oxides. The average aluminium content of the continental areas of the earth's crust is about 15.6 per cent (as alumina,  $Al_2O_3$ ) making it almost twice as common as iron. Abundance, however, does not always signify availability. Commercial

ores of aluminium are only those rich in hydrated oxides of the metal and grouped under the generic term "bauxite". Bauxite consists of a mixture of aluminium oxide trihydrate, gibbsite ( $\text{Al}_2\text{O}_3 \cdot 3\text{H}_2\text{O}$ ), and monohydrates, boehmite and diaspore ( $\text{Al}_2\text{O}_3 \cdot \text{H}_2\text{O}$ ) with varying amounts of such impurities as silica, ferric oxide, titania and other minerals peculiar to certain localities.

There are two main steps in the manufacturing process of aluminium; a) the production of pure alumina, mainly from bauxite by the Bayer process; and b) the reduction of the alumina to metal. The latter step is usually carried out by the Hall-Heroult method. The work represented in this thesis is mainly on the possibility of recovering alumina into solution from aluminium-bearing materials, and therefore no discussions on further treatment of alumina are given.

### The Bayer Process

Of the many processes that had been applied for the preparation of pure alumina from bauxite, the Bayer method, invented by Carl Bayer in 1888, is the only important one for the treatment of high grade bauxites. It has held its own by virtue of the comparative simplicity of its application and also because of the purity of its products. The latter feature is of special importance as the purity of the final metal depends upon the grade of alumina sent forward for electrolysis.

In this process the crushed bauxite is first digested with caustic soda solution, usually under pressure. The alumina is extracted

in the form of soluble sodium aluminate, which leaves behind most of the impurities, predominantly iron oxide, titania and silica, as an insoluble residue. The clear, filtered sodium aluminate solution is diluted and cooled, and a "seed" of alumina trihydrate is added. The sodium aluminate hydrolyses on the surface of the seed to form crystalline alumina trihydrate. The trihydrate is finally filtered off and calcined at about  $1000^{\circ}\text{C}$  to anhydrous alumina.

#### Solubilities of Aluminium Oxide Hydrates

The application of the Bayer method to the extraction of alumina from bauxite may be considered from the view point of the solubilities of the respective hydrates. The trihydrate is more soluble in caustic than the monohydrates and accordingly bauxite containing the majority of its alumina in the former state is more amenable to treatment. Gibbsite is quite soluble in 10-20% solution of NaOH at about  $140^{\circ}\text{C}$ . The pressure at this temperature is below 10 atm. Boehmite is only slightly soluble in weak NaOH solutions under the conditions at which gibbsite is normally extracted. Boehmite, however, is soluble in 20-30% NaOH solutions at  $225^{\circ}\text{C}$  with pressures below 25 atm. Diaspore is insoluble in NaOH solutions under the conditions at which gibbsite and boehmite are soluble. After preheating to  $600-700^{\circ}\text{C}$ , diaspore becomes soluble in NaOH solutions under conditions at which boehmite is also soluble.

Difference in solubilities leads to variations in the procedures of treatment. Bauxites having the great part of its alumina as the trihydrate is usually directly treated in 10% NaOH solutions at  $150^{\circ}\text{C}$  for 1 hr. in a continuous process (American practice). Ores which

contain the major portion of their alumina in the monohydrate form are first calcined at about 600°C, then treated in 30% NaOH solution at 160-170 for 4-5 hrs. in batches (European practice).

Subject to the overall economics, it is occasionally preferable to regard a mixed ore as a simple monohydrate ore and to fix the extraction conditions on this basis, or alternatively to regard the ore as a trihydrate ore and regard monohydrate alumina as non-recoverable.

### Silica Impurities

Silica is a critical impurity in the bauxite ore. It occurs as quartz and as reactive silica as such minerals as kaolinite ( $\text{Al}_2\text{O}_3 \cdot 2\text{SiO}_2 \cdot 2\text{H}_2\text{O}$ ) and hyllosite ( $\text{Al}_2\text{O}_3 \cdot 2\text{SiO}_2 \cdot 3\text{H}_2\text{O}$ ). Silica in the form of quartz is not perceptibly attacked by caustic liquors at low temperatures during the extraction of trihydrate bauxites by the Bayer process. Reactive silica, on the other hand, is rapidly attacked by caustic solutions leading to dissolution of silica. Simultaneously with dissolution of silica, desilication of the solution occurs with the formation of hydrated sodium aluminium silicate which is rejected in the residue and is therefore a serious loss of alumina and alkali. The ore should thus contain as little reactive silica as possible, since its presence entails a loss of 1-2 Kg. of alumina and 0.7 - 1.7 Kg. of  $\text{Na}_2\text{O}$  per 1 Kg. of silica. It is scarcely economical to treat bauxites containing more than 7 per cent reactive silica by the Bayer process.

### Other Processes

As already stated, the Bayer process usually operates with high-grade bauxites containing 50-60% alumina and preferably not more than

5% reactive silica. Although bauxite is known to occur in very large deposits throughout the world, it constitutes only a small proportion of the total alumina content of the earth's crust. It is formed chiefly by laterization, a process assisted by hot, humid climates of tropics and subtropics, and therefore, certain industrial nations are without a domestic supply. Obviously, considerable economic advantage would be gained if it were possible to use a domestic ore and to site the alumina plant in close proximity to the ore deposit. For strategic reasons irrespective of cost, it is also desirable to use local ores if possible.

The great potential source of alumina lies in aluminium silicates occurring as feldspathic rocks and clays; by virtue of its occurrence as silicate, aluminium is the most plentiful metal. Hence, the development of a practicable process for producing aluminium from aluminosilicates is one of the most challenging technologic problems of our times.

Many attempts to prepare alumina from various aluminous materials, such as high-silica bauxites, laterites and clays by methods other than the Bayer process had been done. Some of these attempts were even as early as the history of the aluminium industry itself<sup>(4)</sup>. The literature review showed not only that there were many processes for treating these materials, but that there were many variations for each. The numerous processes have been revised in Gmelin's Handbuch<sup>(5)</sup>, by Edwards, Frary and Jeffies<sup>(1)</sup>, by Tilley, Millar and Ralston<sup>(6)</sup>, by Fulda and Ginsberg<sup>(7)</sup>, and briefly by Pearson<sup>(3)</sup>.

Few of them have, however, proved to be capable of competing with the Bayer process even under special local conditions.

The various processes may be broadly classified into two types:

- a) acid processes in which the raw material is leached with acid solutions; and
- b) alkaline processes in which the raw material is treated with alkaline solutions.

a) Acid Processes

Mineral acids readily dissolve the aluminium both from bauxite and silicate materials particularly if the silicates are subjected to controlled calcination step before leaching. Because none of the so called "acid processes" for the production of alumina have achieved any large scale success, there is no single process which can be described as being typical in the way the Bayer process is typical of alkali digestion processes. In general, however, the acid processes involve the conversion of the aluminium compounds in the raw material into aluminium salts such as aluminium sulphate, sulphite, chloride or nitrate and the purification of such salt. When the aluminium salt has been prepared in suitably pure form, the next problem is to convert it into aluminium oxide and recover the acid radical of the aluminium compound, either for use in the process or in some form which could be sold.

In the acid processes silica is readily eliminated with other insoluble impurities, but the separation of iron and the prevention of contamination of the product by the impurities introduced by

plant corrosion present serious difficulties and require the use of special construction materials for the plant.

#### b) Alkaline Processes

Most of the alkaline processes, as in the Bayer process, depends upon rendering the alumina of the raw material soluble as sodium aluminate by means of alkaline solutions. A measure of success has been achieved with some of these alkaline processes.

Of the more successful of them are the following:

#### The Double-Leach Process

The double-leach process is usually applicable to high-silica bauxites containing 7-15% silica<sup>(8-10)</sup>. In this process the siliceous bauxites is calcined at about 1000°C forming amorphous silica and alumina. The calcine is then leached with dilute (12%) caustic soda solution at about 90°C which dissolves ~70% of the silica as sodium silicate and about 3% of the alumina. Subsequent pressure digestion of the residue with 20-30% caustic soda solution at 220°C dissolves the alumina, which is then precipitated as the hydroxide and subsequently calcined to the oxide.

#### Lime-Soda Sinter Process

In the lime-soda sinter process<sup>(11-19)</sup>, the aluminous raw material is sintered with  $\text{Na}_2\text{CO}_3$  at about 1200°C. Alumina forms sodium aluminate and the other constituents are also attacked with formation of such compounds as silicates, ferrates and titanates causing soda losses. Lime is usually added to form insoluble calcium salts with the impurities, e.g.  $2\text{CaO} \cdot \text{SiO}_2$ , and its addition is essential if the silica content



of the raw material is high. The sintered product is leached with water, caustic soda solution or sodium aluminate liquor to extract the soluble sodium aluminate. The filtered liquor is then either decomposed as in the Bayer process or treated with carbon dioxide to precipitate hydrated alumina, which is then calcined in the usual way.

This process is being in commercial operation in U.S.S.R. since the early 1950's employing nepheline-syenite from the Kola Peninsula, as a raw material. It is inferred that the sale of the by-products (soda ash, potash and dicalcium silicate) in domestic markets renders the process economic. The success of this process encouraged further research into the utilization of nepheline-syenite from large occurrences in Central Siberia, Armenia and South-Eastern Ukraine.

#### Bayer Process, Followed by Lime-Soda Sinter

The high-silica bauxite is treated in the usual way with strong soda solution. The red mud formed is then mixed with the proper quantities of lime and soda ash and sintered. The sinter is leached with caustic soda solution which dissolves most of the alumina and soda and the leach solution is recycled to the Bayer process.

#### Lime-Sinter Process

In the lime-sinter process, a mixture of the aluminous material and limestone is heated to about  $1380^{\circ}\text{C}$  to produce insoluble dicalcium silicate and soluble calcium aluminate<sup>(20-22)</sup>. The cooled sinter is then treated with an alkaline solution or water to extract alumina.

#### Pedersen Process

The Pedersen process was developed by Harold Pedersen, in Norway,

around 1926<sup>(23)</sup>, and it is currently in use in many parts of the world including U.S.S.R., China, Manchuria, Korea, Japan and Sweden<sup>(24,25)</sup>. The Pedersen process operates on the principle of smelting high-silica, high-iron aluminous material in an electric arc furnace with lime and coke to produce a calcium aluminate slag in which the aluminate is leachable by sodium carbonate solution. Such smelting also results in recovery of an iron by-product. Pedersen adapted his process to various aluminous materials that formed slags containing 3.5 to 30 per cent silica and 2 to 3 per cent titania.

#### The Hydrochemical Alkaline Process

Extraction of alumina and alkalies from high-silica aluminous materials can be successfully affected by the most promising hydrochemical alkaline process. This process has been developed in recent years in the Kazakh Mining and Metallurgical Institute, U.S.S.R., employing nepheline-syenite ores (The Ponomarev-Sazhin Process)<sup>(26-28)</sup>. In this method the aluminosilicate raw material, mixed with lime, is decomposed by concentrated aluminate solutions (400-500g Na<sub>2</sub>O/l) of high caustic-to-alumina ratio at 280-290°C for a relatively short period of time (about 30. min). The presence of certain amounts of lime is an essential condition for a high degree of alumina extraction. Under these conditions a hydrated sodium calcium silicate, a phase free from alumina, is formed; while the liberated aluminium oxide goes into solution in the form of alkali aluminate. The alumina in the leach liquor could be recovered by decomposition or carbonation. The residue formed in this process could be decomposed by weak alkaline

solutions or by carbonation to recover the alkali oxides<sup>(29-32)</sup>. The final residue, after the extraction of alkalies, can be used for the production of portland cement.

No preliminary high-temperature sintering of the aluminosilicate raw material with limestone is required in this process, thus reducing equipment, time and capital and accordingly the cost of alumina production would be lower. Ponomarev and Sazhin<sup>(28)</sup> compared the cost of production of alumina from aluminosilicates by the soda-sinter process and the hydrochemical alkaline method. The estimated cost for the production of one ton of calcined alumina by the hydrochemical method was given at 54.5 rubles compared with 61.7 - 69.3 rubles by the sintering method using three different conditions.

In recent years a considerable volume of work had been done in U.S.S.R. on the hydrochemical alkaline method on both laboratory and pilot scales but there is no information in literature whether this method is used on industrial scale or not. The method had been applied for the extraction of alumina from such materials as high-silica bauxites<sup>(33-35)</sup>, blast furnace slags<sup>(36-38)</sup>, clays and nepheline-syenites of different compositions and localities<sup>(26,39-45)</sup>. Ni<sup>(46,47)</sup> treated the red mud from the Bayer process by the hydrochemical alkaline method for alumina extraction. He showed that the application of this process had advantages over the recovery by the sinter method in that it was technically easier, and needed less limestone. Highly-basic alumina slags (gehlenite-dialuminate type), because of the presence of considerable amounts of gehlenite and spirels,

cannot be converted to alumina by means of soda leaching (Pedersen process). These slags could be treated by the hydrochemical alkaline process and the surplus of calcium oxide being precipitated in the form of calcium hydroxide<sup>(37)</sup>. To use the excess amounts of calcium oxide, the slag may be mixed with other aluminosilicates, e.g. nepheline, in proportions to yield a  $\text{CaO}/\text{SiO}_2$  molar ratio of 1.1<sup>(48)</sup>. Isakov et al.<sup>(49)</sup> showed that the addition of nepheline had a favourable effect by compensating the loss of alkali, increasing the alumina content in the aluminate solution during leaching and increasing the degree of utilization of the calcium oxide in the treatment of such slags. They computed the provisional cost for the production of one ton of alumina by this proposed joint hydrochemical treatment of aluminosilicate slags and nepheline and showed that it could be as low as 45 rubles. Ponemarev et al.<sup>(50)</sup>, showed that it was possible to extract alumina, iron, titanium and alkali oxides from high-silica, high-iron bauxites containing titanium by complex treatment. The bauxite was first treated by the usual Bayer process and the red mud obtained was smelted in an electric furnace with charcoal to give pig iron and slag. The alumina was extracted from the slag by the hydrochemical alkaline method. The residue from the hydrochemical process was then treated with 60g  $\text{Na}_2\text{O}/\text{l}$  at 95-100°C to extract sodium oxide. The final residue containing  $\text{TiO}_2$  was chlorinated to obtain titanium. A simplified scheme of this treatment is shown in Figure 1. In laboratory tests they found that the overall recoveries from bauxite were  $\text{Al}_2\text{O}_3$  96-7%, Fe 98%, and Ti about 100%

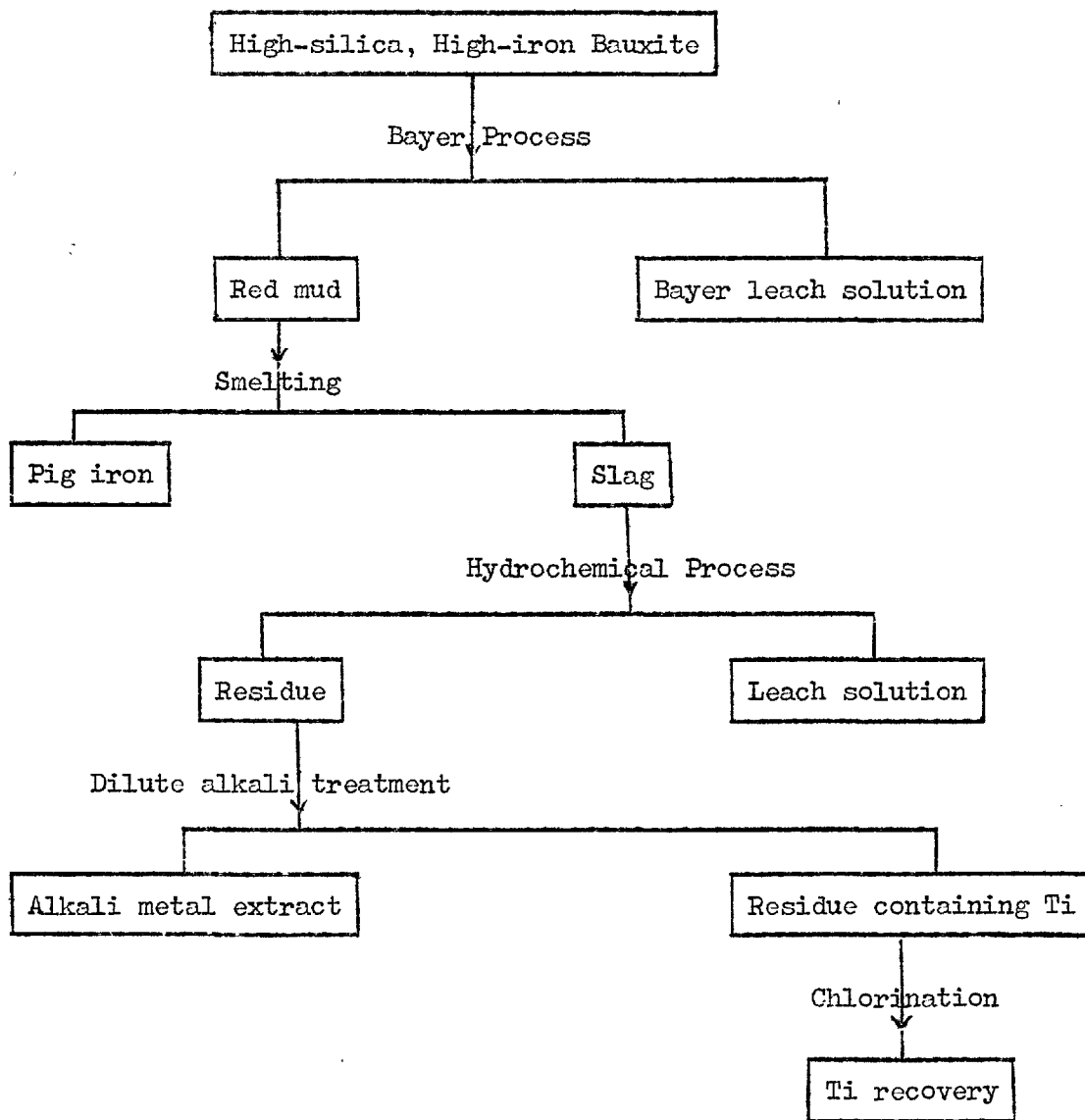


Figure 1. Simplified scheme for a complex treatment of high-silica, high-iron bauxite containing titanium.

and from red mud  $\text{Na}_2\text{O}$  about 80%. The cost of alumina production using this complex treatment of high-silica bauxite was shown to be lower than was the cost of sintering combined with the Bayer process.

The only reported work done on alumina extraction by means of the method outside U.S.S.R. was in South Africa where attempts on laboratory scale have been made to employ domestic aluminous materials such as nepheline, andalusite, clays and coal ashes to produce alumina (51-54).

The hydrochemical process is highly sensitive to all the following factors: caustic ratio (molar ratio of  $\text{Na}_2\text{O}/\text{Al}_2\text{O}_3$ ), molar ratio of  $\text{CaO}/\text{SiO}_2$ , solution concentration, and temperature. Slight changes of any of these conditions result in increase or decrease of alumina extraction. The causes of this are not always clear owing to the chemical complexity of the processes taking place in the five component system:  $\text{Na}_2\text{O} - \text{CaO} - \text{Al}_2\text{O}_3 - \text{SiO}_2 - \text{H}_2\text{O}$ . The process had attracted the attention of numerous investigators, mainly in U.S.S.R., and many papers have been published on the subject, but many of the physico-chemical principles of the process have not yet been worked out fully. Detailed study of the mechanisms of interaction between the different components in this system is necessary for providing a theoretical basis of the hydrochemical process and for searches of new and more advanced methods of production of alumina and other materials by decomposition of aluminosilicates.

The work represented in this thesis was undertaken with the aim of assessing the feasibility of recovering alumina from various types of

aluminosilicate minerals by means of the hydrochemical alkaline method. The minerals of particular interest include those of wide abundance as feldspars, clays and micas; and those of exceptionally high alumina content, e.g. kyanite.

The published work on this process was mainly on nephelines and high-silica bauxites but no systematic investigations appeared which studied the performance of different types of aluminosilicates under the hydrochemical conditions. This study was an attempt to extend the process to include different aluminosilicate minerals and to compare the reactivities of aluminosilicates with various crystal structures and compositions. To contribute to a better understanding of the processes taking place in the five component system:

$\text{Na}_2\text{O} - \text{CaO} - \text{Al}_2\text{O}_3 - \text{SiO}_2 - \text{H}_2\text{O}$ , the process of leaching has been studied in its different stages and the mechanism of the process including solid formation has been discussed.

The thesis has been divided into five chapters. The first discusses the factors affecting alumina recovery and the thermodynamic and kinetic aspects for the leaching process. The second chapter deals with the equipment employed and describes the experimental techniques and materials used in the study. The third chapter describes the preliminary studies done to establish the optimum conditions for the process and the nature of the products formed. The fourth chapter studies the relative reactivities of some common aluminosilicates with detailed investigation on the feldspar group minerals. The last chapter deals with the mechanism of the leaching

process and the solid formation during the treatment of different aluminosilicate minerals in alkali solutions.



C H A P T E R 1

THEORETICAL CONSIDERATIONS

In the study of the reactivities of aluminosilicate minerals in the system:  $\text{Na}_2\text{O} - \text{CaO} - \text{H}_2\text{O}$  under the conditions of the hydrochemical alkaline process, the three important aspects to be considered are:

1) The factors affecting the alumina extraction from the aluminosilicates by this process and the nature of the reaction products,

2) The thermodynamic feasibility of the reactions of the aluminosilicate minerals with caustic soda and lime to form the solid product sodium calcium hydrosilicate. This compound is of particular importance since its formation ensures alumina extraction into solution, and

3) The kinetic aspects of the reactions of the minerals with the alkaline solutions.

### 1.1 Factors Affecting the Hydrochemical Process

In the five component system:  $\text{Na}_2\text{O} - \text{CaO} - \text{Al}_2\text{O}_3 - \text{SiO}_2 - \text{H}_2\text{O}$ , many different solid phases may be formed depending on such factors as relative concentrations of the different components and temperature. Formation of sodium calcium hydrosilicate, a phase free from aluminium oxide, is the basis of the hydrochemical process for production of alumina from aluminosilicate rocks. Any other phase formed containing alumina would lead to serious losses of alumina in the process. Many investigations have been carried out, mostly on synthetic materials, to determine the phase composition and the solubility of various components in the system:  $\text{Na}_2\text{O} - \text{CaO} - \text{Al}_2\text{O}_3 - \text{SiO}_2 - \text{H}_2\text{O}$  over

a wide range of temperature, and concentrations of  $\text{Na}_2\text{O}$  and  $\text{Al}_2\text{O}_3$  (55-59). According to these investigations, the possible phases that may crystallize out in this system and their crystallization regions at  $280^\circ\text{C}$  with a  $\text{CaO}/\text{SiO}_2$  molar ratio of 1.0 are shown in Figure 2. Sodium calcium hydrosilicate (phase I in the figure) crystallizes out below the alumina solubility isotherm with a small amount of unconverted calcium hydroxide (phase II). Above the alumina solubility isotherms the stable phase is sodium calcium hydroaluminosilicate (phase III). At  $\text{Na}_2\text{O}$  contents above 20% this phase crystallizes together with some unconverted calcium hydroxide and at  $\text{Na}_2\text{O}$  contents below 20%, it crystallizes with a hydrogarnet (phase IV).

In the hydrochemical alkaline process, the formation of sodium calcium hydrosilicate (phase I), and hence the recovery of alumina from aluminosilicates, is highly sensitive to the following factors: sodium hydroxide concentration, the calculated caustic ratio of the solution, the molar ratio of  $\text{CaO}/\text{SiO}_2$  in the pulp and the leaching temperature.

#### 1.1.1 Sodium Hydroxide Concentration

Under otherwise equal conditions, the degree of alumina extraction from aluminosilicates increases steadily with the initial concentration of sodium hydroxide solutions (60,61). At concentrations below 200g/l  $\text{Na}_2\text{O}$ , stable sodium hydroaluminosilicate (phase VII in Figure 2), monocalcium hydrosilicate (phase V) and hydrogarnets (phase IV) co-exist, resulting in low alumina extraction in the process.

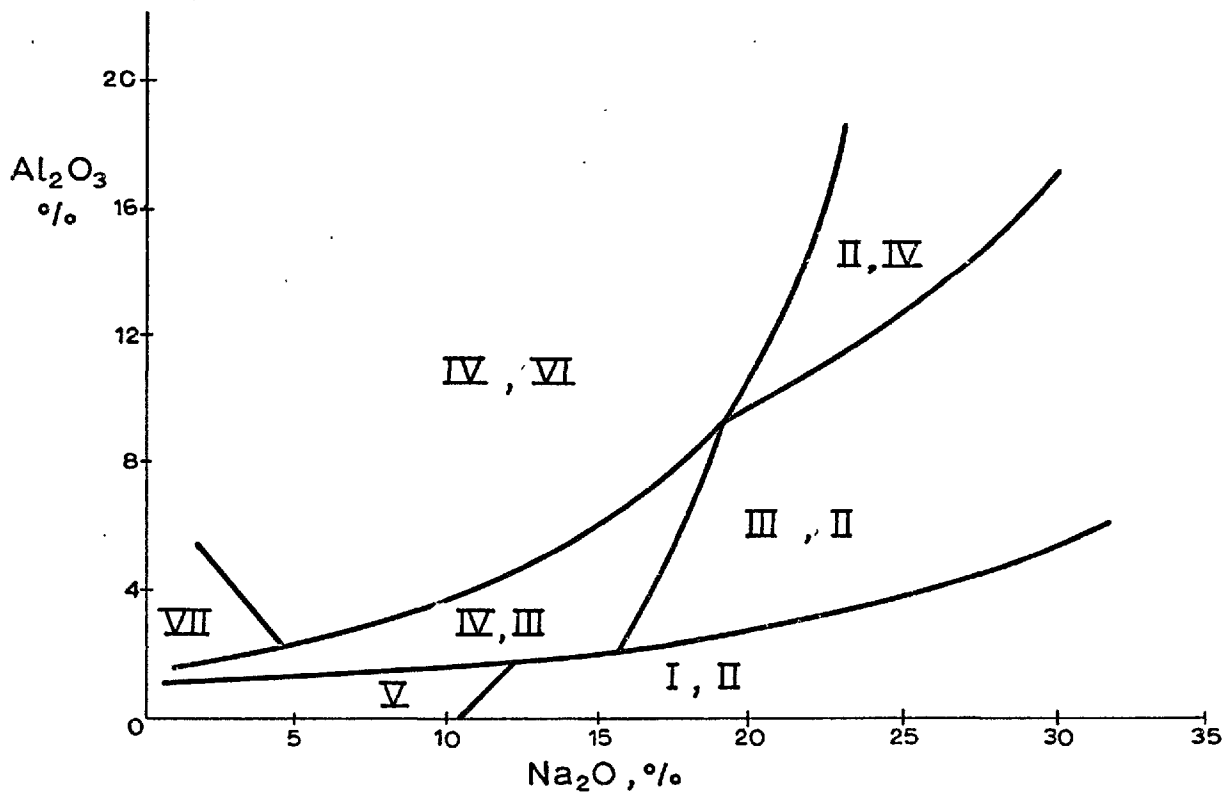


Figure 2. Crystallization fields of the solid phases in the system  $\text{Na}_2\text{O}-\text{CaO}-\text{Al}_2\text{O}_3-\text{SiO}_2-\text{H}_2\text{O}$  at  $280^\circ\text{C}$  with  $\text{CaO}/\text{SiO}_2 = 1.0$ <sup>(59)</sup>

Phases: I)  $\text{Na}_2\text{O} \cdot 2\text{CaO} \cdot 2\text{SiO}_2 \cdot \text{H}_2\text{O}$ ,

II)  $\text{Ca}(\text{OH})_2$ ,

III)  $4\text{Na}_2\text{O} \cdot 2\text{CaO} \cdot 3\text{Al}_2\text{O}_3 \cdot 6\text{SiO}_2 \cdot 3\text{H}_2\text{O}$ ,

IV)  $3\text{CaO} \cdot \text{Al}_2\text{O}_3 \cdot n\text{SiO}_2 \cdot m\text{H}_2\text{O}$ ,

V)  $\text{CaO} \cdot \text{SiO}_2 \cdot n\text{H}_2\text{O}$ ,

VI)  $3(\text{Na}_2\text{O} \cdot \text{Al}_2\text{O}_3 \cdot 2\text{SiO}_2) \cdot 2\text{NaOH} \cdot 2\text{H}_2\text{O}$ ,

VII)  $\text{Na}_2\text{O} \cdot \text{Al}_2\text{O}_3 \cdot 2\text{SiO}_2 \cdot \text{H}_2\text{O}$ .

At concentrations of 200 to 500g/l  $\text{Na}_2\text{O}$ , only sodium calcium hydrosilicate (phase I) is formed which leads to high alumina recovery in solution. With the increase of solution concentration, however, the degree of dispersion of sodium calcium hydrosilicate increases. For efficient alumina extraction, it is usually recommended to use solutions containing 400 - 500g/l  $\text{Na}_2\text{O}$  (about 500 - 645g/l NaOH).

Sazhin and Denisevich<sup>(60)</sup> found that it was possible to extract both alumina and caustic alkali from nepheline in relatively weak alkaline solutions (94.8g/l  $\text{Na}_2\text{O}$ ) in the presence of lime. In 5 min. at 280°C the extraction of alkali oxide and alumina was 70% with the formation of a hydrogarnet (phase IV) and monocalcium hydrosilicate (phase V) but the alumina concentration did not exceed 10g/l in this case.

The molar ratio of  $\text{CaO}/\text{Na}_2\text{O}$  in the sodium calcium hydrosilicate compound formed in the leaching system depends upon the solution concentration. Ponomarev and Shcherban<sup>(61)</sup> reported that a hydrosilicate with the composition of  $2\text{Na}_2\text{O} \cdot 5\text{CaO} \cdot 5\text{SiO}_2 \cdot 3\text{H}_2\text{O}$  would form in a solution containing 200g/l  $\text{Na}_2\text{O}$ . Akhmetov et al<sup>(62)</sup> found that a singular series of sodium calcium hydrosilicates existed at 290°C with decreasing sodium hydroxide concentration from 600g/l  $\text{Na}_2\text{O}$  to zero. This series of compounds and the approximate sodium hydroxide concentration ranges for the stability of each member are summarized in Table 1. The  $\text{CaO}/\text{Na}_2\text{O}$  molar ratio in this series altered stepwise from 2 to  $\infty$ . It is interesting to note

that the end members of this series are the initial and final products in the regeneration of sodium oxide from sodium calcium hydrosilicate (phase I) by hydrolysis.

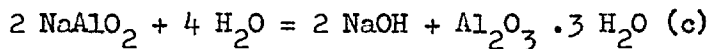
Table 1. The sodium hydroxide concentration ranges for the stability of the sodium calcium hydrosilicate series.

Composition of compound	Concentration range, g/l Na <sub>2</sub> O
Na <sub>2</sub> O.2CaO.2SiO <sub>2</sub> .nH <sub>2</sub> O	600 - 250
2Na <sub>2</sub> O.5CaO.5SiO <sub>2</sub> .3H <sub>2</sub> O	250 - 150
2Na <sub>2</sub> O.11CaO.11SiO <sub>2</sub> .nH <sub>2</sub> O	150 - 75
Na <sub>2</sub> O.13CaO.13SiO <sub>2</sub> .nH <sub>2</sub> O	75 - 25
CaO.SiO <sub>2</sub> .nH <sub>2</sub> O	25 - 0

### 1.1.2 The Caustic Ratio

It is possible in practice to prepare sodium aluminate solutions only with molar ratios Na<sub>2</sub>O/Al<sub>2</sub>O<sub>3</sub> (caustic ratio or caustic modulus) exceeding unity, i.e. with some free sodium hydroxide present.

As the ratio approaches unity, the solutions become unstable and tend to deposit trihydrate alumina according to the equation:



When alumina is extracted from bauxite by the Bayer process, the caustic ratio is usually in the range of 1.6 - 1.8<sup>(3)</sup>. Excess of sodium hydroxide is needed to keep alumina in solution when active silica is present.

Much higher values of the caustic ratio are required for efficient extraction of alumina from aluminosilicates by means of the hydrochemical alkaline process. The optimum values reported for this process are in the range 10-14<sup>(26,63,64)</sup>. In the opinion of Ponomarev and Sazhin<sup>(27)</sup>, the high caustic ratio is necessary in order to retard the formation of hydrated sodium aluminosilicate and thereby to prevent silica removal from the solution at the expense of alumina.

Ponomarev, et al.,<sup>(43)</sup> reported that the recovery of alumina from nepheline rocks by the hydrochemical alkaline process increased sharply when the  $\text{Na}_2\text{O}/\text{Al}_2\text{O}_3$  ratio changed from 7 to 9-10. At higher values the variation of this ratio had no significant effect. Using synthetic materials, Ni, et al.<sup>(65)</sup>, studied the effect of the caustic ratio on the composition of the system:  $\text{Na}_2\text{O} - \text{CaO} - \text{Al}_2\text{O}_3 - \text{SiO}_2 - \text{H}_2\text{O}$  under the hydrochemical alkaline conditions (503g/l  $\text{Na}_2\text{O}$ ,  $\text{CaO}/\text{SiO}_2 = 1.0$ , at  $280^\circ\text{C}$  for 1 hr.). They found four distinct regions at different caustic ratios:

i) A region of caustic ratio above 11, where the stable phase was sodium calcium hydrosilicate. Formation of this sparingly soluble compound transferred silica into the precipitate and ensured the retention of alumina in solution.

ii) A region characterized by the precipitation of sodium calcium hydroaluminosilicate in addition to sodium calcium hydrosilicate. This region was in the range of caustic ratios of 8 - 11.

iii) A region with the predominant formation of sodium

calcium hydroaluminosilicate, high-temperature sodium hydroaluminosilicate and calcium hydroxide. Within this region the caustic ratio was in the range 6 to 8.

iv) A region with the caustic ratio below 6 and in which a high-temperature hydroaluminosilicate, close to permutite in composition was formed. Free calcium hydroxide was found in the precipitate in this region.

### 1.1.3 Effect of Lime

As already stated, the presence of certain amounts of lime is an essential condition for a high degree of alumina extraction from aluminosilicates by means of the hydrochemical alkaline method. Sufficient lime should be present to combine with the silica to form sodium calcium hydrosilicate. If less lime than required is used, silica removal takes place by combination with both lime and alumina.

Lime is usually used in the Bayer process for refractory bauxites. In leaching of boehmite-diaspore bauxites, a small addition of lime (3 to 4% on the weight of bauxite) accelerates their decomposition and favours increased extraction of alumina into solution. There have been many studies of the part played by calcium oxide in bauxite leaching<sup>(55, 66-68)</sup>, but there is no agreed opinion on its intensifying action. Of the explanations of the lime effect is that given by Druzhinina. She showed that in the absence of calcium oxide, titania impurities in the bauxite form finely divided sodium metatitanate. This coats the bauxite particles and thus prevents



further dissolution of the mineral. When calcium oxide is introduced into the digestion zone, perovskite,  $\text{CaO} \cdot \text{TiO}_2$ , is formed. Its crystals are relatively large and have no harmful effect on the leaching process.

Sazhin and Denisevich<sup>(60)</sup>, in their investigations of the rate of decomposition of nepheline by the hydrochemical alkaline method found that calcium oxide introduced into the system not only assisted the formation of compounds not containing alumina but also favoured a considerable increase of the decomposition rate of the native mineral.

Many investigations had been undertaken to study the effect of lime and the molar ratio of  $\text{CaO}/\text{SiO}_2$  on the alumina extraction and on the solid phases formed during the hydrochemical alkaline process<sup>(26,27,43,69,70)</sup>. In the absence of lime, i.e. in the quaternary system:  $\text{Na}_2\text{O}-\text{Al}_2\text{O}_3-\text{SiO}_2-\text{H}_2\text{O}$ , almost all the alumina from the mineral would be in the precipitate and sodium hydroaluminosilicates the main solid phases formed<sup>(58, 71-73)</sup>. With the  $\text{CaO}/\text{SiO}_2$  molar ratio between zero and unity, sodium calcium hydrosilicate and sodium calcium hydroaluminosilicate are formed in different proportions according to the  $\text{CaO}/\text{SiO}_2$  molar ratio<sup>(69)</sup>. The amount of alumina remaining in solution at equilibrium increases with the  $\text{CaO}/\text{SiO}_2$  ratio in the system. Ponomarev and Sazhin<sup>(26)</sup> reported that as the calcium oxide added to the mixture approached the molar equivalent of silica, alumina extraction from nepheline increased from 9% to 96%. At  $\text{CaO}/\text{SiO}_2$  ratio of 1 to 1.1 almost all the alumina passes into

the leaching solution and sodium calcium hydrosilicate is formed as the main solid phase<sup>(43,69,70)</sup>. Further increase in the CaO/SiO<sub>2</sub> ratio above 1.1 has no marked effect on the alumina extraction and the excess of lime crystallizes out in the form of calcium hydroxide.

#### 1.1.4 Behaviour of Potassium Hydroxide

When treating such aluminosilicate minerals as nepheline by the hydrochemical alkaline process, potassium hydroxide is introduced into the system. This potassium hydroxide usually appears in the aluminate solutions. Many investigations have been carried out into the effect of potassium hydroxide on the hydrochemical alkine process<sup>(74-80)</sup>. Ponomarev and Sazhin<sup>(74)</sup> found that potassium hydroxide solutions had a smaller extraction capacity for aluminium than did sodium hydroxide solutions. Up to 60% alumina could be extracted from aluminosilicates with comparatively weak potassium hydroxide solutions (about 80 to 100g/1K<sub>2</sub>O) in the presence of lime and at 280°C. When higher concentrations of KOH were used, the percentage of extracted alumina decreased rapidly.

In solutions containing potassium hydroxide and sodium hydroxide, a high degree of alumina extraction could be achieved under the conditions of the hydrochemical alkaline process. In the presence of potassium hydroxide in amounts up to 4 0% (mol) of the alkali total, there is no drop in the alumina extraction of aluminosilicates by a circulating solution<sup>(74,76)</sup>. Any further increase of the amount

of potassium hydroxide in the starting leaching solution would lead to a proportionate drop in the alumina extraction. To improve and modernize the hydrochemical alkaline method, Ponomarev<sup>(63)</sup> proposed the use of an alkaline solution with a ratio of 70 mole %  $\text{Na}_2\text{O}$  and 30 mole %  $\text{K}_2\text{O}$  at an alkali concentration of 484 g/l (calculated as  $\text{Na}_2\text{O}$ ) instead of the pure sodium hydroxide solutions.

### 1.2 Thermodynamic Assessment

In the hydrochemical alkaline process, the aluminosilicate minerals are decomposed by caustic soda solutions in the presence of lime with the formation of sodium calcium hydrosilicate. The liberated alumina goes into solution in the form of alkali aluminates and silica reacts with calcium hydroxide to form the solid product. To assess the thermodynamic feasibility of the formation of sodium calcium hydrosilicate from aluminosilicate minerals, one needs to investigate the possibility of the following two main step reactions:

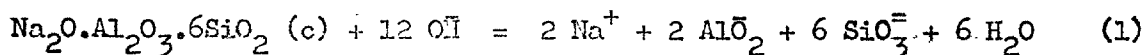
a) dissolution (or decomposition) of the mineral in sodium hydroxide solutions to form mainly soluble sodium aluminate and sodium silicate, and

b) the interaction of the dissolved sodium silicate with calcium hydroxide to form sodium calcium hydrosilicate.

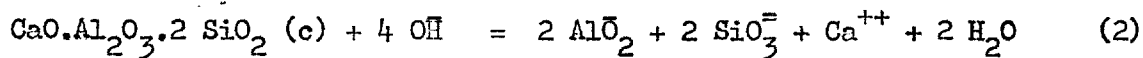
If any of these steps for a particular mineral is not thermodynamically feasible, then the formation of sodium calcium hydrosilicate from that mineral and the extraction of ~~alumina~~ alumina from it by this process would not take place.

The dissolution step reactions of some aluminosilicate minerals used in this study by sodium hydroxide solution are represented in the equations (1 - 6). For purposes of comparison the dissolution of nepheline, which has been used in the hydrochemical alkaline process, is represented by equation (7).

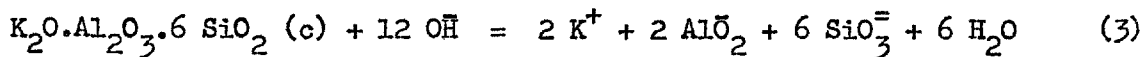
Albite



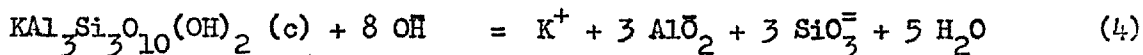
Anorthite



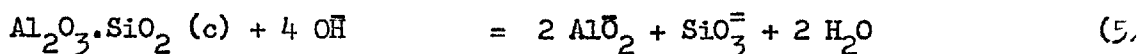
Microcline



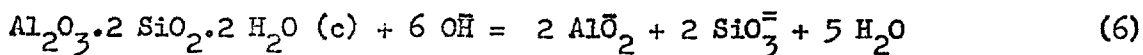
Muscovite



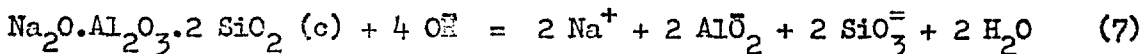
Kyanite



Kaolinite



Nepheline

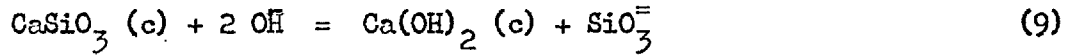


The reactions for the dissolution of quartz and wollastonite by sodium hydroxide solutions are represented in equations (8) and (9) respectively.

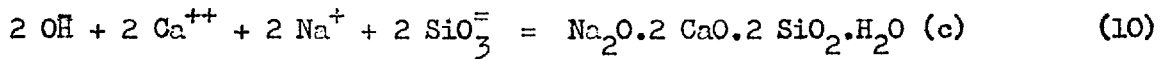
Quartz



Wollastonite



Step (b) of the interaction between the dissolved ionic species to form sodium calcium hydrosilicate may be represented by the equation:



Sodium calcium hydrosilicate is unstable when the solution becomes saturated with alumina. It would be attacked by the aluminate ion with the possible formation of sodium calcium hydroaluminosilicate according to the equation:

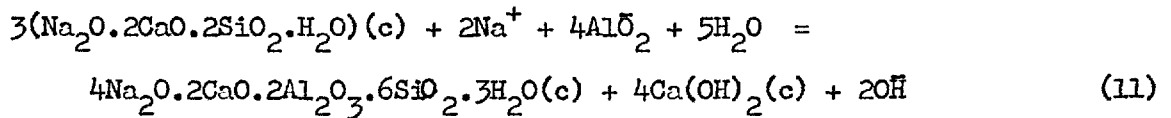


Table 2 shows data of the different thermodynamic functions used for the substances concerned. The missing thermodynamic data for some substances for which no literature values would be found were estimated as shown below.

1.2.1 Estimation of Thermodynamic Data

No thermodynamic data has been reported in the literature for sodium calcium hydrosilicate (phase I in Figure 2) or sodium calcium hydroaluminosilicate (phase III) and they had to be found by calculation. Calculations for phase I were made as follows:

The heat of formation,  $\Delta \text{Hf}_{298}^\circ$ , was calculated as described by Cottrell<sup>(101)</sup> from the formula

$$\Delta \text{Hf}_{298}^\circ = - \sum \epsilon + \sum \sigma + D_{\text{O}_2}$$

where  $\sum \epsilon$  is the sum of the average interatomic bond energies in the

Table 2. Thermochemical data used in the calculations

Substance	$\bar{S}_{298}^{\circ}$	$\bar{C}_p^{\circ}_{298}$	$-\Delta H_f^{\circ}_{298}$	$-\Delta G_f^{\circ}_{298}$	Reference No
Na <sup>+</sup> , aq.	14.0	37	57.48	61.9	81, 82
K <sup>+</sup> , aq.	24.5	31	60.04	67.47	82, 83
Ca <sup>++</sup> , aq.	-13.2	74	129.77	132.18	82, 83
OH <sup>-</sup> , aq.	- 2.52	-57	54.96	37.56	82, 83
AlO <sub>2</sub> <sup>-</sup> , aq.	25	-79	218.6	214.78	81 - 84
SiO <sub>3</sub> <sup>=</sup> , aq.	- 5.45	-86.84	256.0	219.2	81, 82, 85
H <sub>2</sub> O, liq.	16.75	18.03	68.32	56.72	82, 86
Ca(OH) <sub>2</sub> , c	19.93	22.29	235.8	214.33	82, 87
Albite, c	100.93	97.92	1830.9	1724.16	87 - 89
Anorthite, c	48.4	49.5	994.5	940.8	87, 89, 90
Kyanite, c	20.03	29.09	656.4	620.5	87, 91, 92
Quartz, α, c	10.0	10.62	209.9	196.9	87, 93
Kaolinite, c	48.4	58.62	964.7	888.1	94 - 96
Muscovite, c	69.0	76.80	1421.2	1330.1	97 - 99
Microcline, c	105.0	110.93	1816.0	1709.2	82, 87, 95
Wollastonite, β, c	19.6	20.38	378.6	358.2	82, 87
Nepheline, c	59.4	80.04	997.2	926.16	87, 89
Phase I, c	42.4	66.6	985.58	914.6	99, 100
Phase III, c	137.1	-	3493.	3265.	81

molecule of the compound (K.cal./mole),  $\sigma$  is the heat of sublimation of the element (K.cal./mole), and  $Do_2$  is the heat of dissociation of oxygen (K.cal./mole). The heats of sublimation of the elements and the bond energies, taken from the literature<sup>(81)</sup>, are given in Tables 3 and 4 respectively.

Table 3. Heats of sublimation of elements.

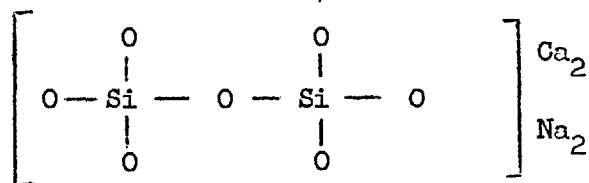
Element	Heat of sublimation, K.cal./mole
Na	25.95
Ca	39.7
Si	67.5
Al	85.0

The heat of dissociation of oxygen molecules was taken as  $Do_2 = 118.32$  K.cal./mole<sup>(83)</sup>.

Table 4. Values of the average bond energy and entropy of the oxygen ion in the molecule.

Bond type	Bond energy, K.cal.	Entropy of oxygen ion, K.cal/deg. g-ion.
Si-O	102.18	2.5
Ca-O	125.38	4.75
Al-O	118.6	2.03
Ca -O-Si	238.21	5.2
Na-O-Si	236.5	3.6
Al-O-Si	243.47	4.94
Ca-O-Al	245.87	8.6

The above equation was used to calculate  $\Delta H_{298}^{\circ}$  of the anhydrous compound. The structural formula of anhydrous sodium calcium silicate may be represented as follows<sup>(102)</sup>:



$$\begin{aligned} - \sum \epsilon &= - [2(\text{Na-O-Si}) + 4(\text{Ca-O-Si}) + 2(\text{Si-O})] \\ &= - (2 \times 236.5 + 4 \times 238.21 + 2 \times 102.18) \\ &= - 1630.2 \text{ K.cal.} \end{aligned}$$

$$\begin{aligned} \sum \sigma &= 2\sigma_{\text{Na}} + 2\sigma_{\text{Ca}} + 2\sigma_{\text{Si}} \\ &= 2 \times 25.95 + 2 \times 39.7 + 2 \times 85.0 \\ &= 301.3 \text{ K.cal.} \end{aligned}$$

$$D_{\text{O}_2} = 118.32 \times \frac{7}{2} = 414.3$$

$$\begin{aligned} \Delta H_{298}^{\circ} &= - 1630.2 + 301.3 + 414.3 \\ &= - 914.6 \text{ K.cal./mole.} \end{aligned}$$

The value of  $\Delta H_{298}^{\circ}$ /mole of water in the lattice of the compound was taken as -71 K.cal./mole water<sup>(81)</sup>, and the heat of formation of sodium calcium hydrosilicate would be

$$\Delta H_{298}^{\circ} = - 914.6 - 71 = - 985.6 \text{ K.cal./mole.}$$

The entropy calculations were based on the assumption of the additivity of the entropy values for the bonds in the molecule<sup>(103)</sup>. The entropy for an equivalent of water was taken as 9.4 K.cal./mole. deg. from Latimer's data<sup>(104)</sup>. Using the entropy values in Table 4, the entropy of sodium calcium hydrosilicate would be



$$\begin{aligned} S_{298}^{\circ} &= 2 \times S_{\text{Na-O-Si}}^{\circ} + 4 \times S_{\text{Ca-O-Si}}^{\circ} + 2 S_{\text{Si-O}}^{\circ} + S_{\text{H}_2\text{O}}^{\circ} \\ &= 2 \times 3.6 + 4 \times 5.2 + 2 \times 2.5 + 9.4 \end{aligned}$$

$$S_{298}^{\circ} = 42.4 \text{ cal./mole-degree.}$$

The standard free energy of formation of sodium calcium hydrosilicate from its elements was then calculated from the equation:

$$\Delta G_{298}^{\circ} = \Delta H_{298}^{\circ} - T \Delta S_{298}^{\circ},$$

and found to be  $\Delta G_{298}^{\circ} = -914.6 \text{ K.cal./mole.}$

In a similar manner data for phase III were estimated.

According to Babushkin<sup>(105)</sup>, the methods used for calculating the thermochemical data give satisfactory agreement with experimental results. Arlyuk<sup>(81)</sup> also found that the thermodynamic calculations based on these assumptions for the reactions of alumina sinters with sodium carbonate solutions and sodium aluminate solutions were in agreement with experimental data.

### 1.2.2 Thermodynamic Feasibility of the Reactions

The free energy changes of the above reactions were calculated at room temperature, 298°K, and at higher temperatures up to 280°C (553°K).

#### 1.2.2.1 Reactions of Room Temperature

The free energy change for the formation of sodium calcium hydrosilicate from its dissolved, ionic species at 298°K has a value of -12.92 K.cal./mole (Table 6) which indicates that step (b) above is thermodynamically feasible. If step (a) for a particular mineral, i.e. its dissolution by sodium hydroxide solution, is possible, the whole process for the formation of sodium calcium hydrosilicate

from that mineral would be feasible. Table 6 shows that this step for most of the minerals investigated is possible at room temperature, since a large negative value for the free energy change is obtained.

The free energy change for the dissolution of silica in sodium hydroxide solutions was calculated to be  $\Delta G_{298}^{\circ} = - 3.9$  K.cal./mole using the thermodynamic data for quartz given in U.S. Bureau of Mines, Bull. 605<sup>(93)</sup>.

Recently it was reported that quartz has a more negative value for its standard free energy of formation than the already known value of - 196.9 K.cal./mole<sup>(106)</sup>. In its latest Technical note edition, the National Bureau of Standards<sup>(91)</sup> has adopted the value - 204.75 K.cal./mole for the standard free energy of formation of quartz. If this value is to be used in equation (8), the free energy change of quartz dissolution in sodium hydroxide solution would be + 3.95 K.cal./mole implying the improbability of the reaction. It is known, however, that quartz could be attacked and dissolved by sodium hydroxide solutions so the value - 3.9 K.cal./mole is more probable and will be used in this analysis.

The free energy change for the dissolution of kyanite in sodium hydroxide solution, based on the National Bureau of Standards data for kyanite<sup>(91)</sup>, was found to be  $\Delta G_{298}^{\circ} = + 8.54$  K.cal./mole indicating that the reaction would not be feasible at room temperature. If earlier data for kyanite<sup>(107)</sup> were used, the free energy change for reaction (5) would be - 27.96 K.cal./mole and the reaction would be possible.

The free energy change for the dissolution of wollastonite at 298°K is so small that it can not be judged with great certainty, but it does show that even if the reaction is possible, it would not be very favourable.

The free energy change for reaction (11), i.e. the interaction of sodium calcium hydrosilicate with saturated aluminate solutions, at room temperature was found to be  $\Delta G_{298}^{\circ} = -62$  K.cal./mole of sodium calcium hydrosilicate, showing that the reaction is feasible.

#### 1.2.2.2 Reactions at Higher Temperatures

The leaching experiments on aluminosilicate minerals in sodium hydroxide solutions were carried out at temperatures up to 280°C (553°K) and in some tests at 300°C. The free energy changes of the different reactions were calculated at 200, 250 and 280°C to find the thermodynamic conditions for the reactions at these temperatures.

The change in the free energy of a reaction,  $\Delta G_{(t_2)}^{\circ}$ , at temperature  $t_2$  is related to the change in the free energy,  $\Delta G_{(t_1)}^{\circ}$ , at temperature  $t_1$  by the equation:

$$\Delta G_{(t_2)}^{\circ} = \Delta G_{(t_1)}^{\circ} + \Delta \bar{C}_p^{\circ} \int_{t_1}^{t_2} \Delta T - \Delta S_{(t_1)}^{\circ} \Delta T - T_2 \Delta \bar{C}_p^{\circ} \int_{t_1}^{t_2} \ln \frac{T_2}{T_1} \quad (12)$$

The  $\Delta \bar{C}_p^{\circ} \int_{t_1}^{t_2}$  term is an average value of the heat capacity change for the reaction between  $t_2$  and  $t_1$  and involves both solid and solute species. The average value of heat capacity for the various solids was obtained in most cases from reliable data but in some cases estimations had to be made. The average value of partial molal

heat capacity for the ionic species was estimated by the Correspondence Principle of Criss and Cobble<sup>(108)</sup>.

Robins<sup>(109)</sup> found that the free energy change data obtained by the correspondence principle were very reliable in predicting equilibria in the uranium-water system, and experimental results<sup>(110)</sup> from hydrothermal precipitation of  $\text{Fe}^{+++}$  solutions were in close agreement with his calculated data. He also used this principle to calculate the free energy change for the sulphate-bisulphate reaction and the results of his calculations were in agreement with experimental data. Cobble calculated solubilities of calcium hydroxide at temperatures up to  $250^{\circ}\text{C}$  by means of this method<sup>(111)</sup>, and the results obtained were in good agreement with the literature data<sup>(112-115)</sup>.

The correspondence principle shows that a standard state can be chosen at every temperature such that the partial molal entropies of one class of ions at that temperature are linearly related to the corresponding entropies at some reference temperature. The entropy standard state at  $25^{\circ}\text{C}$  is a hydrogen ion entropy of  $-5 \text{ cal./mole}\cdot\text{degree}$  and the general relationship can be written:

$$\bar{S}_t^{\circ} = a_t + b_t \bar{S}_{25}^{\circ} (\text{abs}) \quad (13)$$

where  $a_t$  and  $b_t$  are temperature dependent constants for each class of ions (cations, anions, oxyanions and hydroxyanions), and where

$$\bar{S}_{25}^{\circ} (\text{abs}) = \bar{S}_{25}^{\circ} (\text{conventional}) - 5.0z$$

$z$  being the ionic charge.

The calculated values of the partial molal entropies of the different ionic species at high temperatures using equation (13) are

given in Table 5.

No data for the partial molal entropy for the silicate ion are reported in the literature and an estimation of  $\bar{S}_{25}^{\circ}$  had to be made. The partial molal entropy of an oxyanion could be calculated from the equation<sup>(85)</sup>:

$$\bar{S}_{25}^{\circ} = 5.5z + 40.2 + \frac{3}{2} R \ln M - 108.8 z^2/nr \quad (14)$$

where R is the gas constant, M the molecular weight of the ion, n the number of oxygen atoms in the ion and r is the Si-O bond distance plus 1.40 Å<sup>o</sup>. The Si-O bond distance was taken as 1.65Å<sup>o</sup>.<sup>(116)</sup> A value of  $\bar{S}_{25}^{\circ} = -5.45$  cal./mole.degree for the silicate ion was obtained. Using this value, the partial molal entropies at higher temperatures were calculated as above.

The average value of the partial molal heat capacity for the different ionic species between  $t_1$  and  $t_2^{\circ}$ C was calculated from the relation:

$$\bar{C}_p^{\circ} \Big]_{t_1}^{t_2} = \frac{\bar{S}^{\circ}(t_2) - \bar{S}^{\circ}(t_1)}{\ln T_2/T_1}$$

and the values obtained are given in Table 5. The average value of the heat capacity change  $\Delta \bar{C}_p^{\circ} \Big]_{t_1}^{t_2}$  for the different reactions were then calculated (Table 5) and the results were finally used to estimate  $\Delta G^{\circ}(t_2)$  using equation (12). The free energy change for reaction (1) at 473<sup>o</sup>K, for example, would be

Table 5. Partial molal entropies and average molal heat capacities at high temperatures.

Substance	$\bar{S}_{473}^{\circ}$	$\bar{S}_{523}^{\circ}$	$\bar{S}_{553}^{\circ}$	$\bar{C}_P^{\circ} \int_{298}^{473}$	$\bar{C}_P^{\circ} \int_{473}^{523}$	$\bar{C}_P^{\circ} \int_{523}^{553}$
Na <sup>+</sup> , aq.	29.7	35.6	39.14	45	58.8	63.6
K <sup>+</sup> , aq.	37.0	42.2	45.26	39	51.8	54.9
Ca <sup>++</sup> , aq.	6.8	15.3	20.46	66	84.7	92.6
OH, aq.	-27.8	-36.3	-42.6	-65	-84.7	-113
AlO <sub>2</sub> , aq.	-6.4	-16.9	-23.2	-69.1	-105	-113
SiO <sub>3</sub> , aq.	-57.8	-75.95	-86.84	-133.5	-180	-195
H <sub>2</sub> O, liq.	17.59	17.78	17.88	18.17	18.4	18.56
Ca(OH) <sub>2</sub> , c.	30.5	33.01	34.4	23.23	24.45	24.88
Albite, c.	151.90	164.72	171.98	110.54	125.06	127.96
Anorthite, c	74.48	80.99	84.65	56.43	64.39	65.95
Kyanite, c	36.54	40.46	42.59	34.19	39.99	41.04
Quartz, α, c.	15.66	17.1	17.9	12.26	14.21	14.7
Kaolinite, c.	79.25	86.90	91.28	66.75	76.25	78.66
Muscovite, c.	109.77	119.95	125.8	87.74	100.37	102.95
Microcline, c.	157.22	168.94	175.94	110.93	126.66	129.73
Wollastonite, β, c.	30.25	32.83	34.26	22.91	25.79	26.32
Nepheline, c.	89.96	96.84	100.78	74.4	75.22	75.7
Phase I, c.	76.47	84.70	89.36	73.72	81.98	83.72

$$\Delta G_{473}^{\circ} = \Delta G_{298}^{\circ} + \Delta \bar{C}_p^{\circ} \Big]_{298}^{473} \times (473 - 298) - \Delta S_{298}^{\circ} \times (473 - 298) \\ - 473 \times \Delta \bar{C}_p^{\circ} \Big]_{298}^{473} \times 2.303 \log \frac{473}{298}$$

Using the values in Table 5 for the different terms, we obtain

$$\Delta G_{473}^{\circ} = - 34000 + 175 \times 70.72 - 175 \times 75.55 \\ - 2.303 \times 473 \times 70.72 \log \frac{473}{298}$$

$$\Delta G_{473}^{\circ} = - 44140 \text{ cal./mole of albite}$$

Because of the fact that the averages of  $\bar{C}_p^{\circ}$  in equation (12) are not the same over too great a temperature interval, calculations above 200°C were carried out in 50°C intervals. Values of the entropies for the ionic species involved in a given reaction were calculated at 200, 250 and 280°C. These values were then used in turn to generate the corresponding ionic heat capacities according to equation (15). The resulting series of  $\Delta \bar{C}_p^{\circ} \Big]_{t_1}^{t_2}$  above 200°C were finally used to estimate  $\Delta G_{(t_2)}^{\circ}$  using equation (12) as above.

No account was taken of the effect of pressure on free energy changes since it has been shown to be negligible below 300°C (109,111,117). However, the pressure effect is not to be confused with the free energy changes caused by varying the pressure of such gases as oxygen or hydrogen which take part in the reaction.

The changes in the free energy for the different reactions at elevated temperatures, calculated from equation (12), are given in Table 6. The change in the free energy for step (b) reaction, i.e. the formation of sodium calcium hydrosilicate from its ionic species,

Table 6. Thermodynamic data for the different reactions at high temperatures.

Reaction No.	$\Delta S_{298}^{\circ}$	$\Delta S_{473}^{\circ}$	$\Delta S_{523}^{\circ}$	$\Delta \bar{C}_p^{\circ} \Big]_{298}^{473}$	$\Delta \bar{C}_p^{\circ} \Big]_{473}^{523}$	$\Delta \bar{C}_p^{\circ} \Big]_{523}^{553}$	$\Delta G_{298}^{\circ}$	$\Delta G_{473}^{\circ}$	$\Delta G_{523}^{\circ}$	$\Delta G_{553}^{\circ}$
1) Albite	+75.55	-12.96	-40.74	70.72	-170.66	+70.60	-34.0	-44.14	-43.06	-41.90
2) Anorthite	+21.08	-43.3	-70.63	-30.19	-69.09	+12.77	-22.54	-24.91	-24.52	-22.80
3) Microcline	+48.02	-3.68	-31.76	-83.1	-186.26	+25.72	-60.1	-68.14	-67.49	-66.56
4) Muscovite	+132.92	+44.98	+23.0	-45.69	-133.97	+24.75	-22.43	-43.7	-45.61	-46.32
5) Kyanite	+70.94	+39.24	+30.55	-9.55	-54.39	+27.08	48.54	-3.46	-5.29	-6.23
6) Kaolinite	+89.57	+47.10	+34.10	+8.90	-46.05	-76.14	-38.1	-54.16	-56.4	-57.36
7) Nephelite	+51.28	-12.38	-32.58	-93.26	-152.02	-75.7	-28.8	-33.71	-32.71	-31.67
8) Quartz	+7.76	-0.27	-26.03	+2.41	-6.41	+34.86	-3.9	-5.36	-5.33	-4.78
9) Wollastonite	-0.08	-1.95	-3.17	-3.18	+28.66	+29.56	-0.21	-0.057	+0.11	+0.18
10) Phase I	+40.74	+173.99	+206.92	+248.72	+324.38	+387.32	-12.92	-30.9	-40.42	-46.95



becomes steadily more negative with rising temperature. Except for wollastonite, the change in the free energy of step (a) for the dissolution of different minerals in sodium hydroxide also becomes more negative at high temperatures than at 298°K. This indicates that the thermodynamic conditions for these reactions are more favourable at the high temperatures of the hydrochemical alkaline process than at room temperature. Since the thermodynamic conditions for both steps (a) and (b) become more favourable at high temperatures, the whole process of leaching would, therefore, be more favourable.

The results for wollastonite show that its decomposition by sodium hydroxide solutions becomes less favourable with increase of temperature. In fact the free energy change for the reaction at 280°C is + 0.18 K.cal./mole, which indicates that the reaction may be impossible at high temperatures.

The positive value of the free energy change for the dissolution of kyanite at room temperature becomes - 6.23 K.cal./mole at 280°C indicating the feasibility of the reaction at the latter temperature. If the value of  $\Delta G_{298}^{\circ} = - 27.96$  K.cal./mole is to be used, a more negative value would be obtained at 280°C.

The free energy change for reaction (11) was not calculated at higher temperatures. In light of the results for other reactions, however, it is likely that this reaction would be still feasible at temperatures above room temperature.

No thermodynamic calculations have been made for the intermediate

members of the plagioclase series, e.g. oligoclase and labradorite. These intermediate members may be considered as composite mixtures with various proportions of albite and anorthite, the end members of the series, and their thermodynamic properties may also be considered as intermediate between those of the end members.

### 1.3 Kinetics of the Process

The main steps taking place during the process of sodium calcium hydrosilicate formation in the hydrochemical treatment of aluminosilicates could be considered as follows:

- i) The attack and decomposition of the aluminosilicate mineral by sodium hydroxide solution to form ionic species in solution,
- ii) Diffusion or transportation of the various ionic species and in particular silicate and calcium ions, and
- iii) The interaction between the concerned ionic species to form sodium calcium hydrosilicate according to equation (10).

Each of these steps may be composed of one or more sub-steps. The ionic reaction in step (iii) is usually so fast that it could be considered instantaneous once the various reactants come in contact with each other. The overall rate of the leaching process is, therefore, controlled by the rate of one of the other two steps. At low temperatures the process would likely be chemically-controlled, i.e. the dissolution step is the rate-determining step, but as the temperature is raised the part played by diffusion and transportation of species will become more important than at low temperatures. Some of the factors that might have an important influence on the rate of

the dissolution and diffusion steps are discussed in the following:

### 1.3.1 Rate of Mineral Dissolution

Of the factors affecting the rate of dissolution of aluminosilicate minerals in sodium hydroxide solutions, the following are of special importance:

#### 1.3.1.1 Temperature

In general, increase of temperature leads to higher rates of reaction (Arrhenius law). It has also an indirect effect by decreasing the solution viscosity and increasing the solubility of many components in the system.

#### 1.3.1.2 Sodium Hydroxide Concentration

Under otherwise equal conditions, the rate of the dissolution of aluminosilicates in sodium hydroxide solutions would increase with the initial concentration of solution. Low concentrations favour the formation of sodium hydroaluminosilicate which coats the mineral surface preventing further dissolution of the mineral.

#### 1.3.1.3 Particle Size

As the particle size of the mineral decreases, and the surface area increases, the rate of mineral dissolution will increase. Clay minerals, for example, with particle sizes in the micron and sub-micron order would be expected to dissolve with appreciable rates in sodium hydroxide solutions. Because of their very fine particle size, and other factors, clays are readily attacked under the "mild" conditions of the digestion of gibbsitic bauxite by means of the Bayer process.

#### 1.3.1.4 Factors Related to the Mineral

Under equal conditions, the reactivities of the different aluminosilicate minerals would vary from one to another due to factors related to the mineral itself. Of these factors, the following would be of particular importance in the mineral dissolution step during leaching: a) the degree of crystallinity of the mineral, b) crystal structure and compactness, and c) chemical composition of the mineral and impurity inclusions.

#### 1.3.1.5 Impurities

Some impurities may have an indirect effect on the dissolution rates. This effect would be more pronounced if the impurities react under the leaching conditions forming a film of fine particles adherent to the mineral surface thus preventing further dissolution of the mineral. The formation of sodium metatitanate during bauxite leaching (section 1.1.3) is a good example of this effect.

#### 1.3.2. Transport of Solute Species

Because of the large viscosities of the highly concentrated sodium aluminate solutions and the relatively low concentrations of  $\text{Ca}^{++}$  and  $\text{SiO}_3^-$  ions in the system, transportation of these species would be an important factor in the rate of sodium calcium hydrosilicate formation. The concentrations of  $\text{Na}^+$  and  $\text{OH}^-$  ions are so high that they could be considered constant throughout the solution, while those of  $\text{Ca}^{++}$  and  $\text{SiO}_3^-$  ions could vary considerably from one zone to another in the system. The concentration of  $\text{SiO}_3^-$  would be highest in the vicinity of the dissolving mineral surface and lowest where

desilication, i.e. the formation of insoluble silicate phases, takes place. When the rate of mineral dissolution is a fast step, the diffusion of  $\text{SiO}_3^-$  and  $\text{Ca}^{++}$  ions would be a predominant rate-controlling factor in the process, especially if these ions are to diffuse on their own.

Temperature has a favourable effect on diffusion rates since it decreases the viscosity of the solution, increases the individual ionic mobilities and raises the concentration of silica in solution. On the other hand it has a reverse effect on the solubility of calcium hydroxide, decreasing the concentration of  $\text{Ca}^{++}$  ions in solution.

Thorough agitation is necessary during the leaching process. Beside assisting the transportation of different species, it would remove the dissolved silicates and aluminates from the mineral surface vicinity and allow the dissolution of the mineral to proceed unimpeded.

#### 1.3.2.1 Solubility of Calcium Hydroxide

The rate of diffusion depends largely on the concentration and the concentration gradient in the system. In general, calcium hydroxide solubility in aqueous solutions is very low<sup>(112-115)</sup> and decreases rapidly with the increase of temperature. The solubility in water at 30°C, for example, is 1.21 g/l CaO and decreases to 0.037 g/l CaO at 250°C<sup>(113)</sup>. The solubility of calcium hydroxide is greatly reduced in the presence of sodium hydroxide in solution. The solubility drops from 1.177 g/l CaO at 20°C in pure water to

0.146 g/l CaO in solutions containing 8.36 g/l NaOH at the same temperature<sup>(118)</sup>. The particle size of calcium hydroxide has also some influence on its solubility. The solubility of coarse, well-defined crystals, the formation of which is favoured by high temperatures, is usually about 10% lower than the fine particles.

The combined effects of the presence of sodium hydroxide in the leaching system, high temperatures and the large crystals of calcium hydroxide at these temperatures would considerably reduce the amounts of dissolved calcium hydroxide. Its rate of diffusion would, therefore, be a predominant rate-controlling factor in the leaching process at high temperatures.

C H A P T E R 2

EXPERIMENTAL MATERIALS AND TECHNIQUES

## 2.1 Experimental Methods and Techniques

### 2.1.1 Autoclave Leaching Experiments

#### 2.1.1.1 Apparatus.

Most of the leaching experiments were carried out in an Autoclave Engineers' one liter "magnedrive packless autoclave" model AFP-1005. The "dispersimax turbine-type" agitator was driven by an air motor with variable speeds of the range 0 to 2000 r.p.m. It was equipped with two electric heating elements wrapped around the pressure vessel and a cooling coil inside the vessel. The main autoclave parts were made of stainless steel, but the cooling coil, the thermowell and the agitator were made of pure nickel to resist corrosion at high temperatures and high concentrations of sodium hydroxide solutions. A nickel cylindrical container which fitted loosely inside the pressure vessel was used for handling the reaction mixtures.

A chromel-alumel thermocouple was used for solution temperature measurement and control. The temperature of the solution was held constant to within  $\pm 2^{\circ}\text{C}$  by means of an Eurotherm stepless temperature controller fitted with FM2 mains filter unit. The exact temperature was read by means of a "Pye Portable" potentiometer.

Some earlier experiments for the preliminary studies were carried out in a three-liter stainless steel autoclave. No nickel container was used in these tests and the reaction solution was put directly in the pressure vessel. This autoclave was a gas-heated one with an electric-driven agitator. A thermocouple connected to a



Cambridge temperature regulator was placed in the autoclave socket for temperature measurement and control. Compressed air was used to cool the autoclave at the end of the experiment.

#### 2.1.1.2 Experimental Procedure

Leaching experiments were carried out in 250 to 350 ml. batches. Sodium hydroxide solution of the required concentration was prepared from sodium hydroxide flakes in the nickel container. A weighed mineral sample was blended and intimately mixed with calculated quantities of calcium oxide powder to obtain the desired molar ratio of  $\text{CaO}/\text{SiO}_2$  in the mixture. The mixture was then added slowly with continuous stirring to the sodium hydroxide solution and the nickel container was then placed in the autoclave vessel. The autoclave was assembled and heated to the required temperature. The solution was usually agitated at a speed of about 500 r.p.m.

On completion of an experiment the autoclave was cooled to about  $80^\circ\text{C}$  by allowing cold water to flow through the cooling coil before opening it. The nickel container was removed and the solution was immediately filtered by vacuum suction. An aliquot of the filtrate was taken, acidified with hydrochloric acid and then diluted to the required volume. The diluted solution was then analysed for aluminium and, in some cases, for calcium and iron contents. The solid residue was washed with cold, distilled water to remove any sodium hydroxide solution, dried at about  $110^\circ\text{C}$  and then cooled in a desiccator over unhydrated  $\text{CaCl}_2$ . The cool, dried residue, which was in

the form of very fine powder, was kept in sealed polythene bags until used.

The nickel container with reaction mixture was weighed before and after each experiment to allow for water distillation from the nickel container to the outer pressure vessel which took place during the leaching process. Any residue found on the stirrer or the cooling coil after the experiment was washed off, dried and weighed. From the weight change, appropriate corrections were made to the concentration of NaOH, etc. in solution. To improve heat transfer, a thin stainless steel cylindrical sheet was inserted between the nickel container and the autoclave vessel. This reduced the lag of temperature between the container and the autoclave body and helped to damp the solution temperature flocculation. In the presence of this sheet, the water distillation was reduced, but was not completely eliminated.

In the study of the mechanism of solid formation during the leaching process, small lumps of the minerals were treated under various leaching conditions. For this purpose, one face of a roughly cubic lump of the size of about 1-2 cm in length was finely polished. The polished lump was attached to the head of the autoclave agitator and rotated in the leaching solution with an average speed of about 500 r.p.m. At the end of the experiment the lump was taken off, washed with distilled water several times and dried at about 110°C. The reacted lump surface was then examined by different techniques.

#### 2.1.2 Chemical Methods of Analysis

Chemical analysis was used to characterize the different

aluminosilicate minerals examined and the products obtained from leaching experiments. Silica was determined by the gravimetric method. Sodium, calcium, aluminium and iron were determined by atomic absorption spectrophotometry. The apparatus used for these determinations was a Hilger and Watts Atomspek H 1170. Other constituents reported in this thesis were determined by the Analytical Services Laboratory Staff, Imperial College or taken from the manufacturers' specifications.

#### 2.1.2.1 Determination of Silica

An accurately weighed sample of the ground mineral was decomposed by fusion with anhydrous sodium carbonate in a platinum crucible. The contents were then transferred to a basin and neutralized with HCl. In the case of sodium calcium hydrosilicate, it was readily decomposed in hot, concentrated HCl without fusion. The solution was evaporated to dryness twice, then equivalent volumes of concentrated HCl and distilled water were added. The residue was filtered off, dried and heated to bright redness to dehydrate the silica. After cooling, the crucible was weighed. Hydrofluoric acid was added to the contents with 5 drops of conc.  $H_2SO_4$  followed by evaporation and heating to bright redness. The crucible was then weighed. The difference between this weight and the preceding one represented the silica.

#### 2.1.2.2 Determination of Aluminium

Atomic absorption spectrophotometry for aluminium was tested in the range 0 to 1000 ppm Al. It was found that the optimum working

range was 20 to 200 ppm Al. in aqueous solutions using a nitrous oxide - acetylene flame at a wave length of  $3093 \text{ \AA}^{\circ}$ . The influence of sodium, calcium, and iron on aluminium determination was investigated. Addition of sodium chloride had no effect on the determination of aluminium but the addition of sodium hydroxide (2000 - 3000 ppm Na) enhanced aluminium absorption. Calcium and iron had negligible effect in acidic solutions, but they did interfere in an alkaline medium.

Solutions containing the total aluminium content of the minerals were prepared by fusing the mineral with sodium carbonate, removing the silica by HCl precipitation and diluting the acidic solution to the required volume. These solutions were compared against standard acidic, aluminium solutions containing similar quantities of sodium chloride. The solutions obtained from the autoclave tests were made acidic with HCl, diluted to the required volume (two separate portions being used and diluted to different extents), and determined in a similar manner.

The aluminium determination results by this method were reproducible within  $\pm 2\%$  for both mineral samples and leach solutions. The addition method was tried on solutions from both mineral samples and leach solutions. Known quantities of aluminium were added to the unknown solution and the solution was analysed for Al before and after the addition. In all cases the difference between the two readings was exactly equivalent to the quantity of aluminium added to the solution.

### 2.1.2.3 Determination of Sodium

Flame emission photometry and atomic absorption spectrophotometry were tested for the determination of sodium. In the flame emission photometric method calcium and silicon interfered with the results. The interference of calcium could be suppressed by the addition of  $\text{Al}(\text{NO}_3)_3 \cdot 9\text{H}_2\text{O}$  in the ratio of 25:1 with respect to calcium<sup>(119)</sup>. In atomic absorption spectrophotometry calcium, iron, or aluminium did not interfere in the determination of sodium. In this study sodium determinations were made by means of atomic absorption spectrophotometry. This method was found to be superior to flame emission photometry in accuracy and sensitivity and in that reproducible results were obtained. The optimum working range was found to be 0 to 5 ppm Na in aqueous solutions using an air-acetylene flame at a wave length of  $5890 \text{ \AA}$ . The determination could also be carried out in the range 100 to 500 ppm Na at a wave length of  $3302 \text{ \AA}$ .

Solutions from the different minerals were prepared by repeated treatment of a weighed sample with  $\text{HF}-\text{H}_2\text{SO}_4$  mixture and evaporation to dryness. The contents were then dissolved by HCl, diluted to the required volume and compared against standard sodium solutions. Leaching residues were readily decomposed by hot, conc. HCl. After silica filtration, the filtrate was diluted to the required volume and analysed.

### 2.1.2.4 Determination of Calcium

A flame emission photometric method was tested for calcium. The influence of addition of sodium, aluminium, and silicon on the results was studied. The presence of sodium in small amounts had a

slight effect on the results, but large amounts of sodium seriously interfered. Aluminium also interfered and its effect increased with the aluminium concentration. Erratic results were obtained in the presence of silicon. Neither the addition of EDTA nor that of lanthanum chloride improved the results. Hence this method was abandoned.

Atomic absorption spectrophotometric analysis was tested in the concentration range 0 to 50 ppm Ca. The presence of sodium (as chloride) up to 1000 ppm Na had only a slight effect on the results. On the other hand, addition of sodium hydroxide seriously effected the results and in some cases erratic results were obtained. Aluminium and silicon interfered seriously in the calcium determination. In an attempt to prevent the interference of sodium, aluminium, and silicon; magnesium nitrate and perchloric acid, EDTA, and lanthanum chloride were added to the solutions separately. Neither the addition of magnesium nitrate and perchloric acid nor that of EDTA improved the results. Addition of lanthanum chloride (1% La) prevented the interference of sodium, aluminium and silicon, and enabled calcium to be determined in the presence of these substances. The addition of lanthanum chloride, however, enhanced the absorption of calcium. This enhancement increased with the concentration of lanthanum chloride and it was necessary to add the same amounts (1% La) to all the standards and the unknown solutions. The optimum working conditions for the calcium determination were found to be in the range 0 to 10 ppm Ca in aqueous acidic solutions containing 1% La and using air-acetylene flame at a wave length of  $4227 \text{ \AA}$ . Solutions for calcium determination were

prepared as described under aluminium determination, but in the final step of dilution lanthanum chloride was added so that the final concentration of lanthanum was 1%. These solutions were compared against standard, acidic calcium solutions containing similar quantities of sodium chloride and lanthanum chloride. The addition method, described under aluminium determination, was tried with calcium determinations. As in the case of aluminium, the recovery of the added calcium was always 100%.

#### 2.1.2.5 Determination of Iron

Atomic absorption spectrophotometry was tested for iron determination in the concentration range 0 to 40 ppm Fe, and the influence of addition of sodium, calcium, aluminium and silicon on the results was studied. Small amounts of sodium and calcium had a slight effect on the results. In the presence of large amounts of sodium (more than 200 ppm Na) or calcium (more than 50 ppm Ca) no interference occurred. Aluminium and silicon did interfere, but the addition of excess calcium prevented that. Lanthanum chloride did not prevent the interference of aluminium and silicon. It was found that the optimum working conditions for iron determination were in the range of 2 to 20 ppm Fe in aqueous, acidic solutions using an air-acetylene flame at a wave length of 2483 Å. Solutions were prepared as already described under aluminium determination.

#### 2.1.3 Thermo-analytical Methods

##### 2.1.3.1 Differential Thermal Analysis

Differential thermal analysis was mainly used to characterize

the autoclave leaching products. The investigations were carried out with a Bolton's DITA differential thermal analysis apparatus. The sample holder was made of stainless steel with chromel-alumel thermocouples located in the two wells for measurement of the sample temperature and the differential temperature. Calcined alumina was used as the inert reference material. Equal weights of the sample and alumina were moistened with acetone and ground together in a small agate mortar to obtain a uniform mixture. After drying, the mixture was placed in one well and calcined alumina in the other and packed. The tests were conducted under atmospheric conditions with a heating rate of about  $10^{\circ}\text{C} / \text{min}$ .

#### 2.1.3.2 Thermogravimetric Analysis

Thermogravimetric analysis was mainly used for the characterization of the autoclave leaching solid products and for the study of some of the properties of sodium calcium hydrosilicate. Measurements were made using a Stanton's Massflow thermobalance model MF-H5 with an alumina crucible. Some experiments were carried out under atmospheric conditions and others in a stream of nitrogen or carbon dioxide gas. The heating rate was about  $6^{\circ}\text{C} / \text{min}$ . in all the tests run.

#### 2.1.4 X-ray Powder Diffractometry

X-ray powder diffractometry was mainly employed for the characterization of the different mineral samples used and for the identification of the autoclave leaching residues. Charts of the diffraction patterns of the different minerals and leaching products



were obtained by means of a Philips PW 1310 X-ray Diffractometer. The  $2\theta$  values were read directly from the chart and the corresponding d-spacings were calculated using the X-ray conversion tables<sup>(120)</sup>. The intensities were estimated from the heights of the emission peaks.

A Guinier camera was used to produce X-ray powder diffraction films for solid products formed on reacted mineral lump surfaces. The d-spacings were read directly from the film by means of a graduated overlay, and the intensities were estimated.

The interpretation was made by reference to the A.S.T.M. Index<sup>(121)</sup> except where otherwise stated.

#### 2.1.5 Electron-Probe X-ray Microanalysis

A Cambridge "Geoscan" electron-probe microanalyser was used for the characterization of the different natural mineral samples and for the examination of the product layers formed on the surface of mineral lumps treated in the autoclave under various conditions. Natural mineral samples were examined using a polished or thin section of the mineral. To examine the reacted mineral lumps, after autoclave treatment they were covered with a thin layer of clear araldite to protect the product layer formed. The lumps were then cut perpendicular to the previously polished surface, moulded in araldite and graphite powder and the newly cut surface was polished and coated with carbon. This surface was examined by X-ray line scan in the electron-probe microanalyser to follow any changes in composition between the original mineral and the product layer on the mineral.

### 2.1.6 Scanning Electron Microscopy

Scanning electron microscopy was used to examine the reacted mineral lump surfaces and the product layer formed on them. The reacted mineral lumps were covered with a thin metallic coating before examination. The investigations were made by means of a Cambridge "Stereoscan" scanning electron microscope. Pictures of the desired areas were taken using a 35 mm. camera attached to the microscope.

### 2.1.7 Optical Microscopy

Optical microscopic examinations were mainly employed to characterize the different mineral samples used in this study. It was also used for the identification of the solid products obtained from autoclave leaching experiments.

The examinations were carried out by means of a Ziess Ultraphot microscope. Thin sections of the natural minerals were prepared and examined under transmitted light.

The solid reaction products from leaching tests were in the form of very fine powder. A small sample of the residue was placed on a glass slide, moistened with a few drops of alcohol and dispersed by means of a glass rod. When dry, the dispersed sample was covered with a drop or two of immersion oil and then examined under transmitted light.

## 2.2 Experimental Materials

### 2.2.1 Natural Minerals

The mineral samples used in this work which included feldspars of different compositions, mica, kyanite, quartz and clays, were

obtained from various sources. They were characterized by chemical analysis, X-ray powder diffraction, electron-probe X-ray microanalysis and optical microscopy. The following is a brief description of these minerals and of the methods used for preparing them for the leaching experiments.

#### 2.2.1.1 Albite

Large pieces of a Norwegian albite sample was provided by R.F.D. Parkinson Co., Somerset, England. The sample was composed of white cleavable crystalline lumps with quartz and clay material inclusions.

A thin section of the sample was examined by optical microscopy and electron-probe microanalysis. Optical examination showed that it was mainly sodium-rich feldspar with occasional quartz and sericite inclusions. There was also a few scattered small calcite particles. Electron-probe microanalysis confirmed that the main phase was sodium feldspar, with quartz inclusions of up to 100 microns in length. Line and area scans showed that the silicon, aluminium, and sodium contents hardly varied throughout the feldspar matrix. A little calcium could be detected in a few grains of the size 10 to 20 microns, but there was no potassium, iron, or titanium in the sample matrix. X-ray diffraction pattern of an acid-cleaned representative sample of the mineral was in good agreement with that of low-albite (A.S.T.M. Card No. 9-466). The most characteristic maxima of quartz were detected. The acid-cleaned representative sample was also analysed chemically for the major constituents and

the results of analysis are given in Table 7.

After characterization, the whole mineral sample was crushed in a jaw crusher to  $-\frac{1}{4}$  inch and any quartz particles were handpicked and discarded. The crushed sample was then tumbled in a ball mill (without the balls) with water for about 30 min. then sieved on a 100 mesh screen. The undersize, composed mainly of slimes and clay material, was discarded. A few lumps of the oversize were retained for future use and the rest of the sample was ground in a rotating disc pulverizer to pass 72 mesh screen and the oversize was returned for further grinding. The  $-72$  mesh fraction was classified into various size fractions. Each fraction was separately washed with water and then agitated with hot 20% HCl for 30 min. The acid was poured off and the sample was washed with distilled water by beaker-decantation till the pH of the washing water was identical with that of distilled water. The different size fractions were then dried at about  $120^{\circ}\text{C}$  and after cooling kept in sealed polythene bags until required.

All the mineral samples used in this work were cleaned in a similar manner before leaching experiments except clays which were used directly as received, and mica which was only ground and classified to different size fractions.

#### 2.2.1.2 Oligoclase

Large lumps of oligoclase sample from Setersdal, Norway were used. The sample was composed of coarse white to pink crystals with large inclusions of quartz and mica. There were also some dark, fine

particles scattered in the matrix. Optical microscopic examination showed that the mineral was mainly oligoclase feldspar. Electron-probe microanalysis showed that the feldspar contained sodium, calcium, aluminium and silicon in one phase. The aluminium and silicon contents were uniform throughout the mineral. The sodium content was higher than that of calcium and it was almost constant throughout the matrix. The calcium content was, in general, low but there were some areas with higher concentrations. These areas were, however, small and not very common. Potassium was almost absent except for occasional inclusions of small grains (about 10 to 30 microns) where it replaced sodium. Occasional fine grains containing iron and titanium only were detected in the main matrix.

Clean handpicked pieces of the mineral were ground to - 200 mesh and analysed chemically and by X-ray powder diffraction. The results of chemical analysis, given in Table 7, were in agreement with the composition of oligoclase feldspar usually reported in the literature<sup>(122)</sup>. The X-ray diffraction pattern was in good agreement with that of oligoclase (A.S.T.M. Card No. 9-457). The most characteristic maxima for quartz were detected.

The whole mineral sample was crushed to -  $\frac{1}{4}$  inch and quartz and mica particles were handpicked and discarded. Further treatment and cleaning steps were carried out as described under albite. After drying and cooling the acid-cleaned sample, any magnetic material was separated from the mineral by means of a "quick-release" hand magnet. Chemical analysis of a representative sample of the cleaned

Table 7. Chemical analysis of albite and oligoclase samples.

Constituent	Albite	Oligoclase (picked pieces)	Oligoclase (bulk sample)
SiO <sub>2</sub>	70.48	63.31	73.32
Al <sub>2</sub> O <sub>3</sub>	17.10	22.96	15.36
Na <sub>2</sub> O	8.08	6.88	6.5
K <sub>2</sub> O	0.70	1.18	N.D.*
CaO	0.38	1.95	2.44
Fe <sub>2</sub> O <sub>3</sub>	0.26	0.24	N.D.*
TiO <sub>2</sub>	Traces	0.03	N.D.*

\* N.D. = not determined

mineral (Table 7) showed that it contained more free quartz than the handpicked specimen. This result was confirmed by the X-ray diffraction pattern of the sample. No further attempts were made to separate the free quartz from the mineral sample.

#### 2.2.1.3 Andesine

The mineral sample used was white massive lumps of feldspar rock from Kragero, Norway. Optical microscopic examination showed that the sample was mainly plagioclase feldspar with fine sericite particles embedded in the matrix. There were also inclusions of quartz and ilmenite. Electron-probe microanalysis showed that the feldspar sample contained sodium, calcium, aluminium and silicon but there were two distinct phases: a) a calcium-rich phase, and b) a sodium-rich phase. The silicon content was higher and the aluminium content was lower in the sodium-rich phase than in the calcium-rich one. Potassium was found in fine occasional particles. There were also rare inclusions of iron-bearing grains in the matrix.

The mineral lumps were crushed and cleaned as described under albite. X-ray diffraction pattern of the acid-cleaned sample was in good agreement with that of andesine (A.S.T.M. Card No. 10-935). The strongest lines for sericite were also shown on the X-ray diffraction pattern of the sample. Results of chemical analysis of the major constituents in the sample are given in Table 8.

#### 2.2.1.4 Labradorite

Large pieces of a dark pink feldspar sample, of Norwegian origin, were used. The coarse crystals of the feldspar had scattered, white

and black impurity inclusions. Optical examination of a thin section showed that the main phase in the feldspar was an intermediate plagioclase with a little free quartz and occasional inclusions of fine haematite, ilmenite or mica particles. Electron-probe microanalysis showed that the feldspar matrix was mainly of one homogeneous phase containing sodium, calcium, aluminium and silicon. The aluminium and silicon contents were almost constant throughout the matrix. The sodium content was uniform, but it was lower in some areas than the rest of the sample where the calcium content was higher than average. There were some grains of about 30 to 50 microns in length which contained potassium. The iron-containing particles were mainly haematite, but in some cases contained calcium and silicon besides iron.

The mineral lumps were crushed, screened and the different size fractions cleaned with acid followed by magnetic separation as described under albite and oligoclase. A representative sample of the cleaned mineral was analysed chemically and by X-ray diffraction. Results of chemical analysis are given in Table 8. The X-ray diffraction pattern of the sample was in good agreement with that of labradorite (A.S.T.M. Card No. 9-465). The most characteristic maxima for quartz also appeared on the X-ray diffraction pattern of the mineral sample.

#### 2.2.1.5 Anorthosite

Large lumps of white crystalline anorthosite from Ilse of Harris, Herbides, were obtained from P.E. Hines Co., Stoke-on-Trent, England. The white mineral crystals had inclusions of quartz, mica and fine



Table 8 Chemical analysis of some feldspar samples

Constituent	Andesine	Labradorite	Anorthosite	Microcline
SiO <sub>2</sub>	56.4	56.2	48.6	65.52
Al <sub>2</sub> O <sub>3</sub>	25.96	26.74	29.8	17.48
Na <sub>2</sub> O	7.3	5.3	2.58	4.18
K <sub>2</sub> O	0.36	-	0.1	9.63
CaO	9.68	12.2	14.7	-
Fe <sub>2</sub> O <sub>3</sub>	0.32	1.15	1.35	0.51
TiO <sub>2</sub>	trace	-	0.1	0.03

dark hematite particles. Optical microscopic examination showed that the mineral was composed of relatively fine crystals of plagioclase feldspar with frequent quartz particles. Electron-probe microanalysis by X-ray area and line scans of a polished mineral surface showed that the mineral was composed of three main phases: a) a calcium-bearing phase, b) a sodium-bearing phase, and c) free quartz particles distributed between the other two phases. The particle size of the grains varied from about 20 to 200 microns in length. The calcium feldspar phase was more predominant and had larger grains than the sodium feldspar phase. The silicon and aluminium contents were uniform in one particular phase, but the aluminium content was higher and that of silicon was lower in the calcium feldspar phase than in the sodium feldspar phase. Generally there was no calcium in the sodium feldspar nor sodium in the calcium feldspar. The distribution of the three phases was not uniform throughout the mineral sample. Two distinct parts could be easily detected: i) Large areas with large grains mainly of calcium feldspar with some sodium feldspar particles. In these areas there was very little or no free quartz. ii) Smaller areas composed of fine intergrowth of quartz, calcium feldspar and sodium feldspar particles.

The mineral lumps were crushed and screened. The different size fractions were cleaned by acid and magnetic treatments. A sample was analysed chemically and by X-ray powder diffraction. The sample gave an X-ray diffraction pattern very close to that of

anorthite (A.S.T.M. Card No. 12-301). The maxima for quartz were also detected on the chart. The results of chemical analysis are given in Table 8.

#### 2.2.1.6 Microcline

A sample from Pikes Peak District, Colorado, U.S.A., was used in this study. It was in the form of large red cleavable crystalline pieces. Crystallo-optical examination showed that the sample was almost pure microcline with microperthetic texture. A few fine quartz inclusions were present but no other impurities. Electron-probe microanalysis confirmed the microperthetic structure of the mineral. It showed that the mineral was composed of two distinct phases: a) a potassium feldspar phase, and b) a sodium feldspar phase. The potassium feldspar was the predominating phase in the mineral and was usually large grained. The grain size was in the range 50 - 100  $\mu\text{m}$ . The aluminium and silicon contents hardly varied throughout the mineral. Sodium and potassium replaced each other in the matrix. Rarely calcium could be detected in the mineral sample.

The mineral sample was crushed, cleaned and prepared for leaching experiments as already described. X-ray diffraction pattern of the acid-cleaned mineral sample showed that it was mainly microcline (A.S.T.M. Card No. 10-479) with some albite of low-albite structure. Results of chemical analysis of the mineral sample are given in Table 8.

#### 2.2.1.7 Muscovite Mica

A muscovite sample of unknown origin was used. It was in the form of large transparent light brown sheets. Electron-probe

microanalysis showed that it was almost pure potassium aluminium silicate. The contents of these three elements were uniform throughout the mineral sample. Sodium was present in very low quantities, and calcium, magnesium and iron were virtually absent. X-ray diffraction pattern of the ground sample was in agreement with that of muscovite (A.S.T.M. Card No. 6-0263). No other phases were detected. Chemical analysis of the sample showed that the  $\text{SiO}_2$  content was 46.64% and the  $\text{Al}_2\text{O}_3$  content was 33.59%.

The mineral sheets were ground to - 72 mesh in an agate vibrating ring mill (Tima mill) and then classified into different size fractions. No further cleaning steps on the mineral sample were carried out.

#### 2.2.1.8 Kyanite

Large pieces of a Kenyan crystalline kyanite mineral were used. The crystals were silvery-blue in appearance and occurred in clusters associated with quartz inclusions. Closer examination of the mineral by optical microscopy and electron-probe microanalysis showed that it contained thin mica bands besides the quartz inclusions. Occasional rutile particles were scattered in the matrix. The particle sizes of quartz and of kyanite grains were of the order of 0.5 to 2 mm and those of rutile grains roughly 100 to 500 microns. The silicon and aluminium contents in the kyanite grains were very uniform with no other elements present.

Clean pieces were handpicked and any inclusions of quartz or mica were removed. Because of the brittle nature of the mineral,

comminution was carried out in an iron mortar and pestle. The broken material was screened through a 36 mesh screen, the oversize being returned to the mortar. The - 36 mesh mineral fraction was classified into different size fractions by further screening. The - 100 mesh fraction, containing considerable amounts of mica and slimes, was discarded. Further cleaning of the other fractions was necessary to remove any mica or rutile present. This was done by repeated treatment of each size fraction on the super paner. The clean mineral sample was then ground to - 72 mesh and screened. The final cleaning steps were carried out as already described under albite. X-ray diffraction pattern of the clean mineral sample was in agreement with that of kyanite (A.S.T.M. Card No. 11-46). The most characteristic maxima for quartz were detected in the X-ray diffraction pattern of the sample. Chemical analysis of the sample showed that it contained 38.78%  $\text{SiO}_2$  and 59.91%  $\text{Al}_2\text{O}_3$ .

#### 2.2.1.9 Clays

Four clay samples, with different alumina and kaolinite contents, were used. A sample of white paper clay of the "Supreme" grade was obtained from English Clays Co., Cornwall, England and three different ball caly samples were obtained from Mr. R. Best, Geology Department, Imperial College. The chemical analysis of the four clays, and the specifications of the three different ball clays are given in Tables 9-11. Supreme clay was 80% finer than 1 micron. In order to determine the major constituents, i.e. silica and alumina, chemical analysis was carried out on the four clay samples. The results of the analysis agreed with the values given in Table 9 within the

Table 9. Chemical analysis of the clay samples.  
(manufacturers' specifications)

Constituent	Supreme Clay	Ball Clays		
		No. 661	No. 935	No. 961
SiO <sub>2</sub>	46.61	52.41	62.30	53.80
Al <sub>2</sub> O <sub>3</sub>	38.3	32.32	24.60	31.70
Fe <sub>2</sub> O <sub>3</sub>	0.49	1.07	1.05	1.14
TiO <sub>2</sub>	0.05	1.10	1.46	1.11
MgO	0.2	0.16	0.32	0.30
CaO	0.2	0.21	0.15	0.22
K <sub>2</sub> O	0.68	1.56	2.24	2.21
Na <sub>2</sub> O	0.07	0.22	0.23	0.33
L.O.I.	13.43	10.71	7.00	9.41
Total	100.03	99.76	99.35	100.22

Table 10. Rational analysis (mica convention) of the different ball clay samples (manufacturers' specifications)

Component	No. 661	No. 935	No. 961
Clay substance	66.2	41.2	57.9
Micaceous matter	16.1	21.9	22.8
Quartz	14.4	33.2	16.4
Ferric oxide	1.1	1.1	1.1
Lime	0.2	0.2	0.2
Titania	1.1	1.5	1.1
Magnesia	0.2	0.3	0.3
Carbonaceous matter by difference	0.7	0.3	0.4

Table 11. Particle size analysis of the different ball clay samples  
(manufacturers' specifications)

% finer than given Equivalent Spherical Diameter	No. 661	No. 935	No. 961
5 $\mu$ m	89	75	97
2 "	75	61	89
1 "	62	48	79
0.7 "	54	41	73
0.5 "	45	33	65
0.3	30	22	49
0.2	19	14	32



experimental error.

The four clay samples were examined by X-ray powder diffraction. The pattern for supreme clay showed that the sample was composed of kaolinite (A.S.T.M. Card No. 14-164). No quartz, sericite or mica were detected. The patterns for the different ball clays showed that they were composed of various proportions of three main phases: a) kaolinite, b) quartz, and c) mica.

#### 2.2.1.10 Quartz

Large pieces of crystalline quartz from Granite Mountain, Foxdale, Isle of Man were used. The mineral was of clear white crystals with little mica inclusions. Optical examination and electron-probe microanalysis showed that it was almost pure quartz. Clean handpicked pieces were crushed, classified, and cleaned as already described. X-ray diffraction pattern of the cleaned mineral confirmed that it was pure  $\alpha$ -quartz (A.S.T.M. Card No. 5-0494) with no other phases. Chemical analysis of the cleaned sample showed that it contained more than 99.6%  $\text{SiO}_2$ .

#### 2.2.2 Synthetic Minerals

In the early stages of this work it was proposed to carry out the initial leaching studies on synthetic materials in order to avoid excessive time and expense in collecting, purifying and characterizing naturally occurring minerals. Attempts were made to synthesize pure albite and anorthite by the hydrothermal method proposed by Barrer and White<sup>(123)</sup>.

Limited success was achieved in obtaining the required crystal

size of about 100 microns. Crystals of this size were a minor product in albite synthesis; no crystals of anorthite of this size were obtained. In all synthetic experiments done, no pure feldspar phase was obtained. The optimum conditions for the synthesis of a pure crystalline phase by this method do not seem to be well established and more investigations would be required before any satisfactory results could be obtained. Due to the uncertainty of obtaining the required synthetic materials in a reasonable time, this method was abandoned and leaching studies were carried out on natural materials only.

### 2.2.3 Other Materials

Commercial flakes of sodium hydroxide were used for the different leaching experiments unless where otherwise specified. Calcium oxide powder of grade G.P.R., low in sulphur and chlorine was used to blend the mineral samples to obtain the desired  $\text{CaO/SiO}_2$  molar ratio. Chemical analysis showed that it contained about 97 to 98% CaO.

Other chemicals used in this study were of 'ANALAR' grade reagents unless otherwise stated.

C H A P T E R 3

PRELIMINARY STUDIES

### 3.1 Preliminary Leaching Studies

Leaching tests were carried out on a Norwegian labradorite sample to study the effect of different factors on its reactivity (i.e. the readiness with which it is decomposed) in concentrated sodium hydroxide solutions under the conditions of the hydrochemical alkaline method and to determine the optimum leaching conditions for alumina extraction by this method. The characteristics and chemical composition of this mineral and the process of its preparation for the leaching tests have already been described in section 2.2.1.4.

The effect of mineral particle size, sodium hydroxide concentration, leaching temperature, time of leaching and the effect of addition of calcium oxide on the reactivity of the mineral, on the alumina recovery from it, and on the nature of the products formed were investigated. The experiments were carried out in 500 ml batches of solution with a calculated final caustic ratio, i.e.  $\text{Na}_2\text{O}/\text{Al}_2\text{O}_3$  molar ratio in the product solution, of about 30 (on the assumption of complete alumina extraction into solution). The high value of 30 was chosen so that the alumina content in the solution would be far below its solubility limits and so that the sodium hydroxide concentration would be virtually constant while studying the other factors. The effect of the calculated final caustic ratio on the alumina recovery from aluminosilicate minerals is considered later in section 4.1.4.

### 3.1.1 Effect of Particle Size

The effect of particle size of the mineral on its reactivity and on alumina extraction was studied. For this purpose different mineral size fractions in the range -52 mesh to -200 mesh were intimately mixed with the required amounts of calcium oxide powder to obtain a  $\text{CaO}/\text{SiO}_2$  molar ratio of 1.1 in the mixture. The mixtures were then treated in solutions containing 400 g/l NaOH at a leaching temperature of 275°C for 20 min. The residues obtained at the end of the experiments were examined by optical microscopy, X-ray powder diffraction and, in some cases, by chemical analysis. The leach solutions were analysed for aluminium. The results obtained for the different size fractions are given in Table 12. They showed that between -72 mesh and -200 mesh, particle size

Table 12. Effect of particle size on the alumina extraction from labradorite and on the residue formed when treated in 400 g/l NaOH solution at 275 for 20 min.

Particle Size, mesh	Alumina recovery		Length of phase I* crystals X their width, $\mu\text{m}$
	g/l	%	
-52 + 72	13.41	90.1	(35 - 65) x (10 - 20)
-72 + 100	14.54	95.76	(25 - 40) x (5 - 15)
-100 + 150	14.64	98.67	(30 - 45) x (10 - 15)
-200	14.68	98.93	(20 - 30) x (7 - 10)

\*Phase I is sodium calcium hydrosilicate

had little effect on the alumina extraction. The limiting value was obtained with the -100 + 150 mesh size fraction.

Within the size fraction -52 + 72 mesh, some of the mineral remained unreacted in the residue. Elongated prismatic crystals were the main phase in this residue with some unconverted calcium hydroxide (see Figure 4-b). The elongated prismatic crystals were found to be sodium calcium hydrosilicate. The residues obtained from samples finer than 72 mesh were composed of sodium calcium hydrosilicate crystals with small amounts of free calcium hydroxide. No unreacted mineral grains were found in these residues. The size of sodium calcium hydrosilicate crystals in the residues increased with the particle size of the mineral used. Thus with a -200 mesh size fraction, the crystals formed averaged about 25 microns in length and about 10 microns in width; while with a -52 + 72 mesh size fraction the crystals were about 50 x 15 microns (Table 12).

### 3.1.2 Effect of Leaching Time

The time of leaching was taken as the period during which the reaction mixture was held at the required temperature after heating from room temperature. The time required to heat the autoclave to this temperature varied. In this series of tests, where the old autoclave was employed, the time required to reach 275°C was about one hour. With the new autoclave the heating rate was slower and the time required to reach 280°C from room temperature varied between 75 and 90 min.

The effect of time of leaching on the reactivity of labradorite

was determined on a -72 + 100 mesh size fraction in 400 g/l NaOH solution and with a CaO/SiO<sub>2</sub> molar ratio equals 1.1 at a temperature of 275°C.

The results represented in Table 13 showed that the limiting extraction was reached in about 20 min. The residues obtained had sodium calcium hydrosilicate as the main phase with some free calcium hydroxide. Longer times of leaching caused a slight reduction in the size of sodium calcium hydrosilicate crystals in the residues (Table 13).

Table 13. Effect of leaching time on alumina extraction from labradorite and on the residue formed in 400 g/l NaOH solution at 275°C.

Leaching time, min.	Alumina recovery		Length of phase I crystals X their width, μm
	g/l	%	
5	13.41	90.1	(30 - 40) x (6 - 10)
10	14.35	95.76	(30 - 50) x (7 - 10)
20	14.54	98.04	(25 - 40) x (5 - 7)
30	14.64	98.93	~ 20 x 5

### 3.1.3 Effect of Leaching Temperature

The effect of the leaching temperature on labradorite reactivity was studied in the range 200 to 290°C using a -100 + 150 mesh size fraction of the mineral with a CaO/SiO<sub>2</sub> molar ratio of 1.1 in a solution

containing 400 g/l NaOH for a leaching time of 30 min.

The extraction of alumina increased rapidly with temperature from 200 to 240°C (Table 14). At temperatures above 240°C, the alumina extraction increased steadily with temperature at a reduced rate and was complete at 280°C. Above 280°C no significant change in the results was observed.

Table 14. Effect of leaching temperature on alumina recovery from labradorite and on the product formed in 400 g/l NaOH solution for 30 min of treatment.

Leaching temp., °C	Alumina recovery		Length of phase I crystals X width, µm
	g/l	%	
200	12.47	83.2	(25 - 40) x (10 - 15)
240	14.35	95.8	(40 - 50) x (15 - 20)
265	14.54	98.0	(30 - 50) x (5 - 10)
275	14.64	98.7	(20 - 25) x (5 - 10)
280	14.92	100.3	(20 - 25) x (5 - 7)
290	14.91	100.3	(15 - 25) x (5 - 7)

The residue obtained from treatment at 200°C contained sodium calcium hydrosilicate crystals, free calcium hydroxide and occasional unreacted mineral particles. Residues obtained at temperatures of 240°C and above had no unreacted mineral particles and were composed of sodium calcium hydrosilicate crystals as the main phase with small amount of free calcium hydroxide.



### 3.1.4 Effect of Sodium Hydroxide Concentration

The effect of the concentration of sodium hydroxide in the leaching solution on the reactivity of the mineral and the nature of the products was studied in the range 200 to 600g/l NaOH on a -72 + 100 mesh size fraction and with CaO/SiO<sub>2</sub> molar ratio equals to 1.1. The tests were carried out at a leaching temperature of 275°C for 30 min.

The results showed that the recovery of alumina from the mineral increased rapidly with increasing sodium hydroxide concentration from 200 g/l to 300 g/l NaOH and at a reduced rate above 300 g/l NaOH (Table 15). There was no significant effect of concentration on the extraction above 500 g/l NaOH.

Table 15. Effect of sodium hydroxide concentration on the alumina recovery from labradorite when treated at 275°C for 30 min.

NaOH concn.		Alumina recovery		Length of phase I crystals X their width, μm
NaOH g/l	Na <sub>2</sub> OHg/l	g/l	%	
200	155	6.23	83.2	(20 - 40) x (10 - 15)
300	232.5	10.39	92.3	(20 - 30) x (5 - 10)
400	310	14.64	98.7	(15 - 25) x (5 - 7)
500	387.5	19.26	102.6	(10 - 25) x (3 - 7)
600	465	22.91	101.7	(10 - 20) x (3 - 5)

The residue formed in 200 g/l NaOH solution contained small amounts

of sodium calcium hydroaluminosilicate (phase III in Figure 2, section 1.1) and free calcium hydroxide beside the main phase of sodium calcium hydroxide. Occasional unreacted mineral grains were also found in the residue. With a solution concentration of 300 g/l, the unreacted mineral grains were absent and the proportions of sodium calcium hydroaluminosilicate and free calcium hydroxide in the precipitate decreased. Sodium calcium hydrosilicate was the only phase in the residues obtained from solution concentrations of 400 g/l NaOH and more. The increase of solution concentration was accompanied by an increased dispersion of sodium calcium hydrosilicate crystals in the residue (Table 15).

### 3.1.5 Effect of Addition of Calcium Oxide

The effect of addition of varying amounts of calcium oxide and the molar ratio of  $\text{CaO}/\text{SiO}_2$  in the pulp on the recovery of alumina from labradorite and on the solid products formed was investigated. Varying quantities of calcium oxide powder were intimately mixed with a constant weight of the -200 mesh size fraction of the mineral and the mixture was then added to the leaching solution. The leaching tests were carried out in solutions containing 500 g/l NaOH at a temperature of  $280^\circ\text{C}$  for 30 min.

The results showed that the degree of alumina extraction increased rapidly with increase of the molar ratio of  $\text{CaO}/\text{SiO}_2$  in the mixture (Table 16). The extraction reached a maximum when this ratio was 1.1. At  $\text{CaO}/\text{SiO}_2$  molar ratios higher than 1.1, a slight decrease in alumina recovery in solution was noticed.

Table 16. The Effect of addition of lime and the CaO/SiO<sub>2</sub> molar ratio on the recovery of alumina from 39.75 g labradorite treated in 500 g/l NaOH solution at 280°C for 30 min.

CaO added, g.	CaO/SiO <sub>2</sub> molar ratio	Alumina recovery	
		g/l	%
5.6	0.5	5.0	26.2
11.8	0.8	10.77	58.1
14.0	0.9	16.24	86.6
16.0	1.0	17.28	92.3
17.0	1.05	18.32	98.1
18.0	1.1	19.25	102.1
26.0	1.48	18.12	97.2

The leaching residues obtained from mixtures with CaO/SiO<sub>2</sub> molar ratios between 0.9 and 1.1 contained sodium calcium hydrosilicate crystals as the main phase. With the molar ratio CaO/SiO<sub>2</sub> of 0.9 and below, the residues contained sodium calcium hydroaluminosilicate and sodium hydroaluminosilicate (phase VI in Figure 2, section 1.1) and sodium calcium hydrosilicate in proportions depending on the quantities of lime added. Mixtures with CaO/SiO<sub>2</sub> molar ratios of 1.1 and above yielded sodium calcium hydrosilicate crystals together with varying amounts of free calcium hydroxide.

### 3.1.6 Leaching Residues

The precipitates which formed in all leaching tests carried out

on labradorite under different conditions were examined by optical microscopy, X-ray powder diffraction, differential thermal analysis (D.T.A.) and thermogravimetric analysis (T.G.A.) and in some cases by chemical analysis.

Microscopic examination showed that almost all the residues contained elongated prismatic crystals as the main phase (see figure 4). The size of these crystals varied according to the various leaching conditions (Tables 12-15). The residue obtained with 200 g/l NaOH solution contained fine tetrahedral crystals of sodium calcium hydroaluminosilicate and hexagonal platy crystals of calcium hydroxide beside the elongated prismatic crystals. Precipitates obtained from leaching experiments using a  $\text{CaO/SiO}_2$  molar ratio less than 0.9 contained three phases in varying proportions; a) elongated prismatic crystals; b) fine rounded crystals of sodium hydroaluminosilicate; and c) tetrahedral crystals of sodium calcium hydroaluminosilicate.

The X-ray diffraction patterns were very similar for all the precipitates, and particularly those with the elongated prismatic crystals as the main solid phase. The X-ray diffraction patterns for these residues were in agreement with the pattern assigned for sodium calcium hydrosilicate of the composition  $\text{Na}_2\text{O} \cdot 2\text{CaO} \cdot 2\text{SiO}_2 \cdot \text{H}_2\text{O}$  (57,62,124) which was similar to that obtained from the pure synthetic compound (see Table 18). The X-ray diffraction pattern for the residue formed in 200 g/l NaOH solution had in addition the strongest lines characteristic for sodium calcium hydroaluminosilicate (124,125,126).

The X-ray diffraction patterns for residues from leaching tests with  $\text{CaO/SiO}_2$  ratio less than 0.9 had the strongest lines for both sodium calcium hydroaluminosilicate and sodium hydroaluminosilicate (127) along with the pattern of sodium calcium hydrosilicate phase.

Differential thermal analysis of the different leaching residues gave patterns with a sharp endothermic effect between the temperatures 550 and 560°C. The D.T.A. curve obtained for the residue from the treatment of labradorite in 500 g/l NaOH solution with  $\text{CaO/SiO}_2$  molar ratio of 1.0 at 280°C for 30 min. is given in Figure 3. The other leach residues gave D.T.A. curves similar to that in the figure. The endothermic effect for the residues obtained from the studies on the effect of calcium oxide addition increased in prominence with the molar ratio of  $\text{CaO/SiO}_2$  in the reaction mixture up to a ratio of 1.0 after which the effect was constant. The differential thermal analysis for a -200 mesh size fraction of the original labradorite mineral gave a pattern with no thermal peaks when heated up to 1100°C.

The endothermic effect between the temperatures 550 and 560°C obtained with the leach residues was characteristic of sodium calcium hydrosilicate (57,71,124) and was due to its dehydration. This dehydration effect was confirmed by thermogravimetric analysis which gave a rapid loss of weight between the temperatures 510 and 590°C. The total weight loss for the residues varied between 5.6 and 6.0%.

Some of the leaching residues were analysed chemically for their major constituents. The results for four of these residues and that

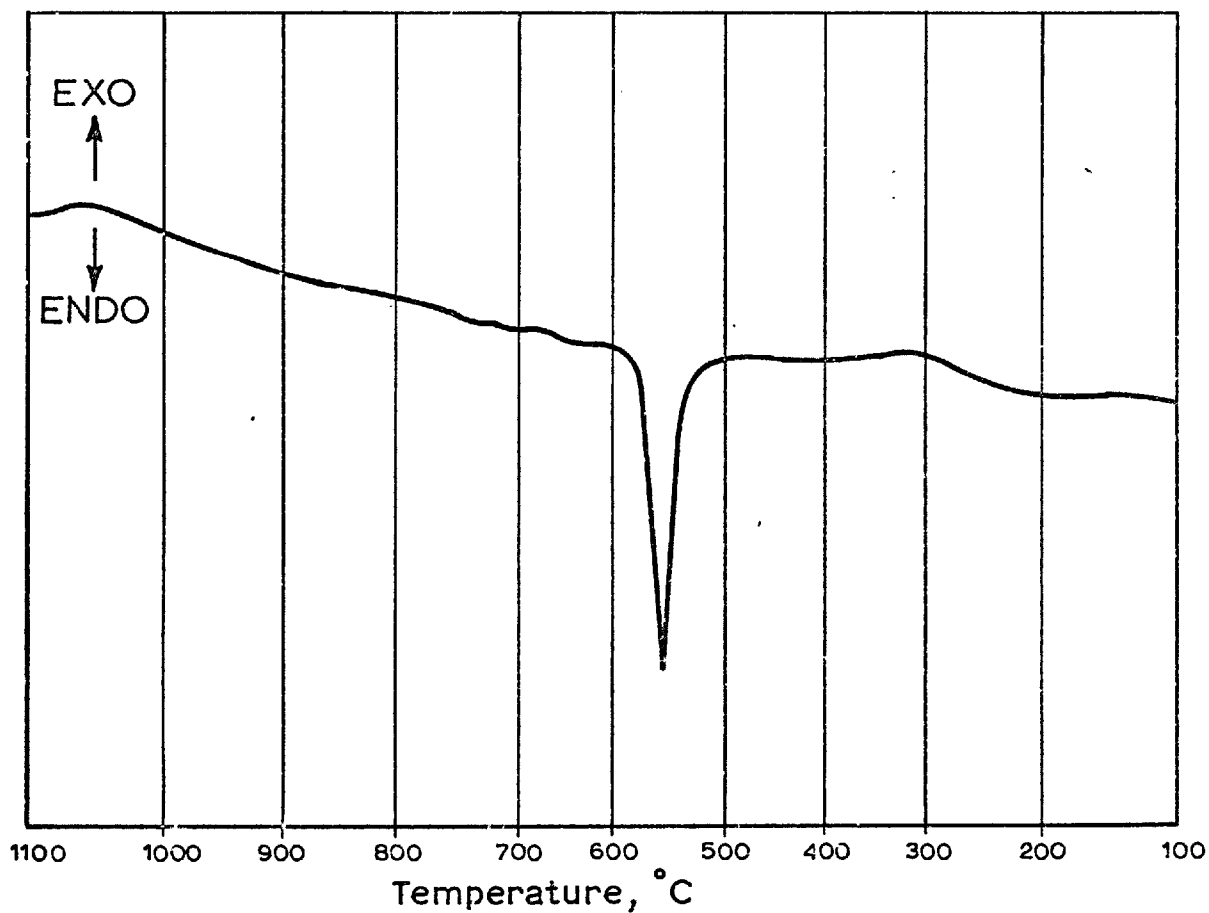


Figure 3. D.T.A. curve for leach residue from labradorite treated in 500 g/l NaOH with  $CaO/SiO_2 = 1.0$  at  $280^\circ C$  for 30 min.

for pure synthetic sodium calcium hydrosilicate are given in Table 17. The main constituents of the residues were  $\text{Na}_2\text{O}$ ,  $\text{CaO}$ ,  $\text{SiO}_2$  and  $\text{H}_2\text{O}$ . The alumina content in the residues was low in general and in particular in residues which had the elongated prismatic crystals of sodium calcium hydrosilicate as the main phase. The results of the chemical analysis showed that the composition of the leaching precipitates were similar to Table 17. Chemical analysis of synthetic sodium calcium hydrosilicate and some leaching residues from labradorite.

Constituents	Synthetic Compound	Residue 1	Residue 2	Residue 3	Residue 4
$\text{SiO}_2$	37.92	36.61	37.70	37.67	36.94
$\text{Na}_2\text{O}$	19.80	18.95	19.74	20.0	20.37
$\text{CaO}$	36.13	34.95	33.96	34.79	34.65
$\text{Al}_2\text{O}_3$	7	0.48	0.30	0.59	0.17
$\text{Fe}_2\text{O}_3$	-	0.78	0.04	0.78	0.73
L.O.I.	6.41	7.15	8.16	6.59	6.83
Total	100.26	98.92	99.90	100.42	99.69

Residues 1 and 2 were those obtained from -100 + 150 mesh size fraction treated in 400 g/l NaOH with  $\text{CaO}/\text{SiO}_2 = 1.1$  at  $275^\circ\text{C}$  for 20 and 30 min. respectively.

Residues 3 and 4 were those obtained from -200 mesh size fraction treated in 500 g/l NaOH at  $280^\circ\text{C}$  for 30 min. with  $\text{CaO}/\text{SiO}_2$  molar ratio of 1.0 and 1.05 respectively.

each other and to that of synthetic sodium calcium hydrosilicate which was very close to the theoretical composition of the compound  $\text{Na}_2\text{O} \cdot 2\text{CaO} \cdot 2\text{SiO}_2 \cdot \text{H}_2\text{O}$ .

The above series of leaching tests showed that labradorite could be decomposed in concentrated sodium hydroxide solutions at high temperatures and pressures and in the presence of a certain amount of lime. The liberated alumina from the mineral went into solution and calcium oxide reacted with silica to produce sodium calcium hydrosilicate of the composition  $\text{Na}_2\text{O} \cdot 2\text{CaO} \cdot 2\text{SiO}_2 \cdot \text{H}_2\text{O}$ . The optimum leaching conditions for alumina recovery from the mineral were; sodium hydroxide solutions containing about 500 g/l NaOH heated to a temperature of  $280^\circ\text{C}$  and a leaching time of about 20 min. The mineral should be ground to -100 mesh and mixed with calcium oxide powder in such amounts that the molar ratio of  $\text{CaO}/\text{SiO}_2$  in the mixture would be 1.1. Under these conditions almost all the alumina reported in solution and sodium calcium hydrosilicate was the main phase in the leaching residues.

### 3.2. Sodium Calcium Hydrosilicate

In all the above leaching experiments carried out on labradorite, the main solid phase in the residues was the elongated prismatic crystals of sodium calcium hydrosilicate. This compound, which plays an important role in the hydrochemical alkaline process for the conversion of aluminosilicates, was first synthesized and described by Leiteizen and Arakelyan<sup>(62)</sup>. In subsequent investigations



by numerous workers (57,65,71,102,124), it has been shown that this compound crystallizes in the four component system:

$\text{Na}_2\text{O} - \text{CaO} - \text{SiO}_2 - \text{H}_2\text{O}$ , and in the five component system:

$\text{Na}_2\text{O} - \text{CaO} - \text{Al}_2\text{O}_3 - \text{SiO}_2 - \text{H}_2\text{O}$  containing 150-600 g/l  $\text{Na}_2\text{O}$  at temperatures in the range 160 to 300°C with the molar ratios of  $\text{CaO}/\text{SiO}_2$  equal to 1.0 and that of  $\text{Na}_2\text{O}/\text{Al}_2\text{O}_3$  to 12 or over.

### 3.2.1 Synthesis of the Pure Compound

To prepare a pure sample of sodium calcium hydrosilicate, a -150 + 200 mesh size fraction of the acid-cleaned crystalline quartz sample (see section 2.2.1.10) was treated in sodium hydroxide solution containing 500 g/l of 'Analar' NaOH pellets with  $\text{CaO}/\text{SiO}_2$  molar ratio of 1.0 at a temperature of 280°C for 3 hours. The calcium oxide used in this experiment was prepared by the ignition of 'Analar'  $\text{CaCO}_3$ . At the end of the experiment, the residue was filtered off; washed several times with cold, distilled water and then dried at 110°C for 2 hours. The product was then examined by different analytical techniques.

### 3.2.2 Some Properties of Sodium Calcium Hydrosilicate

Determinations of the chemical composition of the synthetic sample (see Table 17) showed that it was almost identical with the theoretical composition of sodium calcium hydrosilicate ( $\text{Na}_2\text{O} \cdot 2\text{CaO} \cdot 2\text{SiO}_2 \cdot \text{H}_2\text{O}$ ). Its composition was also very close to those of the residues obtained from most of the leaching experiments carried out on labradorite (Table 17).

The synthetic compound was composed of well-formed crystals in

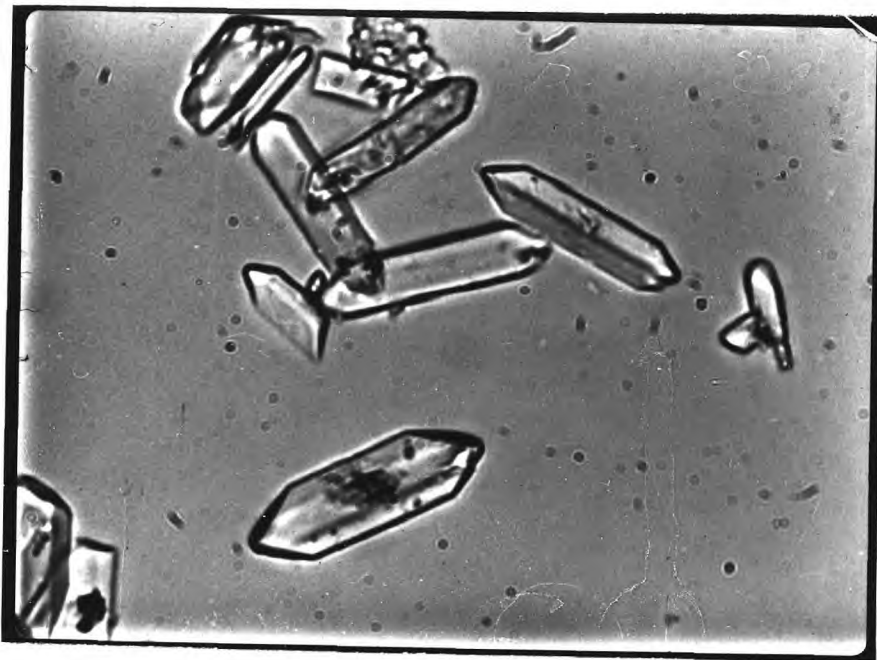
the form of elongated prisms with pointed or truncated vertices (Figure 4a). The crystals were about 20 to 40 microns in length and about 5 to 10 microns in breadth.

When the compound was examined by X-ray powder diffraction, it gave patterns with the strongest lines being found at  $d/n = 3.869$ ,  $2.853$  and  $2.729$ . The X-ray diffraction pattern obtained (Table 18) was similar to that reported in literature for sodium calcium hydrosilicate (57,62,71,124).

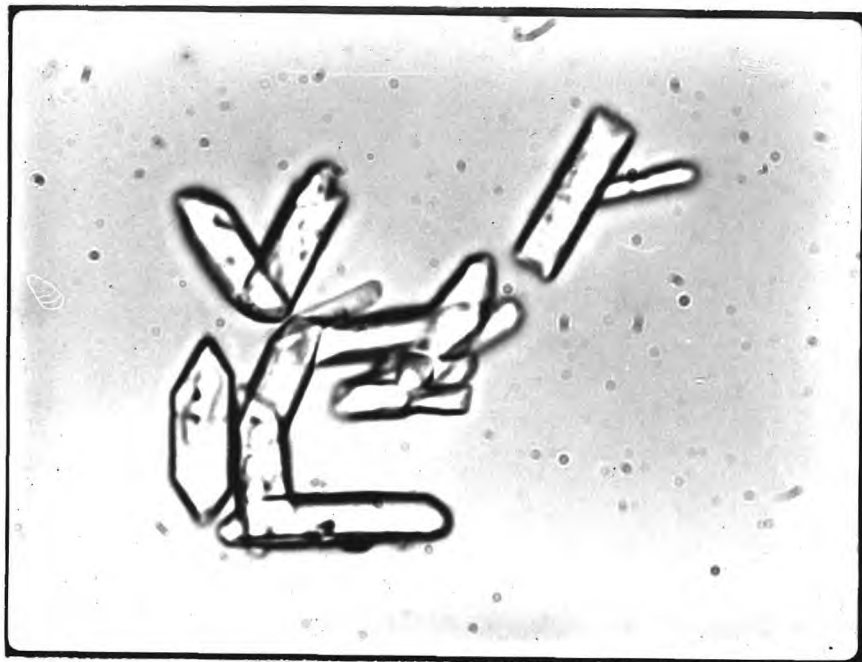
Differential thermal analysis results for the synthetic compound, were similar to those obtained for the leaching residues of labradorite and which gave a sharp endothermic peak between the temperatures  $550$  and  $560^{\circ}\text{C}$  (see figure 3). Thermogravimetric analysis gave a rapid loss of weight between  $510$  and  $580^{\circ}\text{C}$ . The total weight loss of the compound was about  $5.8\%$  which corresponded to one molecule of water in the structure.

To study the effect of carbon dioxide on sodium calcium hydrosilicate, it was treated with  $\text{CO}_2$  gas both at room temperature and during the heating of the compound in the thermobalance. At room temperature, a suspension of 10g sample of the compound in 100 ml of distilled water was treated by a stream of one litre  $\text{CO}_2/\text{min}$  bubbled through the mixture. The compound decomposed and formed sodium carbonate which went into solution and a gelatinous precipitate which was a homogenous mixture of calcium carbonate and silica gel. The reaction may be represented by the equation:

$$\text{Na}_2\text{O} \cdot 2\text{CaO} \cdot 2\text{SiO}_2 \cdot \text{H}_2\text{O}(\text{c}) + \text{CO}_2 + \text{aq.} = \text{Na}_2\text{CO}_3 + \text{CaCO}_3 + \text{SiO}_2 \cdot n\text{H}_2\text{O}$$



(a)



(b)

Figure 4. Sodium calcium hydrosilicate crystals (a) synthetic sample, 1000X; (b) from labradorite leach residue, 1000X.

Table 18. X-ray diffraction pattern for synthetic sodium calcium hydrosilicate

d/n	I	d/n	I
4.895	2	1.857	2
4.829	5	1.779	5
4.627	3	1.769	6
4.020	4	1.761	14
3.984	13	1.642	10
3.869	27	1.628	5
3.531	3	1.608	11
2.853	100	1.589	13
2.729	45	1.577	3
2.694	25	1.567	5
2.647	7	1.499	4
2.445	4	1.480	7
2.413	3	1.475	8
2.311	10	1.458	1
2.282	3	1.427	4
2.219	10	1.412	3
2.196	8	1.399	1
2.118	4	1.364	3
2.094	3	1.339	5
2.010	17	1.323	1
1.991	13		
1.933	20		

After about 30 min. of  $\text{CO}_2$  treatment the decomposition of sodium calcium hydrosilicate was almost complete and the sodium oxide extraction into solution exceeded 95%. The reaction was exothermic and the reaction temperature increased from  $24^\circ\text{C}$  to about  $38^\circ\text{C}$ .

The reaction of sodium calcium hydrosilicate with  $\text{CO}_2$  gas in the thermobalance was studied with a heating rate of about  $6^\circ\text{C}/\text{min}$ . When heated alone, the material lost its water of crystallization between the temperatures of  $510$  and  $580^\circ\text{C}$ . The same results were obtained when the heating process was carried out in a stream of  $100$  ml/min. of nitrogen gas. In a stream of  $100$  ml/min of dry  $\text{CO}_2$  the weight loss of the sample between  $510^\circ\text{C}$  and  $580^\circ\text{C}$  was only 2.8% compared with 5.8% in the absence of  $\text{CO}_2$  (Table 19). At temperatures above  $580^\circ\text{C}$ , there was no significant weight change until a temperature of about  $830^\circ\text{C}$  was reached, when a second weight loss of about 3.2% took place between  $830^\circ\text{C}$  and  $900^\circ\text{C}$ .

The effect of the presence of water vapour at different pressures in the  $\text{CO}_2$  stream on the reaction with sodium hydrosilicate during heating in the thermobalance was investigated. Carbon dioxide gas with the same rate as in the previous test ( $100\text{ml}/\text{min}$ ) was bubbled through distilled water held at constant temperatures of  $45$ ,  $60$  and  $80^\circ\text{C}$  before it was allowed in the thermobalance. The introduction of water vapour in the system did not affect the position or the the magnitude of the two steps of weight losses which took place between the temperatures  $510$  and  $580^\circ\text{C}$  and between  $830$  and  $900^\circ\text{C}$  (Table 19).

Table 19. Results of heating sodium calcium hydrosilicate in the thermobalance and its weight loss when treated under different conditions.

Gas used	Water vapour Temperature, °C	Weight loss, %	
		between 510-580°C	between 830-900°C
-	-	5.8	-
N <sub>2</sub>	-	5.9	-
CO <sub>2</sub>	-	2.8	3.1
CO <sub>2</sub>	45	2.6	3.2
CO <sub>2</sub>	60	2.8	3.0
CO <sub>2</sub>	80	2.8	3.0

In all the thermogravimetric tests on sodium calcium hydrosilicate, no significant weight changes took place below the temperature of 510°C. Between the temperatures of 580°C and 830°C, there was a slight weight gain in the presence of CO<sub>2</sub> gas, but this gain did not exceed 0.4%.

The above results indicated that when the dehydration step of sodium calcium hydrosilicate between 510 and 580°C took place, the dehydrated material absorbed carbon dioxide and formed different carbonates, thus reducing the apparent weight loss during this step from 5.8 to about 2.8%. That the reaction of carbon dioxide with the dehydrated material was not complete could be attributed to lack of contact between CO<sub>2</sub> and the material, which was in a small

alumina crucible. The newly formed carbonates were then decomposed and gave up their  $\text{CO}_2$  when the temperature rised above  $830^\circ\text{C}$ . The reaction between carbon dioxide gas and the original compound before dehydration seemed to be so slow that no weight gain could be recorded by the thermobalance. The presence of water vapour did not have any significant effect on the reaction of  $\text{CO}_2$  gas with sodium calcium hydrosilicate before and after dehydration took place.

C H A P T E R 4

THE REACTIVITY OF SOME

ALUMINOSILICATE MINERALS



Many types of the aluminosilicate minerals are of particular interest for alumina production. These minerals include those which occur in great abundance, e.g. feldspars, clays and micas and those minerals of exceptionally high alumina content, e.g. kyanite. The performance of mineral samples representing these different types of aluminosilicates under the conditions of the hydrochemical alkaline process and the possibility of recovering alumina from them by this method were investigated.

Quartz is usually found associated with aluminosilicate minerals in various proportions. Its reactivity in alkaline solutions under the hydrochemical alkaline process would, therefore, be of particular interest.

A detailed study of the reactivity (the readiness with which the mineral is decomposed) of six feldspar samples with different compositions in the alkaline leaching solutions and the effect of some important factors on the alumina extraction are given in the first section in this chapter. In the second section the relative reactivities of quartz and different aluminosilicates other than feldspars were investigated.

#### 4.1 Detailed Study of the Reactivities of Feldspars

The majority of feldspars may be classified as members of the ternary system:  $\text{NaAlSi}_3\text{O}_8$  -  $\text{KAlSi}_3\text{O}_8$  -  $\text{CaAl}_2\text{Si}_2\text{O}_8$ . These compositions are referred to as sodium, potassium and calcium feldspar. Members of the series between  $\text{NaAlSi}_3\text{O}_8$  and  $\text{KAlSi}_3\text{O}_8$  are called alkali feldspars and those between  $\text{NaAlSi}_3\text{O}_8$  and  $\text{CaAl}_2\text{Si}_2\text{O}_8$  plagioclase

feldspars.

Although  $KAlSi_3O_8$  and  $NaAlSi_3O_8$  form a continuous solid solution series at high temperature, segregation takes place on cooling and the gap in the isomorphous series increases with decreasing temperature. Thus the alkali feldspars in general, and the low-albite-microcline series in particular, consist of two phases; one potassium rich, the other sodium-rich, and the resulting textures are described as cryptoperthetic, microperthetic or perthetic according to the size of exsolved phase.

A purely chemical definition of a plagioclase can be given in terms of albite (Ab) anorthite (An) "molecule" percentages, but specific names are used to denote the six compositional ranges into which the series has been divided. Thus albite, oligoclase, andesine, labradorite, bytownite and anorthite refer to (An) percentages of 0-10, 10-30, 30-50, 50-70, 70-90 and 90-100 respectively. These divisions have been chosen merely for convenience and have no structural significance. The high-temperature series from albite to anorthite is one of almost complete solid solution, but X-ray investigations have shown that the low-temperature series is structurally complex<sup>(122)</sup>. It contains at least six structural divisions ranging from low-albite structure to the most stable primitive anorthite structure depending on the (An) percentage in the molecule.

The alkali feldspar varieties used in this study were albite and microcline. As already mentioned in section 2.2.1 ,

the albite sample was of low-albite structure and the microcline sample was of microperthetic texture with the grain size in the range 30 to 100 microns and with the potassium feldspar as the predominating phase in the mineral.

The plagioclase varieties included, beside albite, oligoclase, andesine, labradorite and anorthosite samples. The chemical composition and the characteristics of these different samples were described in section 2.2.1.

The reactivities of the different feldspar samples were compared under different leaching conditions. The influence of calcium oxide addition, leaching temperature, the presence of alumina in the leaching solution and the calculated caustic ratio on the mineral reactivity and on alumina recovery in solution were investigated. Unless otherwise stated, a size fraction of -200 mesh of the different ground mineral samples, prepared as described in section 2.2.1, were used in the different leaching tests.

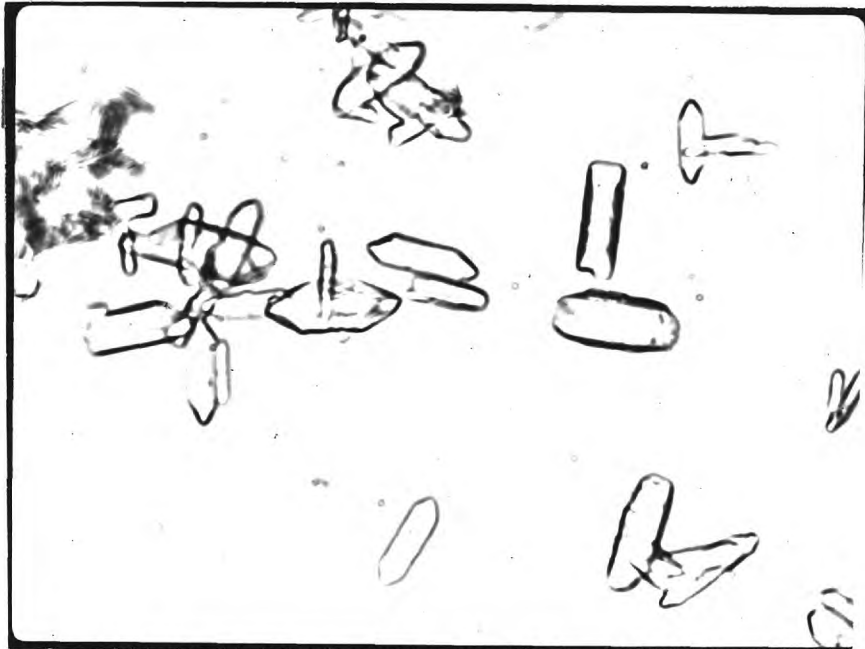
#### 4.1.1 Effect of Calcium Oxide Addition

Leaching experiments were carried out on the six different feldspar samples in a solution containing 500 g/l NaOH with a calculated caustic ratio about 30 at the leaching temperature of 280°C for one hour. Calcium oxide powder was mixed with the mineral sample to give a CaO/SiO<sub>2</sub> ratio of 1.1. The experimental results (Table 20) indicated that all the feldspars examined were completely decomposed and gave almost all their alumina into solution. Under

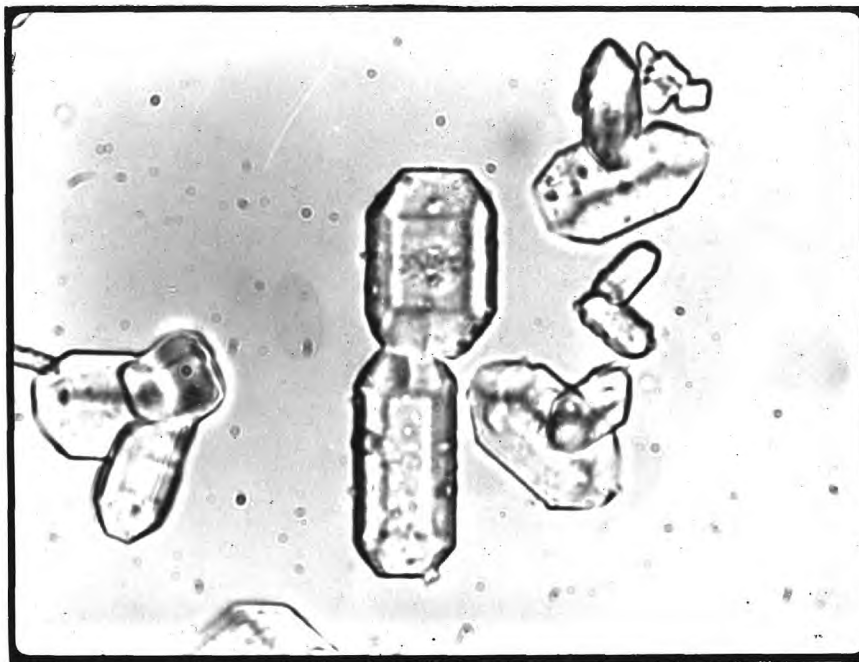
the above mentioned leaching conditions no significant differences in the reactivities of the different feldspars were noticed. The residues obtained in all cases were found to contain elongated prismatic crystals of sodium calcium hydrosilicate as the main phase with small amounts of free calcium hydroxide. The size and the shape of the sodium calcium hydrosilicate crystals varied slightly from one mineral to another (Figures 5 and 6). The X-ray diffraction patterns for all the precipitates were similar to that of pure sodium calcium hydrosilicate sample (section 3.2.2). The strongest lines characteristic for calcium hydroxide were found in the X-ray diffraction patterns of some of these precipitates.

Table 20. The recovery of alumina from feldspars with different molar ratios of  $Al_2O_3/SiO_2$  when treated in 500 g/l NaOH solution at  $280^\circ C$  for one hour with a  $CaO/SiO_2$  molar ratio of 0.97 and 1.1.

Mineral	$Al_2O_3/SiO_2$ ratio in mineral	$Al_2O_3$ recovery, %	
		with $CaO/SiO_2 = 0.97$	with $CaO/SiO_2 = 1.1$
Microcline	0.22	56.0	97.4
Albite	0.14	34.1	96.7
Oligoclase	0.13	32.4	101.2
Andesine	0.27	67.1	95.3
Labradorite	0.28	79.3	102.1
Anorthosite	0.35	81.9	97.5

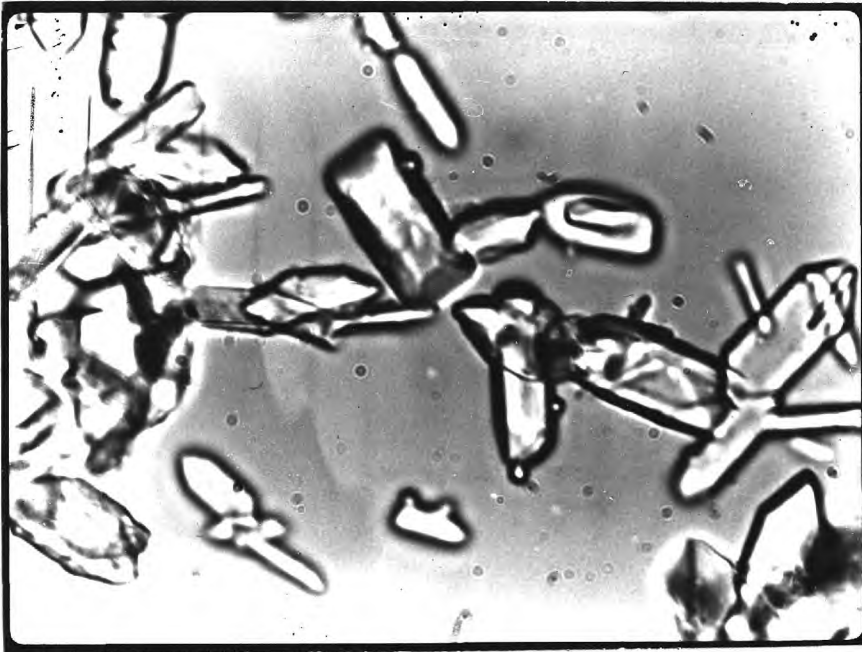


(a)

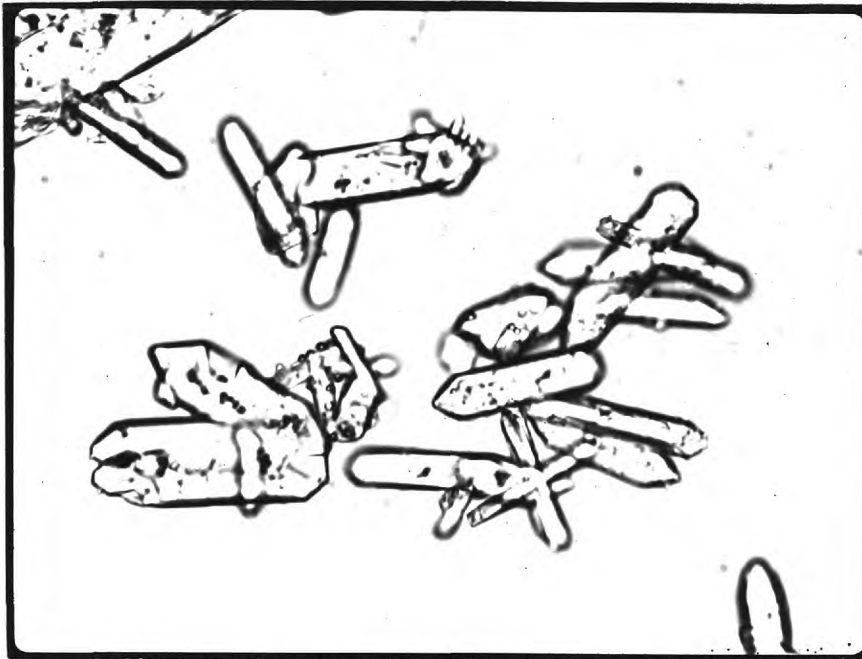


(b)

Figure 5. Sodium calcium hydrosilicate crystals obtained from leaching tests on, (a) Albite, 800X; (b) Microcline, 1000X.



(a)



(b)

Figure 6. Sodium calcium hydrosilicate crystals obtained from leaching tests on, (a) Oligoclase, 1000X; (b) Anorthosite, 625X.

When, however, the  $\text{CaO}/\text{SiO}_2$  molar ratio used was slightly less than unity (about 0.97) in the mixture, the recovered alumina under the above mentioned leaching conditions varied widely from one mineral to another as shown in Table 20. The precipitates obtained from the different feldspar samples using  $\text{CaO}/\text{SiO}_2$  molar ratio 0.97 were examined by optical microscopy and X-ray powder diffraction. These examinations showed that the residues contained sodium calcium hydrosilicate crystals, but no unreacted mineral particles. There was another phase in these residues. Its crystals were rose-like in shape with pinkish colour under transmitted light and were generally attached to the sodium calcium hydrosilicate crystals (Figure 7).

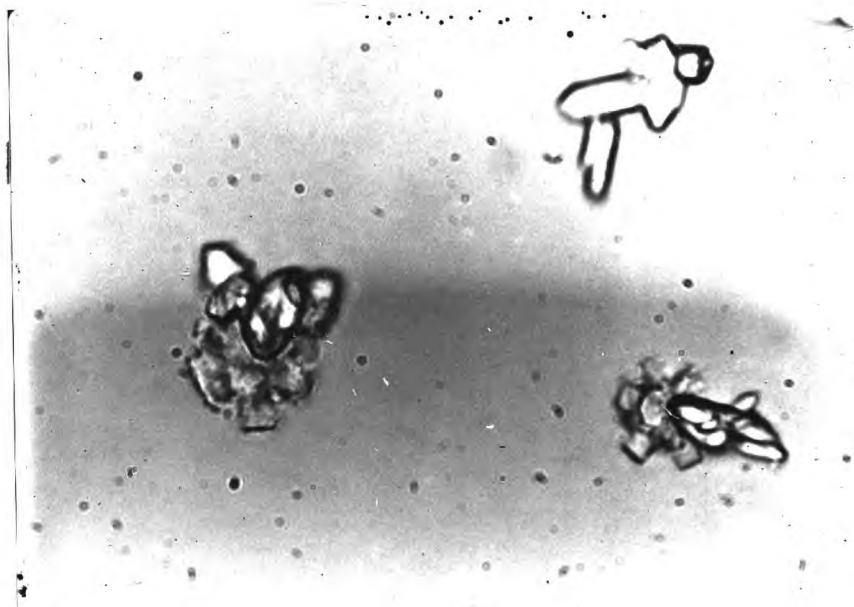


Figure 7. Rose-like crystals of natrodavyne, 800X, obtained from anorthosite sample leached with  $\text{CaO}/\text{SiO}_2 = 0.97$ .

The X-ray diffraction pattern obtained for this phase was in good agreement with that of natrodavyne (low form) of the composition  $3\text{NaAlSiO}_4 \cdot \text{Na}_2\text{CO}_3$ . (A.S.T.M. Card No. 15-594). The results showed that there was a high correlation between the alumina recovered and the molar ratio of  $\text{Al}_2\text{O}_3/\text{SiO}_2$  in the mineral (Table 20). Increase of this ratio was accompanied by a parallel increase in alumina extraction. This could be explained by the fact that in the presence of lime, the silica removal from solution would take place by the formation of sodium calcium hydrosilicate and the alumina would be retained in the solution. When there was a deficit in lime, i.e. the molar ratio  $\text{CaO}/\text{SiO}_2$  was less than unity, the silica removal took place at the expense of alumina forming such compounds as sodium hydroaluminosilicates. When the excess of silica was relatively large, as in the case of minerals with low  $\text{Al}_2\text{O}_3/\text{SiO}_2$  ratios, the alumina losses were great and alumina recovery in solution was low.

#### 4.1.2 Effect of Leaching Temperature

The reactivities of the different feldspars and the degree of alumina extraction from them at different leaching temperatures were investigated. Leaching tests were carried out in 500 g/l NaOH solutions with a calculated caustic ratio of 30 and a  $\text{CaO}/\text{SiO}_2$  molar ratio of 1.1 at constant temperatures of 160, 220, 250 and 280°C for one hour. The results are summarized in Table 21. All the feldspars studied gave almost complete alumina extraction at temperatures of 220°C and above except the anorthosite sample which gave only about 58% recovery at 220°C. When the leaching temperature used was 160°C, the alumina



extraction dropped to about 25% for anorthosite and between about 40 - 57% for the other feldspar samples.

Table 21. Percentage of alumina extracted from the different feldspars when treated in 500 g/l NaOH solution with a CaO/SiO<sub>2</sub> ratio of 1.1 and a caustic ratio of about 30 at different leaching temperatures for one hour. .

Mineral	Temperature, °C			
	280	250	220	160
Microcline	97.40	100	95.68	51.60
Albite	96.70	99.46	80.38	41.68
Oligoclase	101.2	100	96.36	39.68
Andesine	95.25	99.62	91.82	57.22
Labradorite	102.1	94.75	86.20	38.73
Anorthosite	97.5	93.74	58.11	25.02

X-ray powder diffraction and microscopic examinations of the residues formed showed that all the feldspars treated above the temperature of 220°C yielded sodium calcium hydrosilicate as the main reaction product. Small quantities of free calcium hydroxide were also present in the residues. No unreacted mineral particles were detected in these residues except in that obtained from anorthosite treatment at 220°C where partially decomposed mineral particles were found. The residues obtained at 160°C contained in all cases a

mixture of unreacted feldspar particles, free calcium hydroxide and sodium calcium hydrosilicate crystals. Some residues obtained at this temperature contained also minute amounts of calcium hydroaluminosilicate, a hydrogarnet of the composition  $3 \text{CaO} \cdot \text{Al}_2\text{O}_3 \cdot \text{SiO}_2 \cdot 4 \text{H}_2\text{O}$ <sup>(55)</sup>. The X-ray diffraction lines for the sodium calcium hydrosilicate phase obtained at 160°C were not as sharp as those obtained at higher temperatures which suggested that the compound had a poor crystal structure.

Above 220°C, no significant differences were noticed between the reactivities of the alkali and plagioclase feldspars or between those of members in the same series. By decreasing the leaching temperature, the differences in the reactivities of the different feldspars became more pronounced. As would be expected, anorthorite, the calcium-rich feldspar, was the least reactive member in the plagioclase series. It was the only feldspar which did not dissolve completely when treated at 220°C for one hour. Alkali feldspar members were of comparable reactivities but microcline, the potassium rich-member, was generally more reactive than albite, the sodium-rich one.

#### 4.1.3 Effect of Alumina in the Initial Leaching Solutions

The effect of the addition of alumina to the starting leaching solutions and the variation of the initial caustic ratio on the reactivity of the different feldspars and on the alumina recovery were studied. Sodium aluminate solutions containing about 10, 15 and 35 g/l  $\text{Al}_2\text{O}_3$  were prepared by dissolving the required amounts of 'aluminium hydroxide moist gel.' of Laboratory Reagent grade in

500 g/l NaOH solutions. The leaching tests were carried out at a temperature of 280°C for 30 min. with a CaO/SiO<sub>2</sub> molar ratio of 1.1.

The results of these tests (Table 22) showed that the reactivity of the different feldspar minerals and the recovery of alumina from them was not significantly affected by the presence of alumina in the initial leaching solutions as long as the solubility limit of alumina was not exceeded. The change of the initial caustic ratio,  $\alpha_c$ , from about 68 for solutions containing 10g/l Al<sub>2</sub>O<sub>3</sub> to about 18 for solutions containing 35 g/l did not affect the alumina recovery from the minerals as long as the calculated final caustic ratio,  $\alpha_f$ , was not less than about 12.

All the residues obtained from tests in aluminate solutions with the calculated final caustic ratio more than 12 were found to be composed of sodium calcium hydrosilicate crystals with some free calcium hydroxide, regardless of the initial alumina concentration in solution. No unreacted feldspar particles or other phases were found in these residues.

It seemed likely that the only effect of the presence of alumina in the initial leaching solution was to reduce the amount of the aluminosilicate mineral which could be added to the solution to reach the solubility limit of alumina. The larger the amount of alumina in the starting solution, and the lower the initial caustic ratio, the smaller the amount of the mineral which could be used in the leaching process with complete alumina recovery.

Table 22. The effect of the presence of alumina in the leaching solution and of the initial caustic ratio on the alumina extraction from the different feldspars when treated at a temperature of  $280^{\circ}\text{C}$  for 30 min. with a  $\text{CaO}/\text{SiO}_2$  ratio of 1.1 .

Mineral	Initial $\text{Al}_2\text{O}_3$ concn., g/l	Initial caustic ratio	Calculated final caustic ratio	$\text{Al}_2\text{O}_3$ recovery %
Microcline	9.26	68.87	20.79	97.8
"	15.11	42.19	17.46	98.7
"	35.89	17.76	11.69	88.73
Albite	9.63	66.17	20.85	98.2
"	14.73	43.27	17.87	97.9
"	32.53	22.73	13.41	95.7
Oligoclase	9.73	65.53	30.79	97.83
"	15.42	41.34	24.16	99.33
"	34.0	18.75	12.10	95.95
Andesine	9.48	67.25	20.79	95
"	14.92	42.72	17.65	96.4
"	34.0	18.75	12.15	97.36
Labradorite	9.44	67.50	19.70	98.7
"	15.29	41.69	16.68	97.3
Anorthorite	10.01	63.7	19.64	96
"	15.3	41.7	16.89	97.5
"	28.8	22.13	13.65	96.45

#### 4.1.4 Effect of Calculated Final Caustic Ratio

The effect of the calculated final caustic ratio on the reactivity of the different feldspars and the recovery of alumina was investigated. The calculated weight of the mineral sample to give the desired final caustic ratio (assuming complete alumina extraction into solution) was intimately mixed with the required amount of lime ( $\text{CaO}/\text{SiO}_2$  molar ratio of 1.1) which was then treated in 500 g/l NaOH solutions at a temperature of  $280^\circ\text{C}$  for 30 min.

The results (Table 23) showed that the calculated final caustic ratio,  $\alpha_f$ , of about 12 seemed to be a critical value for the leaching process. Almost complete alumina extraction was obtained from the different feldspars when the calculated caustic ratio was above this critical value. The actual final caustic ratio was in this case almost identical to that already calculated (see Tables 22 and 23). On the other hand, with calculated final caustic ratios below 12 there was a sharp drop in the alumina recovered in solution. From the results given in Table 23, the lower the calculated final caustic ratio below 12, the lower the alumina recovery in solution and the higher the actual final caustic ratio would be at the end of the experiment. Treatment of microcline, for example, with a calculated final caustic ratio of 11.7 gave an alumina recovery of about 88% compared with more than 98% when the ratio was about 12 (Tables 22 and 23). When the calculated final caustic ratio was about 10, the alumina recovery dropped to about 55% and the actual final caustic ratio was about 18. With a ratio of about 7, the recovery was only

Table 23. The effect of the calculated final caustic ratio,  $\alpha_f$ , on the actual final caustic ratio and on the alumina recovery from aluminosilicate minerals when treated in 500 g/l NaOH solutions at 280°C for 30 min. and with a CaO/SiO<sub>2</sub> ratio of 1.1

Mineral	Calculated $\alpha_f$	Al <sub>2</sub> O <sub>3</sub> recovery, %	Actual $\alpha_f$
Anorthosite	13.16	96.45	13.65
Andesine	12.15	97.36	12.26
Oligoclase	12.10	95.95	12.60
Microcline	11.69	88.73	13.18
Microcline	9.99	54.67	18.28
Andesine	9.42	57.87	16.27
Anorthosite	7.05	36.63	19.25
Supreme clay	7.02	34.48	20.35
Supreme clay *	7.01	35.53	19.7

\*

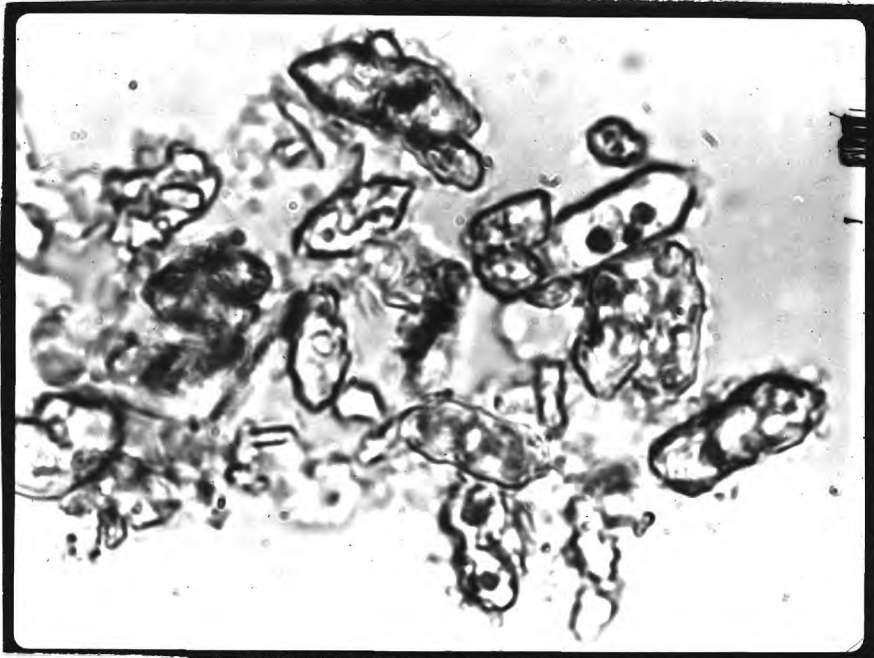
This sample was treated for 4 hours instead of 30 min.

about 35% and the actual final caustic ratio was about 20.

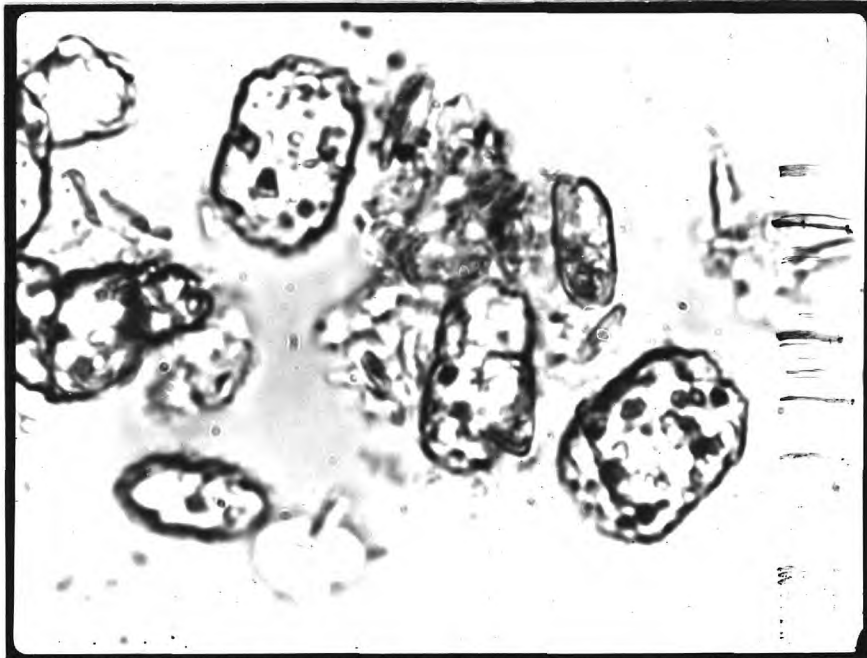
All the feldspars gave the same results at equal values of the calculated final caustic ratios,  $\alpha_f$ , regardless of their composition.

The main phase in the residues obtained with calculated final caustic ratios above 12 was the elongated prismatic crystals of sodium calcium hydrosilicate with small amounts of free calcium hydroxide. When this ratio was less than 12, some new solid phases containing alumina were found in the residues beside sodium calcium hydrosilicate. The residues obtained with a calculated caustic ratio of about 10 contained sodium calcium hydroxide crystals which were at the break down stage and transversely strained and spotted, or present in the form of fragments (Figure 8). There were also large amounts of hexagonal calcium hydroxide crystals and tetragonal crystals of sodium calcium hydroaluminosilicate,  $4\text{Na}_2\text{O} \cdot 2\text{CaO} \cdot 2\text{Al}_2\text{O}_3 \cdot 6\text{SiO}_2 \cdot 3\text{H}_2\text{O}$ , and some sodalite compounds as cancrinite,  $3(\text{Na}_2\text{O} \cdot \text{Al}_2\text{O}_3 \cdot 2\text{SiO}_2) \cdot \text{Na}_2\text{O} \cdot 3\text{H}_2\text{O}$ , and natrodavyne,  $3(\text{Na}_2\text{O} \cdot \text{Al}_2\text{O}_3 \cdot 2\text{SiO}_2) \cdot \text{Na}_2\text{CO}_3$ . The residues from treatment of the mineral samples with a calculated caustic ratio of about 7 contained less sodium calcium hydrosilicate crystals, and more of the sodium calcium hydroaluminosilicate and the sodalite-type compounds than in the residues obtained with a calculated caustic ratio about 10. The sodium calcium hydrosilicate crystals were in a more advanced stage of break down (Figure 9a).

The results were not affected by the presence of alumina in the initial leaching solution: the same results were obtained from the treatment of feldspars in both sodium hydroxide and sodium aluminate



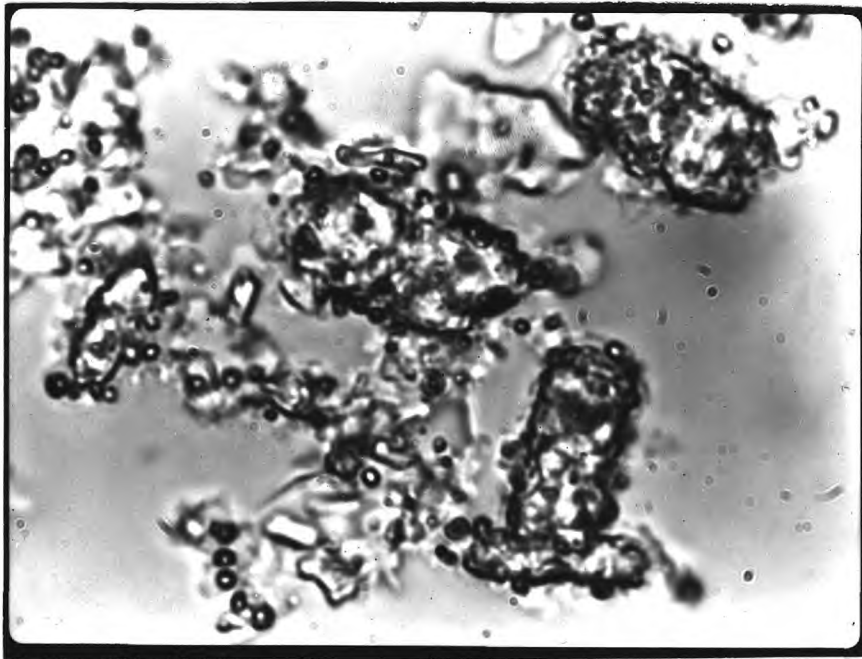
(a)



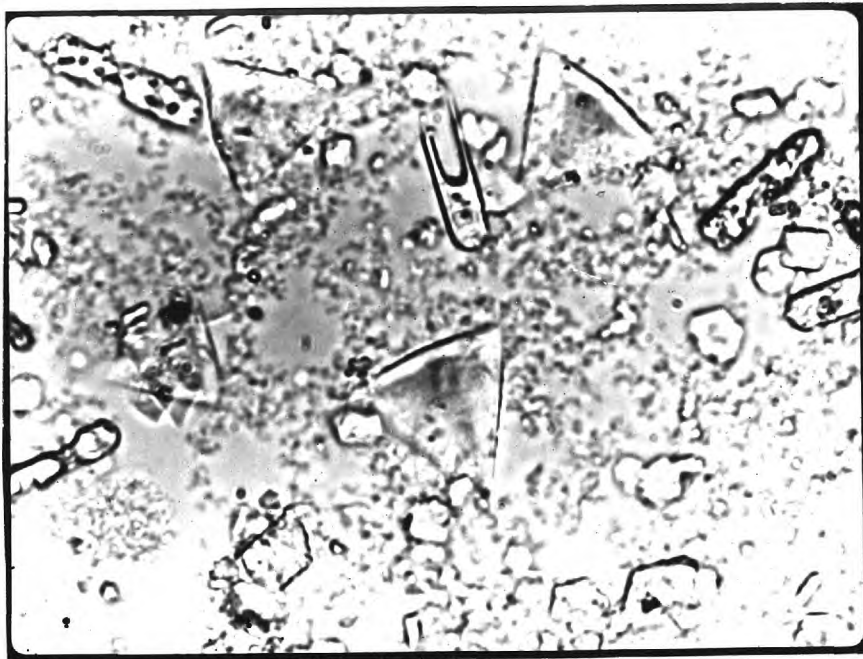
(b)

Figure 8. Sodium calcium hydrosilicate crystals at the break down stage obtained when treating feldspars with calculated final caustic ratio of about 10 at 280°C for 30 min. (a) from Andesine, 1100X; (b) from Microcline, 1000X.





(a)



(b)

Figure 9. Leaching residues obtained from the treatment of aluminosilicate with a calculated caustic ratio of about 7; (a) Sodium calcium hydrosilicate crystals in advanced stages of decomposition, 1000X, obtained from anorthosite treated for 30 min; (b) Tetragonal crystals of sodium calcium hydroaluminosilicate, 750X, obtained from supreme clay treated for 4 hours.

solutions having the same calculated final caustic ratio.

It should be noted that other aluminosilicate minerals gave the same results as those obtained from feldspars treated with sodium hydroxide solutions at the same calculated final caustic ratio. It was found, e.g., that the treatment of the supreme clay sample (see section 2.2.1.9) with a calculated final caustic ratio of 7 gave the same alumina recovery in solution as that obtained from the treatment of anorthosite under the same conditions (Table 23). The residues in both cases contained the same solid phases. Longer leaching times than 30 min. had no significant effect on the results. For example, when the supreme clay sample was treated, with a calculated final caustic ratio of about 7 for 4 hours instead of 30 min., no change in the alumina recovery in solution was observed (Table 23) and the residues contained basically the same reaction products. Sodium calcium hydroaluminosilicate crystals in this case became, however, larger in size and better crystalline than those obtained after 30 min. of treatment (Figure 9b).

From these results it was obvious that the calculated final caustic ratio was an important factor in the formation and stability of sodium calcium hydrosilicate, and consequently the alumina recovery from aluminosilicate minerals. When this ratio was above the critical value of 12, sodium calcium hydrosilicate was the stable phase in the system and the liberated alumina from the mineral was retained in solution with almost complete recovery. When the ratio was lowered below 12, sodium calcium hydrosilicate compound became unstable

and was attacked by the aluminate solution with the formation of sodium calcium hydroaluminosilicate. This reaction could be represented by equation (11) in section 1.2. This result was in agreement with the thermodynamic calculations represented in section 1.2 and which showed that the above mentioned reaction would be thermodynamically feasible. To obtain sodium calcium hydrosilicate as the stable solid phase in the leaching system and to obtain a high degree of alumina recovery from aluminosilicate minerals, the calculated final caustic ratio should, therefore, be above the critical value of 12.

#### 4.2 The Reactivities of Quartz and Some Aluminosilicates Other than Feldspars.

The reactivities of quartz and some aluminosilicate minerals other than feldspars were examined in sodium hydroxide solutions under leaching temperatures in the range of 160 to 280°C. The types of aluminosilicate minerals studied included mica, kyanite and clays. Of the mica group only an almost pure muscovite sample was used. A Kenyan kyanite sample was used to represent the group of aluminosilicates which had high alumina content (about 60%  $Al_2O_3$ ). The clays included a paper clay sample, which was almost pure kaolinite, and three ball clays which had different alumina, quartz and kaolinite contents. The chemical composition and the characteristics of these minerals were discussed in section 2.2.1.

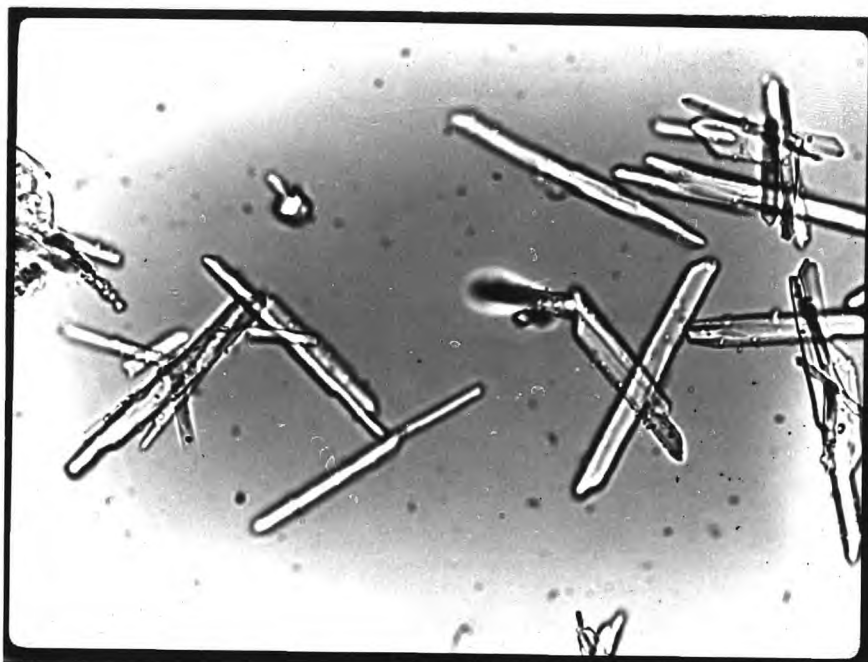
Unless otherwise stated, a size fraction of a -200 mesh of the ground mineral sample, prepared as described in section 2.2.1, was used in the different leaching tests.

#### 4.2.1 Reactivities at 280°C

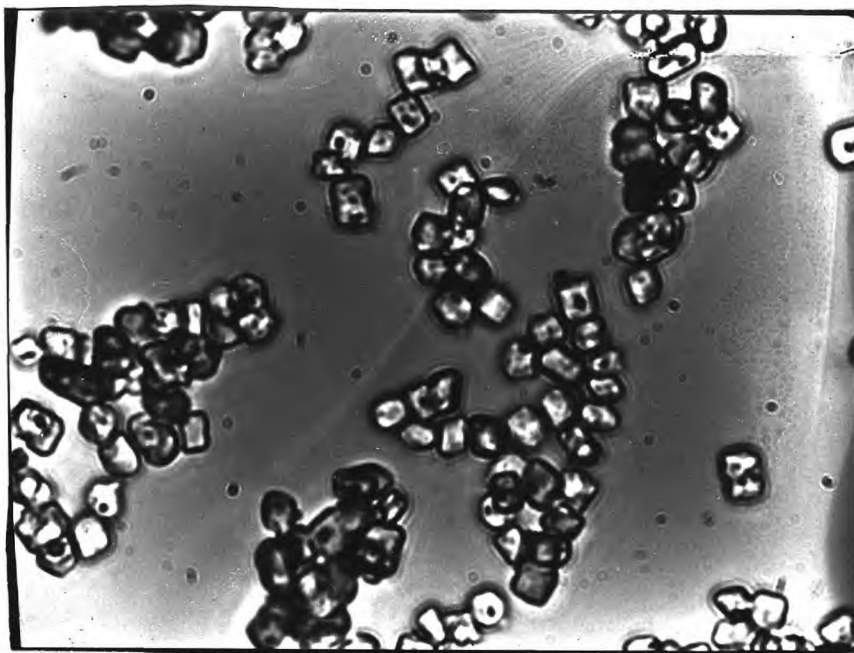
Samples of quartz and the different aluminosilicate minerals were separately treated in a solution containing 500 g/l NaOH with a calculated caustic ratio of about 30 and a CaO/SiO<sub>2</sub> molar ratio of 1.1 at a temperature of 280°C for one hour. The results of alumina recovery from the different aluminosilicate minerals are given in Table 24. With the exception of kyanite, all the minerals examined dissolved completely and gave almost all their alumina in solution. In the case of kyanite, the alumina extraction did not exceed 57% under the above mentioned conditions and the residue obtained contained considerable amounts of unreacted mineral grains beside free calcium hydroxide and sodium calcium hydrosilicate crystals. The sodium calcium hydrosilicate crystals in the residue were large, thin and very elongated (Figure 10a).

Table 24. The percentages of alumina recovery from different aluminosilicate minerals when treated in 500 g/l NaOH solutions for one hour with a CaO/SiO<sub>2</sub> molar ratio of 1.1 at different leaching temperatures.

Mineral	Temperature, °C			
	280	250	220	160
Muscovite	98.63	97.91	96.37	37.41
Kyanite	56.74	23.42	15.33	4.78
Supreme Clay	96.55	96.74	90.26	57.51
Ball Clay 661	99.02	97.55	95.78	55.28
Ball Clay 935	96.72	96.41	97.05	57.86
Ball Clay 961	98.41	97.12	94.17	57.13

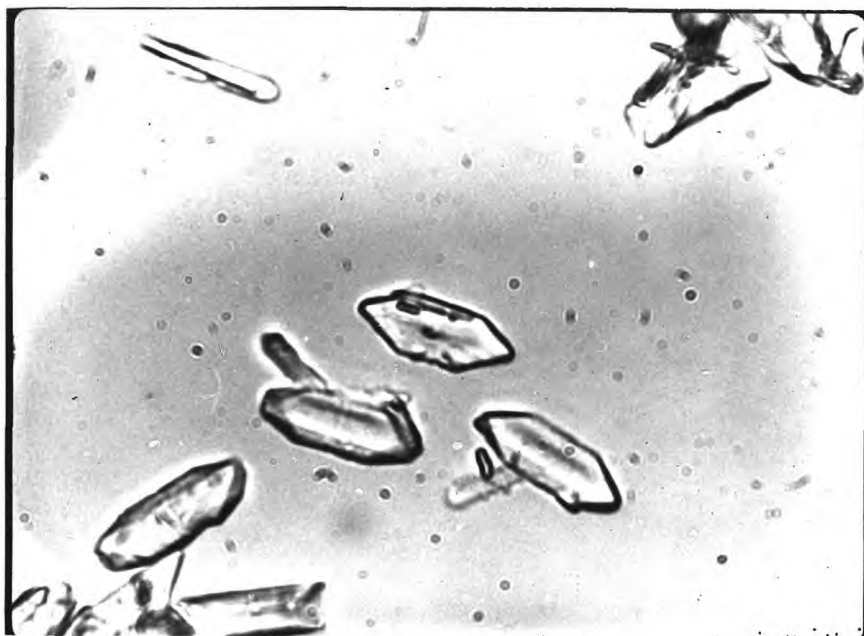


(a)



(b)

Figure 10. Sodium calcium hydrosilicate crystals obtained from the treatment of (a) Kyanite, 625X; and (b) Ball clay No.661, 1000X; in 500g/l NaOH solutions at 280°C for 1 hour.



(a)



(b)

Figure 11. Sodium calcium hydrosilicate crystals obtained from the treatment of (a) Quartz, 1000X; and (b) Muscovite, 800X, in 500 g/l NaOH solutions at 280°C for 1 hour.

The precipitates obtained from minerals other than kyanite were composed mainly of sodium calcium hydrosilicate crystals with small amounts of free calcium hydroxide, but no unreacted mineral grains were found. The lengths and the sizes of the sodium calcium hydrosilicate crystals in the residues varied from one mineral to another (Figures 10 and 11). Sodium calcium hydrosilicate crystals obtained from the different clays were similar to each other in shape and size. They were in the form of very fine, almost equidimensional prisms of about 3 to 5 microns in length (Figure 10b). Quartz and other aluminosilicate minerals yielded sodium calcium hydrosilicate crystals with sizes and shapes intermediate between those obtained from kyanite and clays.

#### 4.2.2 Reactivities at Temperatures Below 280°C

Samples of quartz and the different aluminosilicate minerals were treated separately in sodium hydroxide solutions containing 500 g/l NaOH with a calculated caustic ratio of about 30 and a CaO/SiO<sub>2</sub> molar ratio of 1.1 at temperatures of 160, 220 and 250°C for one hour. The results of treatment for the various minerals may be summarized in the following:

##### 4.2.2.1 Treatment of Muscovite

The muscovite sample decomposed completely and its alumina was extracted into solution when treated at temperatures of 250 and 220°C (Table 24) with the formation of sodium calcium hydrosilicate as the main phase in the residues. The residues contained also small amounts of free calcium hydroxide but no unreacted mineral grains were detected.

When the mineral was treated at a temperature of 160°C, it did not decompose completely and only 37% of its alumina was extracted into solution (Table 24) sodium calcium hydrosilicate and free calcium hydroxide were found in the precipitate besides unreacted mineral grains. No other phases were detected in the residue.

#### 4.2.2.2 Treatment of Kyanite

Kyanite was found to be the most refractory aluminosilicate mineral examined. As already mentioned, it did not decompose completely when treated at a temperature of 280°C for one hour. At temperatures lower than 280°C, the percentage of the mineral decomposed, and consequently the percentage of the alumina extracted, decreased with the decrease of the leaching temperature. When treated at 160°C, a slight amount of the mineral was dissolved and the alumina recovery was less than 5% (Table 24).

The residues formed at all the temperatures employed contained sodium calcium hydrosilicate crystals, free calcium hydroxide and unreacted mineral in varying proportions according to the leaching temperatures.

#### 4.2.2.3 Treatment of Clays

The different clays examined had similar reactivities in the alkaline solutions at the various leaching temperatures employed. They gave high degrees of alumina extraction into solution and yielded sodium calcium hydrosilicate as the main solid phase in all the residues when treated at temperatures of 220°C and above (Table 24).



The sodium calcium hydrosilicate crystals were of similar shape and size in all the residues obtained. They were in the form of small prisms of about 3 to 5 microns in length. The crystals shown in Figure 10b were typical.

When the different clay samples were treated at a temperature of 160°C, they decomposed almost completely but only about 57% of their alumina was extracted into solution (Table 24). The residues obtained at this temperature contained sodium calcium hydrosilicate, free calcium hydroxide and other phases which retained alumina in the residues. The alumina-containing phases in the residues were found to be sodium hydroaluminosilicate,  $3(\text{Na}_2\text{O} \cdot \text{Al}_2\text{O}_3 \cdot 2\text{SiO}_2) \cdot \text{Na}_2\text{O} \cdot 3\text{H}_2\text{O}$ , sodium calcium hydroaluminosilicate,  $4\text{Na}_2\text{O} \cdot 2\text{CaO} \cdot 2\text{Al}_2\text{O}_3 \cdot 6\text{SiO}_2 \cdot 3\text{H}_2\text{O}$ , and calcium hydroaluminosilicate,  $3\text{CaO} \cdot \text{Al}_2\text{O}_3 \cdot \text{SiO}_2 \cdot 4\text{H}_2\text{O}$ . The X-ray diffraction lines for the different phases were diffuse indicating that they had a poor crystal structure. Unlike with the other aluminosilicate minerals, no unreacted kaolin material from the clays could be detected in the residues when they were treated at 160°C.

#### 4.2.2.4 Treatment of Quartz

When the quartz sample was treated in 500 g/l NaOH solutions with equivalent amounts of lime, i.e. CaO/SiO<sub>2</sub> molar ratio equals unity, at temperatures of 220 and 280°C for one hour, the mineral was completely decomposed and formed elongated prismatic crystals of sodium calcium hydrosilicate as the solid phase (Figure 11a). The same results were obtained when solutions containing 500 g/l NaOH and

about 10 g/l  $Al_2O_3$  were used. No alumina-containing solids were formed and all the alumina reported in the solution.

When excess of calcium oxide was used ( $CaO/SiO_2$  molar ratio equals 1.5), the surplus of lime deposited in the form of hexagonal platy crystals of calcium hydroxide in both sodium hydroxide and sodium aluminate solutions.

When treated at a temperature of  $160^{\circ}C$  for one hour, quartz did not decompose completely and the residue obtained contained sodium calcium hydrosilicate, free calcium hydroxide and partially decomposed quartz particles.

#### 4.2.3 Treatment of Kyanite Under More Severe Conditions

Due to its low reactivity, kyanite was treated in stronger sodium hydroxide solutions than 500 g/l NaOH at temperatures up to  $300^{\circ}C$  and using very fine size fractions of the mineral sample.

An increase in the sodium hydroxide concentration and the leaching temperature increased the alumina recovery from the mineral. When, e.g., two samples of -300 mesh size fraction were treated, one in 580 g/l NaOH at  $280^{\circ}C$  and the other in 646 g/l NaOH at  $300^{\circ}C$  for two hours, the alumina extraction was 87% and 93% respectively. Unreacted mineral grains were found in the residue obtained in both cases. The residues contained also very elongated prismatic crystals of sodium calcium hydrosilicate and well-defined hexagonal platy crystals of free calcium hydroxide. (Figure 12).

The particle size had a considerable effect on the reactivity of kyanite. Treating a -72 + 100 mesh size fraction in 500 g/l NaOH solution at  $280^{\circ}C$  for one hour gave an alumina recovery of about 20%

compared with about 57% recovery when a -200 mesh size fraction was treated under the same conditions.

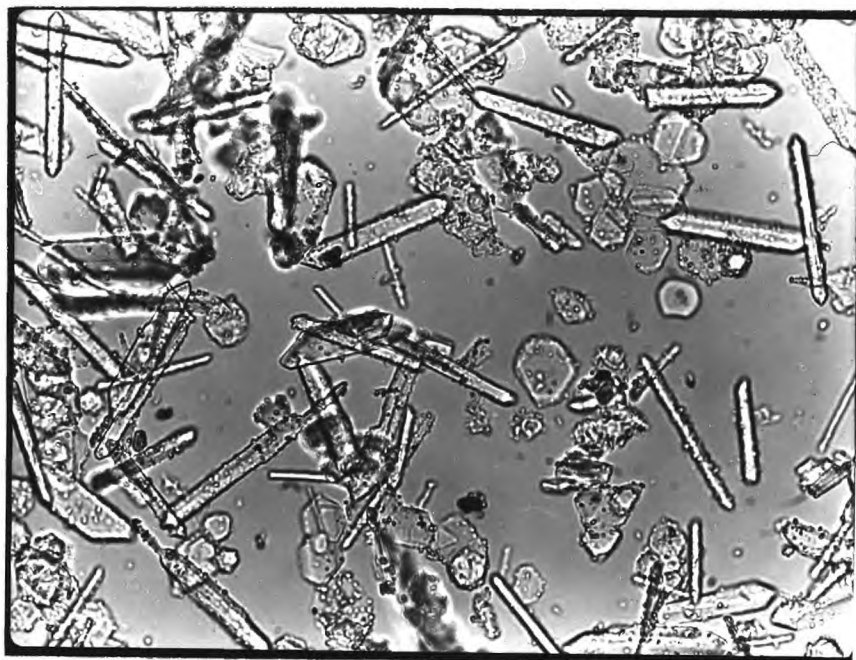


Figure 12. Elongated prismatic crystals of sodium calcium hydrosilicate and hexagonal plates of calcium hydroxide obtained from kyanite treatment in 646 g/l NaOH solution at 300°C for 2 hours.

In another experiment, a -200 + 300 mesh size fraction of the mineral gave 82% recovery while a -300 mesh fraction yielded 93% when both were treated in 646 g/l NaOH solution at 300°C for two hours.

It should be noted that the great influences caused by the change of reaction temperature, solution concentration and the mineral particle size on the reactivity of the kyanite mineral are characteristic features of chemically-controlled processes. In other words, the chemical dissolution of kyanite seemed to be the slowest step in the leaching process of the mineral under all the leaching conditions

employed. The low reactivity of kyanite could be partially attributed to the compactness of its structure. With a volume of  $15.3 \text{ \AA}^3$  per oxygen atom, kyanite has the closest packing of the aluminosilicate minerals<sup>(128)</sup>. This would make its decomposition more difficult and the rate of its dissolution lower than the other aluminosilicates.

#### 4.3 Discussion of Results

The results obtained for the different aluminosilicates and quartz showed that all the minerals examined could be decomposed by the sodium hydroxide solutions and gave sodium calcium hydrosilicate crystals under the conditions of the hydrochemical alkaline process. These results were in agreement with the thermodynamic calculations represented in section 1.2 and which indicated the thermodynamic feasibility of the process for the different minerals examined.

Among the aluminosilicates examined, clay minerals were the most reactive and kyanite the most refractory mineral in the leaching solutions. The clays were completely decomposed in sodium hydroxide solutions at temperatures as low as  $160^\circ\text{C}$ . On the other hand, treatment of kyanite at a temperature of  $300^\circ\text{C}$  for two hours failed to dissolve all the mineral. The reactivities of different feldspars, muscovite and quartz were intermediate between those of kyanite and the clay minerals.

Sodium calcium hydrosilicate crystallization was favoured by high temperatures. At leaching temperatures of  $220^\circ\text{C}$  and above, well crystalline crystals were obtained. At a temperature of  $160^\circ\text{C}$

sodium calcium hydrosilicate crystals had poor crystal structure and some aluminium-containing compounds were found in the residues in spite of the fact that sufficient lime was present in the leaching system.

There seemed to be a certain correlation between the size and the relative length of sodium calcium hydrosilicate crystals and between the reactivity of the mineral from which they were produced. Kyanite, the most refractory mineral studied, gave large, thin and very elongated crystals of about 100 to 150 microns in length and 5 to 10 microns in breadth (Figure 10a). On the other hand, clays yielded under the same leaching conditions small, short and thick prisms of about 3 to 5 microns in length (Figure 10b). The sodium calcium hydrosilicate crystals obtained from the other minerals were intermediate in size and relative thickness between these two extremes. (Figures 5, 6, 10 and 11). In the feldspar group itself, microcline produced relatively the shortest and thickest crystals and anorthosite the longest and thinnest ones.

CHAPTER 5

MECHANISM OF SOLID FORMATION

DURING THE LEACHING PROCESS.

To obtain a better understanding of the chemistry of the hydrochemical alkaline process and to elucidate the roles of sodium hydroxide and calcium hydroxide during the different stages of the process, an attempt was made to study the mechanism of the solid formation during the leaching step. This would also demonstrate whether the solids form a layer on the mineral surface or the mineral goes into solution first followed by the formation of different phases.

For this purpose polished mineral lumps were treated in leaching solutions and the changes that took place on the mineral surface during the different stages of the process were followed by scanning electron microscopy, electron-probe microanalysis and by X-ray powder diffraction.

This procedure proved to be very useful for the study of the relative reactivities of the different minerals in sodium hydroxide solutions.

## 5.1 Experimental Results

### 5.1.1 Results Obtained During the Heating Period

Changes on the surfaces of the different aluminosilicate minerals during the heating step and before equilibrium was attained in the leaching system were followed. Polished lumps of albite, microcline, oligoclase and anorthosite minerals were heated in 500 g/l NaOH solutions with suspended lime up to temperatures of 160, 190, 220 and 250°C. The heating rate for the reaction mixtures was about 140 to 150°C/hr. When the desired temperature was reached, the autoclave was cooled

quickly to about 80°C. After taking out the lumps from solution, they were carefully and thoroughly washed with distilled water and then dried at 110°C. The lumps were weighed before and after the treatment.

No product layer was formed on the surface of the lumps heated to temperatures of 160, 190, or 220°C. The surfaces of the minerals had, however, been attacked and the degree of attack increased with temperature as shown by the weight losses of the treated minerals (Table 25). The weight losses of the treated lumps also indicated that the reactivities of the minerals in the alkaline solution were in the following order: microcline > albite ≈ oligoclase > anorthosite. The oligoclase sample had a reactivity comparable to that of albite. It, however, showed a larger percentage weight loss than albite did at lower temperatures (Table 25), presumably because of the presence of the reactive quartz inclusions in the mineral sample. At higher temperatures, oligoclase weight losses were comparable to or slightly less than those for albite.

A porous layer firmly attached to the surface was observed on the anorthosite mineral heated to 250°C. On the surfaces of the other feldspar minerals heated to this temperature, loose, porous layers which peeled off readily were formed.

The results of closer examinations by scanning electron microscopy and electron-probe microanalysis of the surfaces of the minerals heated to the different temperatures were as follows:

#### 5.1.1.1 Lumps Heated to 160°C

The albite mineral was slightly attacked by the caustic solution



Table 25. The percentage weight losses of treated mineral lumps in NaOH leaching solutions at different stages and conditions of the leaching process.

Leaching conditions	Microcline	Albite	Oligoclase	Anorthosite
Heating to 160°C in NaOH	0.15	0.07	0.1	- 0.1
Heating to 190°C in NaOH	1.50	0.6	0.8	0.24
Heating to 220°C in NaOH	7.05	3.6	4.1	1.1
Heating to 250°C in NaOH	35.7	23.5	22.1	10.35
160°C, NaAlO <sub>2</sub> , 60 min.	2.3	0.4	-	0.1
160°C, NaOH, 60 min.	5.5	2.7	-	1.3
220°C, NaAlO <sub>2</sub> , 60 min.	31.7	21.1	-	3.5
220°C, NaOH, 60 min.	64.1	38.8	-	8.6

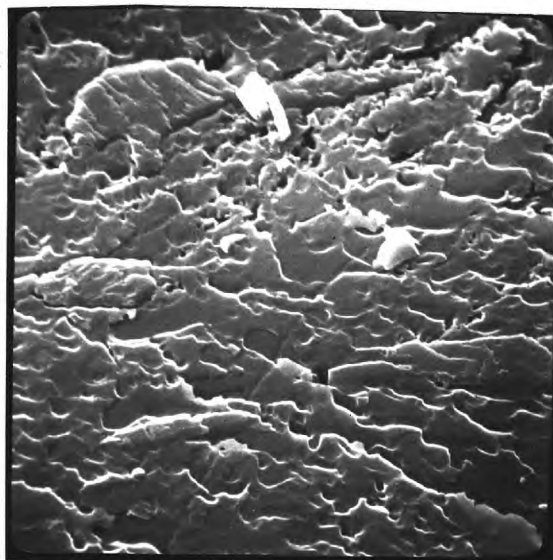
when heated to 160°C. The lump surface became rough and developed fine cracks as shown in Figure 13a. No solid product was deposited on the mineral surface.

The microcline surface, like that of albite, was almost evenly etched with no product solids formed on the surface (Figure 13b).

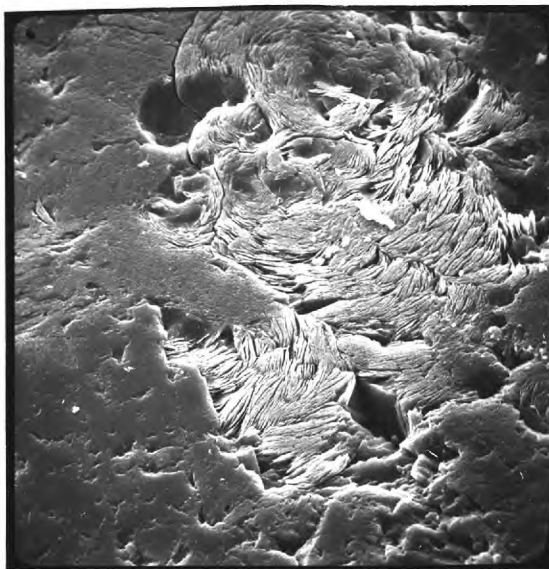
Different parts of the anorthosite mineral surface were attacked to varying extents. Most of its surface was almost smooth and slightly affected by the alkali solution when heated to 160°C, but some areas were relatively deeply attacked (Figure 13c & d). The outer surface



(a)



(b)



(c)



(d)

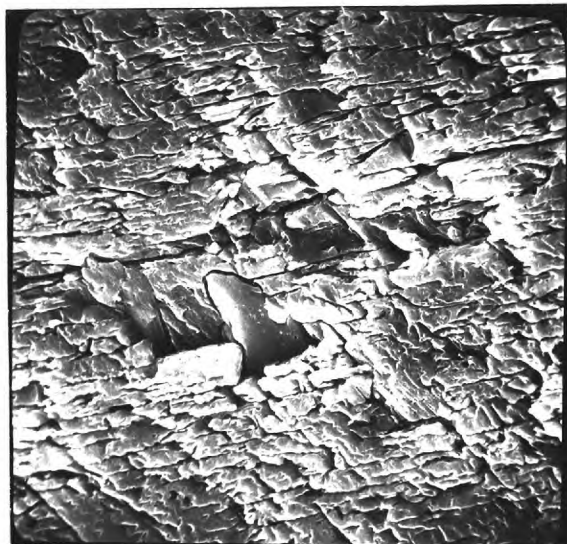
Figure 13. Scanning electromicrographs for mineral surfaces heated to 160°C in 500 g/l NaOH solutions; (a) Albite, 9135x; (b) Microcline, 4470x; (c) Anorthosite, 410x; and (d) Attacked parts in central area of micrograph c, 4100x.

of the areas which were least attacked were found by electron-probe microanalysis to be composed of relatively large grains of a calcium aluminosilicate phase (calcium-feldspar). On the other hand, the outer surface of the deeply attacked areas was found to contain very fine intergrowths of quartz particles and calcium- and sodium-feldspar particles.

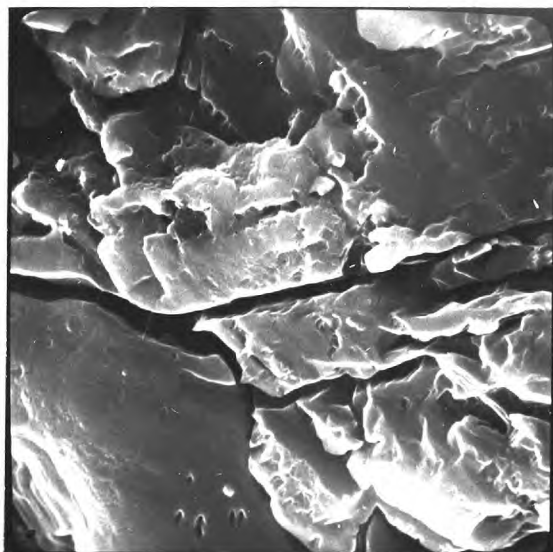
#### 5.1.1.2 Lumps Heated to 190°C

When heated to 190°C, the albite mineral surface was attacked to a greater extent than when heated to 160°C and the surface became rough with deep fissures. As shown in Figure 14a & b, the attack was almost even on the whole surface. No product layer was found on the mineral surface at this temperature.

The microcline surface was unevenly attacked by the caustic solution when heated to this temperature: some areas were deeply attacked and became very rough and porous and others were only slightly affected (Figure 14c & d). The latter areas seemed to be attacked to a similar extent as the albite mineral surface treated under the same conditions (Figure 14a & b). The whole microcline surface was composed of alternating strips of slightly reacted and deeply attacked parts. Examination of the mineral surface by electron-probe microanalysis showed that the slightly attacked parts of the surface were the sodium-rich phase in the mineral sample (see section 2.2.1.6) and the deeply attacked areas were mainly the potassium-rich phase (Figure 15). No product solids were found on the surface of the mineral.



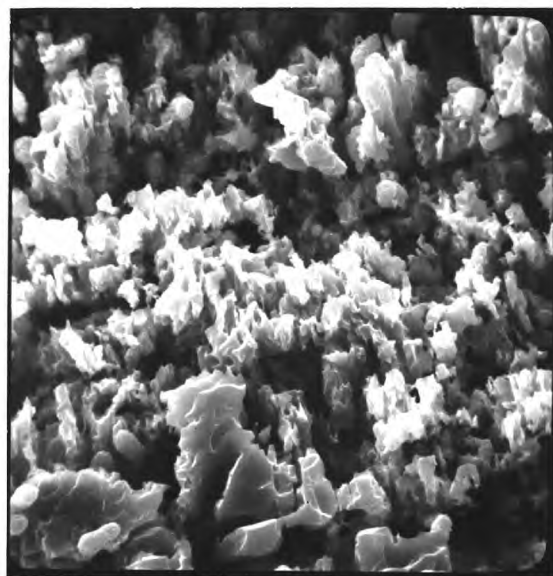
(a)



(b)



(c)



(d)

Figure 14. Scanning electronmicrographs for mineral surfaces heated to  $190^{\circ}\text{C}$  in 500 g/l NaOH solutions; (a) Albite, 980x; (b) Central area of micrograph (a), 4440x; (c) Microcline, 440x; and (d) Central area of micrograph (c), 1180x.

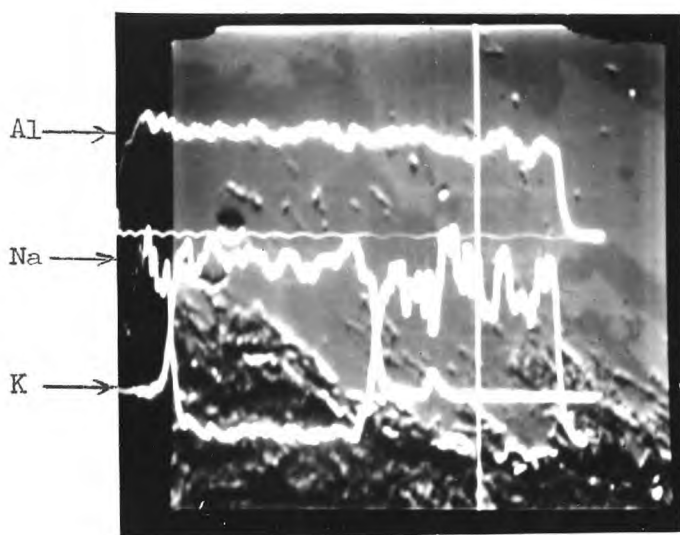
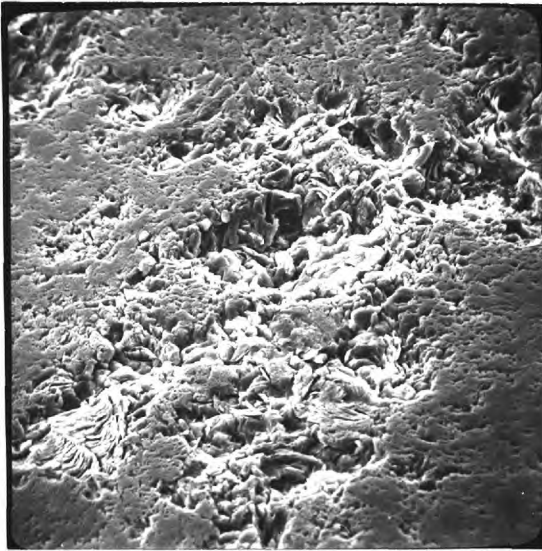
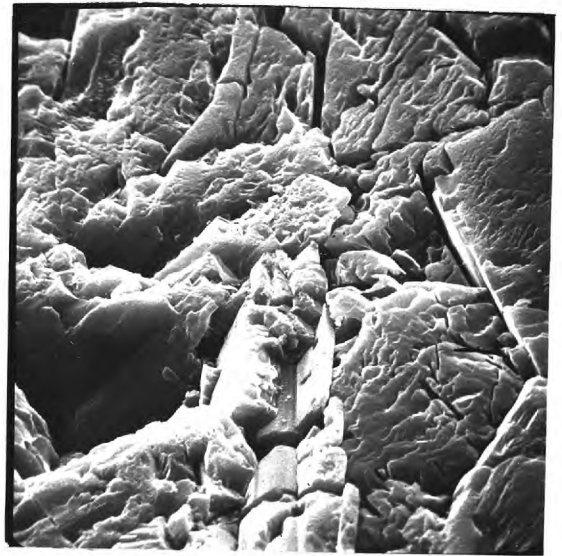


Figure 15. Electron image of a vertical section through reacted surface of microcline, when heated to  $190^{\circ}\text{C}$  in 500 g/l NaOH solution, superimposed on the X-ray line scans for aluminium, sodium and potassium. The vertical line represents the scanning line. Magnification 320x.

When the anorthosite mineral was heated to  $190^{\circ}\text{C}$ , the degree of attack on the mineral surface by the sodium hydroxide solution varied for the different parts of the surface (Figure 16). Some areas were quite reactive and became very rough after being deeply attacked. The rest of the surface was less affected but developed deep cracks. Figure 16 shows that the slightly attacked areas were composed of relatively large grains while the more reactive parts were in the form of thin layers. Electron-probe microanalysis showed that the large, slightly attacked particles were calcium feldspar crystals and the thin layers of the reactive areas were intergrowths of fine



(a)



(b)



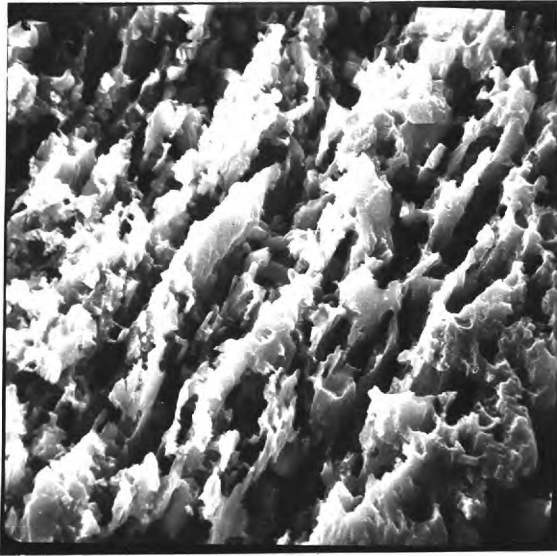
(c)



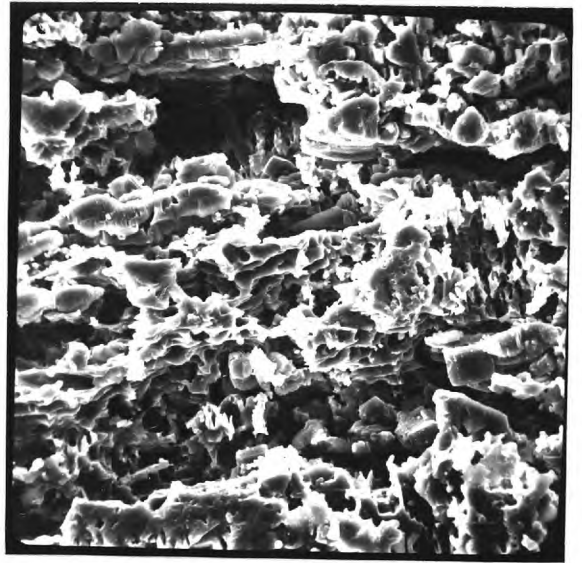
(d)

Figure 16. Scanning electronmicrographs for the anorthosite surface heated to  $190^{\circ}\text{C}$  in 500 g/l NaOH solution; (a) General view of the treated surface, 168x; (b) Slightly attacked areas of the surface, 1700x; (c) Deeply attacked parts in the central area of micrograph (a), 840x; and (d) Central area of micrograph (c), 4200x.

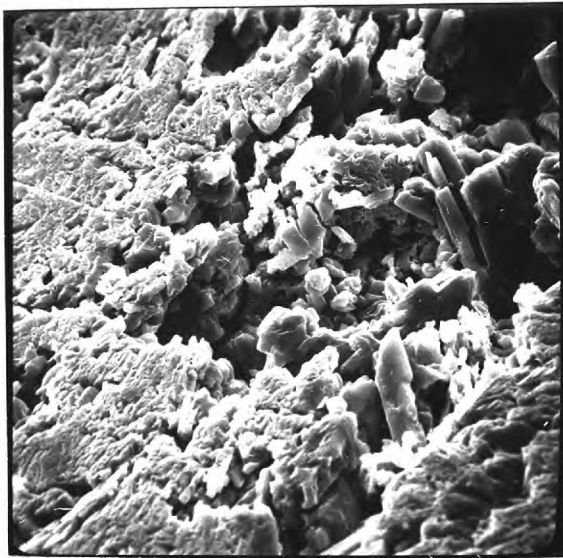




(a)



(b)



(c)



(d)

Figure 17. Scanning electronmicrographs for mineral surfaces heated to 220°C in 500 g/l NaOH solutions; (a) Albite, 835x; (b) Microcline, 440x; (c) Anorthosite, 440x; and (d) Deeply attacked parts in central area of micrograph (c), 1770x.

grains of quartz, sodium-feldspar and calcium feldspar. Like albite and microcline, no product layer was found on the anorthosite surface when heated to 190°C.

#### 5.1.1.3 Lumps Heated to 220°C

When heated to 220°C, albite and microcline surfaces became very rough and porous but no product layer was found on the mineral surfaces (Figure 17a & b). The microcline mineral was attacked to a greater extent than albite and when examined by electron-probe microanalysis the outer, rough surface was found to be composed of the sodium-rich phase only (Figure 18). The rate of dissolution

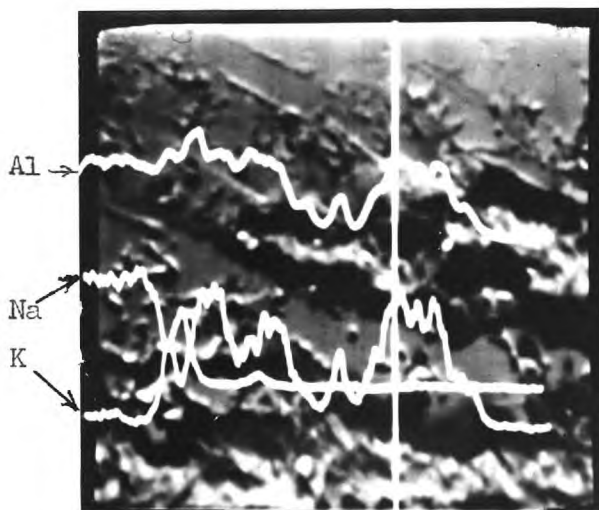


Figure 18. Electron image of a vertical section through the reacted surface of microcline, heated to 220°C in 500 g/l NaOH solution, superimposed on the X-ray line scans for aluminium, sodium and potassium. The vertical line in the micrograph represents the scanning line. Magnification, 600x.



of the potassium-rich phase in the mineral by the sodium hydroxide solution seemed to be higher than that of the sodium-rich one. Thus the former phase was leached from the outer surface of the mineral lump leaving the less reactive sodium-rich phase as a rough, porous layer.

The anorthosite lump heated to  $220^{\circ}\text{C}$  was generally attacked to a lesser extent and the mineral surface was smoother than those of albite and microcline heated to the same temperature. Some areas in the anorthosite surface were more deeply attacked than the rest of the surface (Figure 17c & d). As in the case of lumps heated to  $160$  and  $190^{\circ}\text{C}$ , the least affected areas of the surface were found to be the calcium feldspar crystals and the most reactive parts those composed of intergrowths of fine grains of quartz, sodium feldspar and calcium feldspar. Where the outer surface of the lump was composed of the sodium feldspar, the attack by the caustic solution was intermediate between the above two extremes. No product layer was found on the anorthosite surface heated to the temperature of  $220^{\circ}\text{C}$ , but occasional aggregates of hexagonal platy crystals of free calcium hydroxide were deposited on the surface.

#### 5.1.1.4 Lumps Heated to $250^{\circ}\text{C}$

When the mineral lumps were heated to  $250^{\circ}\text{C}$ , a product layer of elongated prismatic crystals of sodium calcium hydrosilicate with some hexagonal crystals of free calcium hydroxide was found on the mineral surfaces of all the minerals examined. The product layer

was found in particular in the cracks and the deeply attacked parts of the surfaces (Figure 19). Product layers on albite, microcline, and oligoclase surfaces were very porous and loose and peeled off readily. The peeled surface of the mineral looked very rough with large, deep cracks (Figure 19-b). On the anorthosite mineral surface, a thin and more firmly attached product layer was obtained.

Examination of the product layers formed on the different minerals by X-ray powder diffraction and electron-probe microanalysis confirmed that it was composed of sodium calcium hydrosilicate crystals with little free calcium hydroxide. There was no 'inner' or 'intermediate' layer between the original mineral surface and the layer of sodium calcium hydrosilicate crystals.

The results for oligoclase mineral heated to the different temperatures were similar to those of albite at the corresponding temperatures and, therefore, no detailed results for the treated oligoclase lumps are given.

The results obtained from the treatment of the different mineral lumps during the heating period showed that among the feldspars, the potassium member was the most reactive and the calcium member was the most refractory in the sodium hydroxide solutions. When the mineral sample was composed of more than one phase, e.g. microcline sample, the more reactive phase was attacked to greater extents than the less reactive phases.

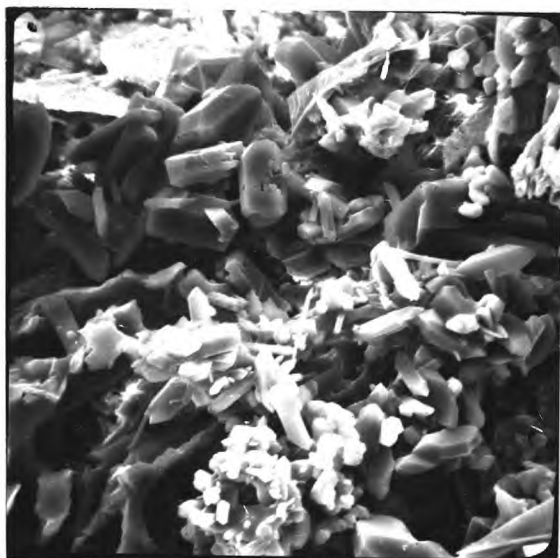
The results also showed that the leaching solution attacked the mineral surface, dissolving it without any product formation on the



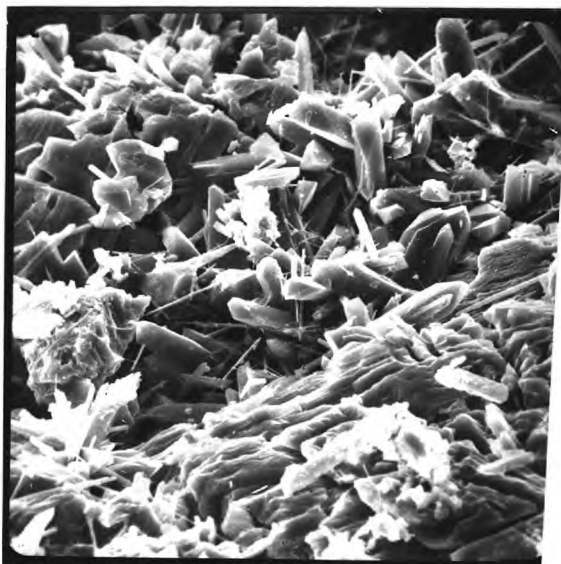
(a)



(b)



(c)



(d)

Figure 19. Scanning electronmicrographs of aluminosilicate minerals heated to 250°C in 500 g/l NaOH solutions;  
(a) Albite, 182x; (b) peeled surface of albite, 880x;  
(c) Mincrocline, 870x; and (d) Anorthosite, 430.

surface at low temperatures. When the mineral surface became very rough and cracked at higher temperatures, product crystals formed on the surface and in particular in cracks and deeply attacked areas.

### 5.1.2 The Effect of Alumina in the Leaching Solutions

To study the effect of the presence of alumina in the leaching solutions on the degree of the mineral attack and on the product layer formation, two parallel sets of experiments were carried out. In one set, solutions containing 500 g/l NaOH were used, and in the other sodium aluminate solutions containing 500 g/l NaOH and about 10 g/l  $Al_2O_3$ . Calcium oxide powder was added to both solutions. Polished lumps of albite, microcline and anorthosite were treated in these solutions at leaching temperatures of 160 and 220°C for one hour.

#### 5.1.2.1 Results of Treatment at 160°C

When the minerals were treated at 160°C, no product layer was noticed on any of the mineral surfaces treated in either sodium hydroxide or sodium aluminate solutions. Judged from the weight losses of the treated mineral lumps (Table 25), the reactivities of the minerals were higher and the degree of the surface attack was greater in the former solutions. The surfaces and the weight losses of the minerals treated in the sodium hydroxide solutions were similar to those of the corresponding minerals when heated to the temperature of 220°C during the heating period in section 5.1.1.3 (see Figures 17, 20, 21 and 22). In sodium aluminate solutions the results were similar to those obtained

when the mineral lumps were heated to the temperature of  $190^{\circ}\text{C}$  only in section 5.1.1.2 (see Figures 14, 16, 20, 21 and 22).

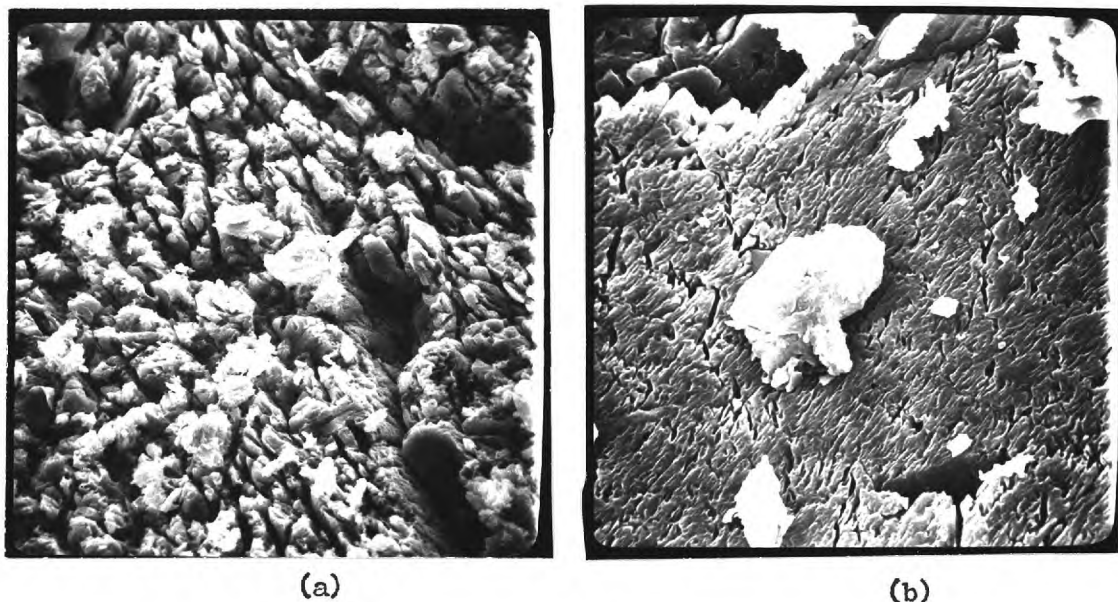
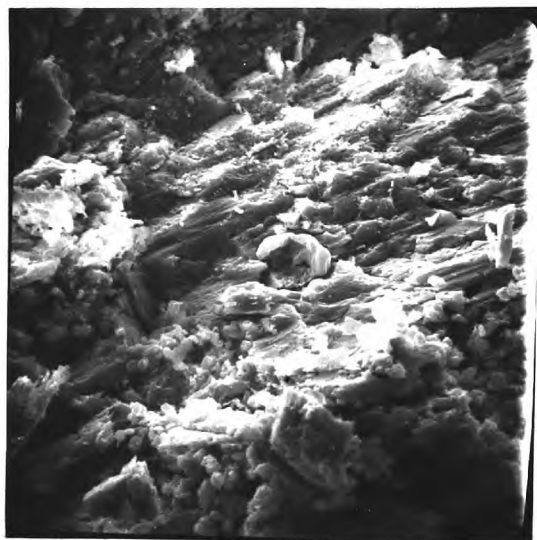


Figure 20. Scanning electromicrographs of reacted surfaces of albite treated at  $160^{\circ}\text{C}$  for one hour; (a) In sodium hydroxide solutions, 390x, and (b) In sodium aluminate solutions, 800x.

From the percentage weight losses of the lumps, the reactivity of the microcline mineral in the sodium hydroxide solution was shown to be about twice that in the aluminate solutions (Table 25). The difference between the reactivities in the sodium hydroxide solutions and in the sodium aluminate solutions were much greater even for albite and anorthosite than for microcline (Table 25).

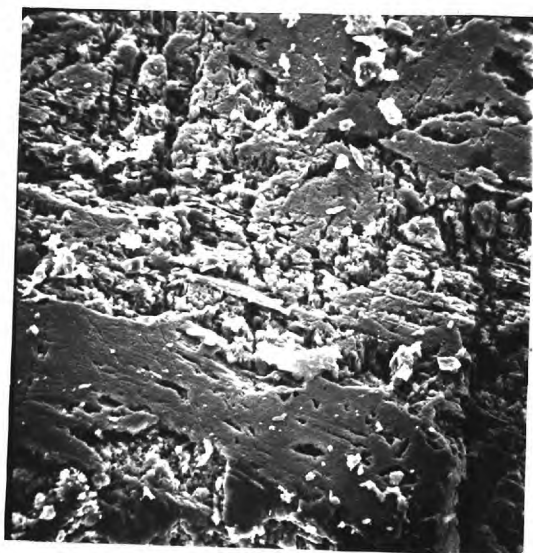
Preferential attack of the different parts of the microcline surface was observed on the lump treated in the aluminate solution, the potassium-rich areas being attacked to a greater extent than



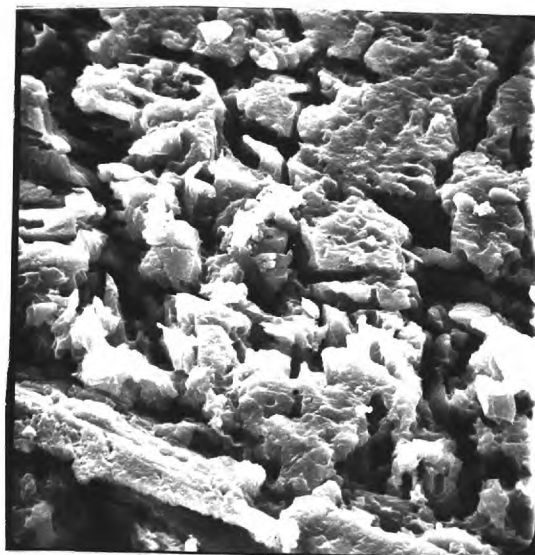
(a)



(b)

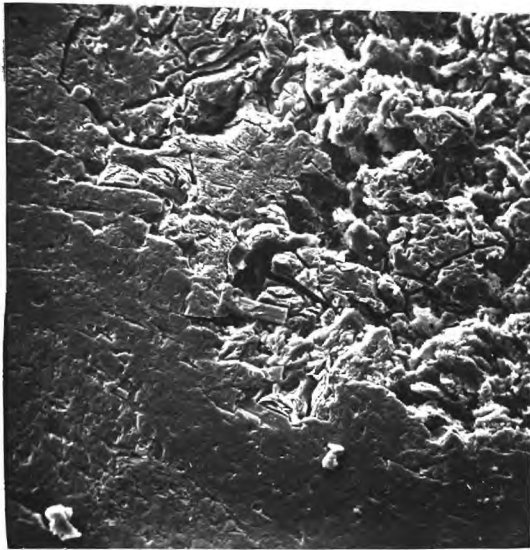


(c)

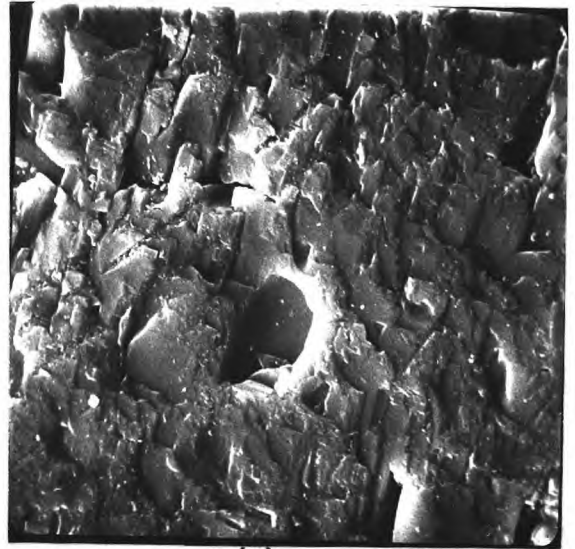


(d)

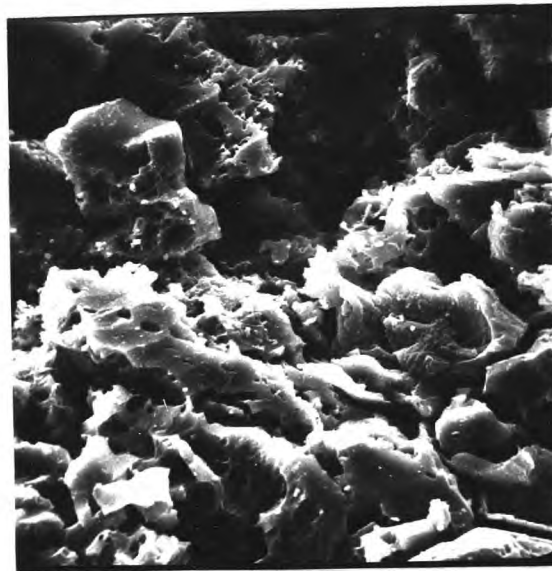
Figure 21. Scanning electronmicrographs of reacted surfaces of microcline treated in sodium hydroxide solutions (a & b) and in sodium aluminate solutions (c & d) at  $160^{\circ}\text{C}$  for one hr. Magnification, (a) 417x; (b) central area of micrographs (a), 1670x; (c) 155x; and (d) central area of micrograph (c), 760x.



(a)



(b)



(c)

Figure 22. Scanning electronmicrographs of Anorthosite surface treated in sodium aluminate solution at  $160^{\circ}\text{C}$  for one hour (a) General view of the surface, 202x; (b) Slightly attacked areas of the surface, 2020x; and (c) Deeply attacked parts of the surface, 1000x.



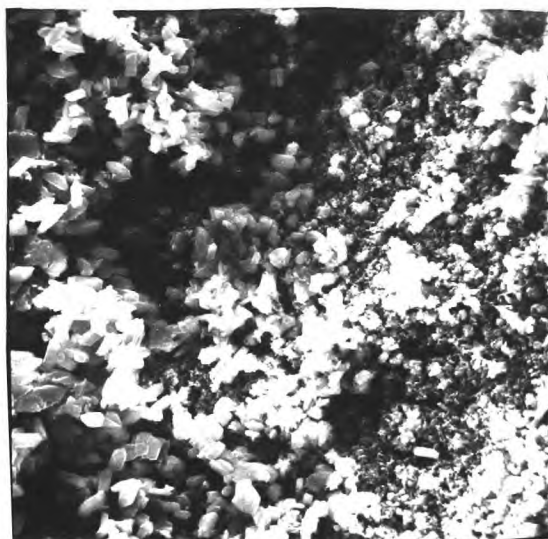
the sodium-rich parts (Figure 21). In the sodium hydroxide solutions the attack was generally deeper and the preferential attack was less obvious than in the aluminate solutions.

The appearance of the anorthosite surface treated in the sodium hydroxide solutions and that treated in the aluminate solutions were essentially the same. Those obtained from treatment in the aluminate solutions are shown in Figure 22. The degree of attack of the surface was generally low and the calcium feldspar areas of the surface were hardly affected in both solutions. The more reactive parts of the surface, which were composed of the quart-feldspar intergrowths, were more deeply attacked in the sodium hydroxide solutions than in the aluminate solutions.

#### 5.1.2.2 Results of Treatment at 220°C

When treated at a temperature of 220°C, the albite and the microcline minerals were strongly attacked in the sodium hydroxide solutions and their surfaces became rough and porous and covered with a thin, loose product layer of slightly elongated crystals. Figure 23 shows the surfaces of albite treated in sodium hydroxide and sodium aluminate solutions. Those of microcline were similar to these in the figure. The product layer formed on both albite and microcline surfaces in sodium hydroxide solutions was found by X-ray powder diffraction to be sodium calcium hydrosilicate with little free calcium hydroxide.

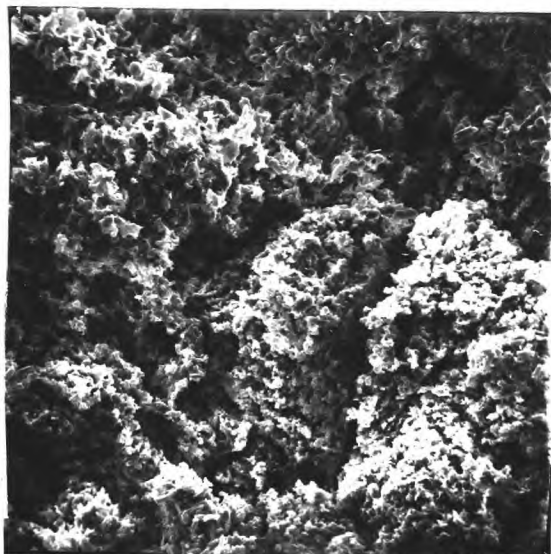




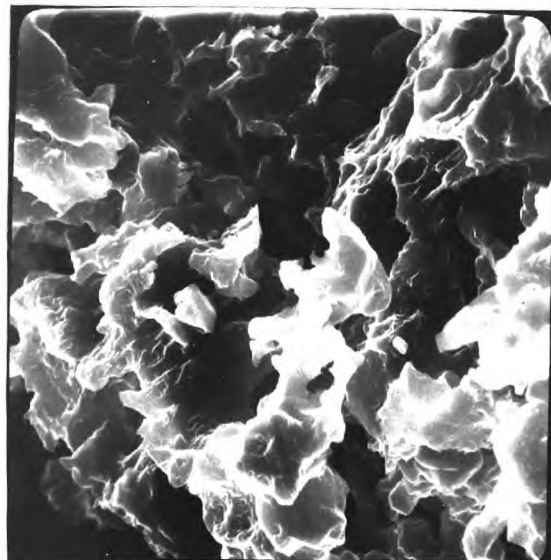
(a)



(b)



(c)



(d)

Figure 23. Scanning electronmicrographs of Albite surface treated in sodium hydroxide solution (a & b) and in sodium aluminate solution (c & d) at 220°C for one hour. Magnification (a) 490x; (b) Central area of micrograph (a), 1950x; (c) 168x; and (d) Central area of micrograph (c), 1680x.

In the sodium aluminate solutions, the degree of attack of albite and microcline was less and there were occasional aggregates of product crystals on their surfaces but no continuous layer, such as that obtained in the sodium hydroxide solutions, was noticed. The percentage weight losses of the albite and microcline lumps treated in the sodium hydroxide solutions were about twice those for lumps treated in the aluminate solutions, in spite of the fact that the latter had less product layer on their surfaces (Table 25)

A thin product layer of sodium calcium hydrosilicate crystals was found on the anorthosite surfaces treated in sodium hydroxide solution and in sodium aluminate solutions. The surfaces looked essentially similar to those in Figure 24a, but the product layer was thinner. In both the hydroxide and aluminate solutions the degree of attack on the mineral surface varied for the different areas, the large calcium feldspar grains being only slightly affected by the solutions and the areas with the fine intergrowths of quartz and feldspar being deeply attacked. Like albite and microcline, the anorthosite mineral was more reactive in sodium hydroxide solutions and the percentage weight loss of the lump was more than twice that found in the aluminate solutions at the same temperature.

The above results showed that alumina present in the leaching solutions had no significant effect on the formation of the product layer on the aluminosilicate minerals surfaces. It has also been shown in section 4.1.3 that the presence of alumina in the initial

leaching solutions did not affect the degree of alumina recovery from ground aluminosilicate mineral samples as long as the calculated final caustic ratio,  $\alpha_f$ , was higher than 12. Its presence, however, reduced the rates of dissolution of aluminosilicate minerals to about half their values in the pure sodium hydroxide solutions under the same experimental conditions. No satisfactory explanation could be given for this effect.

### 5.1.3 Results of Treatment at 280°C for Two Hours

Polished lumps of the different aluminosilicate minerals were treated in alkaline solutions at a constant leaching temperature of 280°C for a period of two hours. The experiments were carried out in sodium aluminate solutions containing 500 g/l NaOH and about 16 g/l  $Al_2O_3$  in the presence of suspended lime. The heating rate for the reaction mixtures in these tests was about 170°C/hr.

The surfaces of the treated mineral lumps were examined by scanning electron microscopy and electron-probe microanalysis. When a product layer was found on the treated mineral surface the layer was scrapped off and examined by X-ray powder diffraction. When this layer was relatively thick the outer part and the inner part of it were examined separately.

Porous product layers of varying thicknesses were found on the surface of all the aluminosilicate minerals treated under the above mentioned conditions except on the kyanite mineral surface. The results obtained for the different minerals studied may be

summerized in the following:

#### 5.1.3.1 Anorthosite

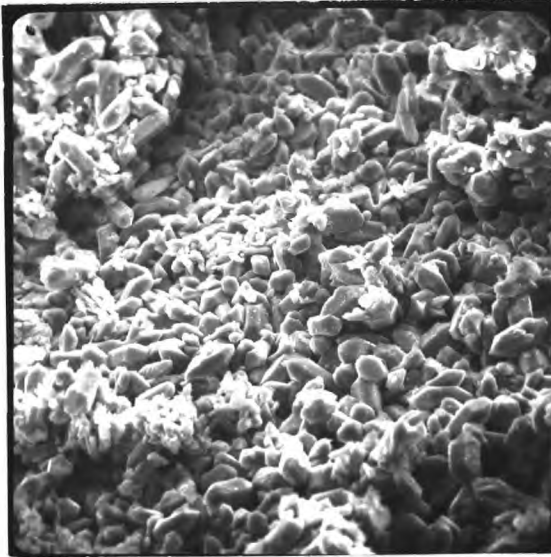
When an anorthosite mineral lump was treated under the above mentioned conditions, it was attacked with the formation of a thin product layer of well-formed, slightly elongated, prismatic crystals on the surface (Figure 24 a). These crystals were found to be sodium calcium hydrosilicate. No 'inner' layer was found between these crystals and the original mineral surface. The apparent weight loss of the treated lump was about 10%.

#### 5.1.3.2 Muscovite

When a sheet of the muscovite mineral was treated, it was strongly attacked by the solution with an apparent weight loss of about 25%. Examination of the surface showed that it had occasional aggregates of sodium calcium hydrosilicate crystals, but it was not completely covered with a product layer (Figure 24 b).

#### 5.1.3.3 Kyanite

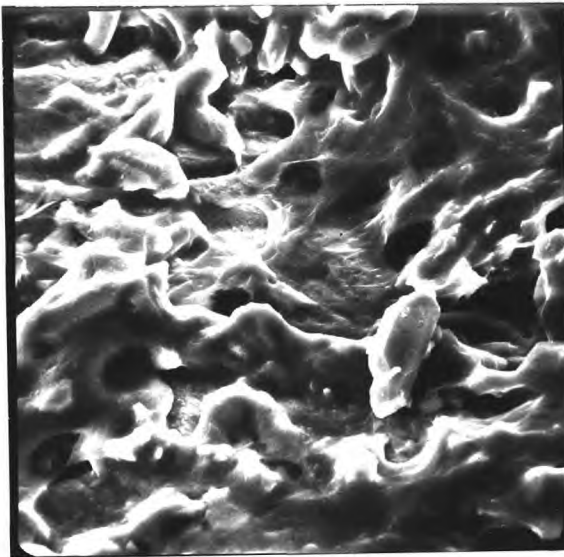
The kyanite surface looked as though it had been attacked, but there was almost no adherent product layer on the mineral surface (Figure 24 c & d). The absence of this product layer was confirmed by X-ray powder diffraction and electron-probe microanalysis. The weight loss of the mineral after the treatment was about 7.7%. It should be noted that this weight loss was not due to the kyanite dissolution only, but included the loss due to the dissolution of quartz inclusions which were associated with the mineral sample.



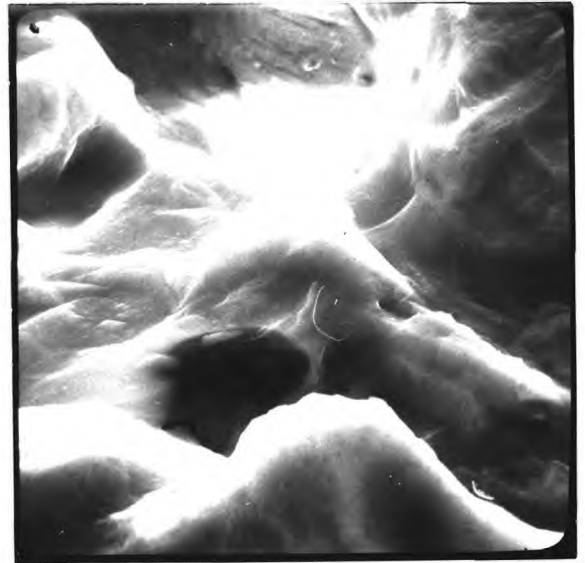
(a)



(b)



(c)



(d)

Figure 24. Scanning electron micrographs of treated surfaces of aluminosilicates treated in sodium aluminate solutions at 280°C for two hours; (a) Anorthosite, 190x; (b) Muscovite, 140x; (c) Kyanite, 413x; and (d) Central area of micrograph (c), 1655x.

#### 5.1.3.4 Feldspars Other than Anorthosite

When lumps of albite, microcline, oligoclase, labradorite and andesine minerals were treated separately under the above mentioned leaching conditions, all the minerals were strongly attacked by the solution and developed a product layer on their surfaces. Almost uniform, thick product layers were found on albite, microcline and oligoclase surfaces, and thinner layers on labradorite and andesine. These layers were occasionally as much as a few millimeters in thickness. After scraping the product layer off the reacted mineral surface, the weight losses were found to be about 42, 33, 31, 20 and 15% for microcline, albite, oligoclase, labradorite and andesine respectively.

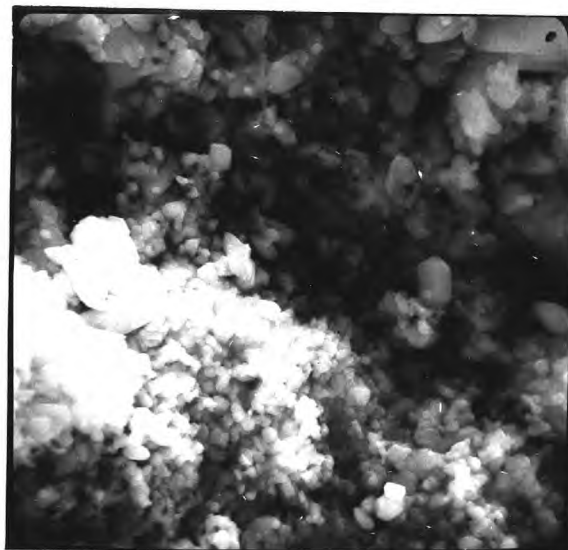
The product layers on these minerals were found to consist of two distinct, inner and outer layers of different chemical and structural compositions:

a) The outer, highly porous layer consisted of relatively large, elongated prismatic crystals similar to those obtained in the residues when treating the ground mineral samples (section 4.1.1). Micrographs of this outer layer on oligoclase and microcline mineral lumps are shown in Figure 25.a & c. Those on albite, andesine and labradorite are similar to the above mentioned figure. These outer layers were found to be composed of sodium calcium hydrosilicate crystals with small amounts of free calcium hydroxide.

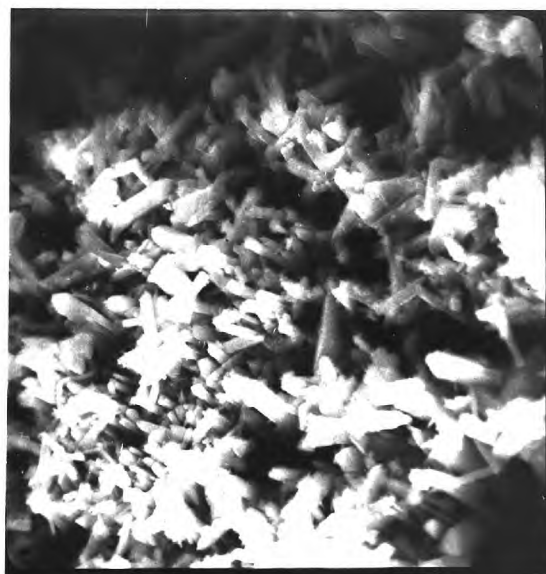
b) The inner layer, which was situated between the outer layer and the mineral surface, was more compact than the outer layer and



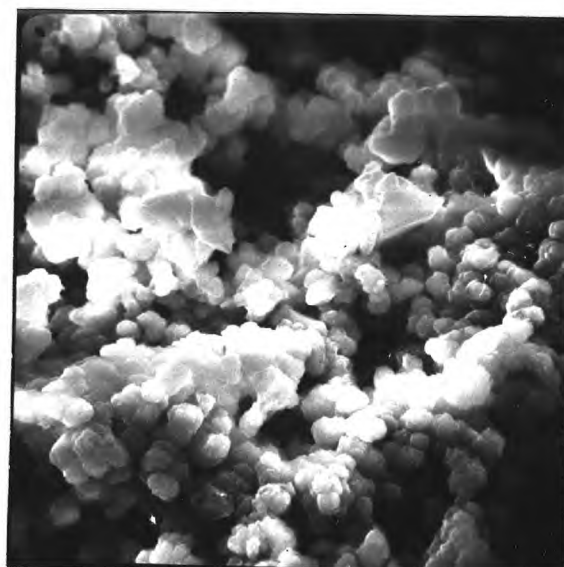
(a)



(b)



(c)



(d)

Figure 25. Product layers formed on the surface of aluminosilicate minerals when treated in sodium aluminate solutions at  $280^{\circ}\text{C}$  for two hours; (a) Outer layer on Oligoclase, 815x; (b) Inner layer on Oligoclase, 2215; (c) Outer layer on Microcline, 1040x; and (d) Inner layer on Microcline, 1775x.

consisted of smaller, rounded crystals. This type of crystal is represented in Figure 25-b & d for the inner layers formed on oligoclase and microcline respectively.

When this inner layer was examined by electron-probe microanalysis, it was found to contain sodium, aluminium, silicon and very little calcium, as distinct from the outer layer which contained sodium, calcium and silicon but no aluminium. Figure 26 a & b shows the relative distributions of the major elements in the inner layer and the original mineral, for oligoclase and microcline minerals. It also shows that the sodium and aluminium contents in the inner layer on the mineral surface (From A to B in the figure) were higher than those in the original mineral (From B to C in the figure). The silicon decreased to about half the level in the original mineral. In the inner layer on the microcline surface, potassium was completely replaced by sodium. The composition of the inner layers formed on albite, andesine and labradorite were essentially similar to those in Figure 26.

X-ray powder diffraction showed that this inner layer was composed mainly of sodium hydroaluminosilicate crystals of the composition  $3(\text{Na}_2\text{O} \cdot \text{Al}_2\text{O}_3 \cdot 2\text{SiO}_2) \cdot \text{Na}_2\text{O} \cdot \text{H}_2\text{O}$  (127).

It seemed that when the outer layer of sodium calcium hydrosilicate reached a certain thickness on the surface of these minerals, the sodium hydroxide solution continued to attack and dissolve the mineral and the attack was followed by the crystallization of a sodium hydroaluminosilicate phase. Due to the deficiency of lime in



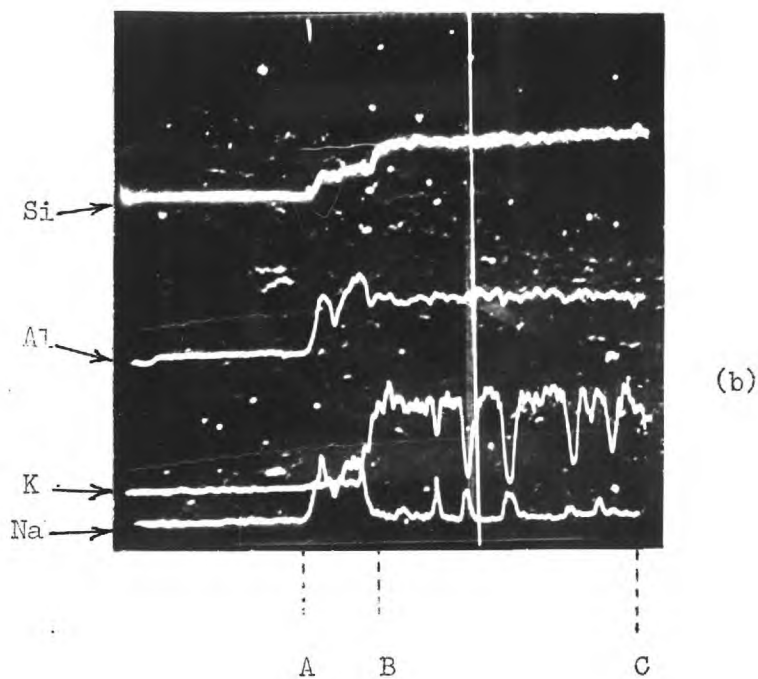
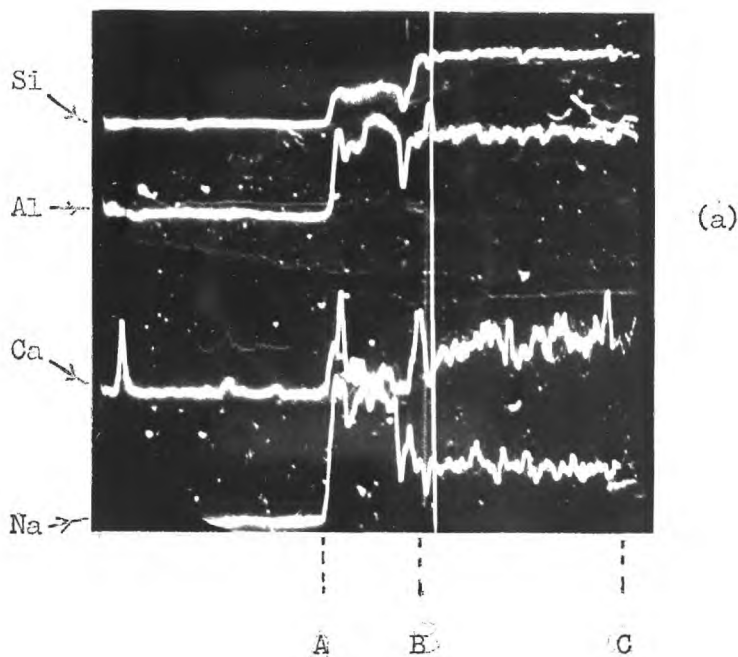


Figure 26. Electronmicroprobe X-ray line scans showing the relative distributions of the major elements in the inner product layer (from A to B) and in the original mineral (from B to C); (a) for Oligoclase, 70x; and (b) for Microcline, 140x.

this zone, which had to diffuse from the bulk solution through the outer layer, sodium calcium hydrosilicate was not formed. In otherwords, under these conditions the rate of the mineral dissolution was higher than that for the diffusion of the silicate ions and the calcium ions through the outer product layer.

Comparison between the results of treatment and weight losses of albite and microcline minerals under the above mentioned conditions and between those obtained at 220°C (section 5.1.2.2) indicated that the rate of mineral dissolution at 280°C should have been greatly reduced part way through the treatment. It should be noted that the principal difference between the two cases was that no 'inner' product layer of the small, compact crystals of sodium hydroaluminosilicate was formed on the mineral surfaces treated at 220°C, such as those obtained at 280°C. Thus the formation of these crystals on the mineral surface must have been the cause of the great reduction in the rate of mineral dissolution at 280°C.

#### 5.1.4 Kyanite Treatment at 300°C

It was shown in the previous section that the kyanite mineral was slightly attacked when treated at 280°C for two hours, with no product formation on its surface. To find out whether it was possible to produce a product layer on the mineral surface, the mineral was treated under more severe conditions than those mentioned above. A polished lump was treated in 646 g/l NaOH solution containing 10 g/l Al<sub>2</sub>O<sub>3</sub> at a constant temperature of 300°C for two hours.

The mineral surface was not deeply attacked but it became rough.

It looked essentially similar to that treated at 280°C (Figure 24 c & d). No product layer, except some free calcium hydroxide crystals, was found on the treated mineral surface. The apparent weight loss of the lump was about 15% compared with the 7.7% when it was treated in 500 g/l NaOH at 280°C for two hours.

These results demonstrated the low reactivity of the kyanite mineral in the sodium hydroxide solutions and showed that the rate of mineral dissolution was so slow at temperatures as high as 300°C that the leaching process continued to be chemically-controlled at these temperatures. These results were in agreement with the results obtained on the ground mineral samples given in section 4.2.3 and showed that the mineral reactivity depended greatly on leaching temperature, solution concentration and on the mineral particle size.

#### 5.1.5 Reactivity of Quartz in the Leaching Solutions

The reactivity of quartz in sodium hydroxide solutions and the charges on the mineral surface during the heating step were investigated. Lumps of the crystalline quartz sample were heated in 500 g/l NaOH solutions in the absence of lime to temperatures of 160°C and 190°C.

When the lumps were heated to 160°C, the surface was nonuniformly etched and fine fissures developed on the mineral surface, as shown in Figure 27. At 190°C the mineral surface became very rough and the cracks large and deep (Figure 28 a & b). The weight losses of the treated mineral lumps were 0.4% and 1.7% at 160 and 190°C respectively.

The results showed that the quartz mineral surface was attacked

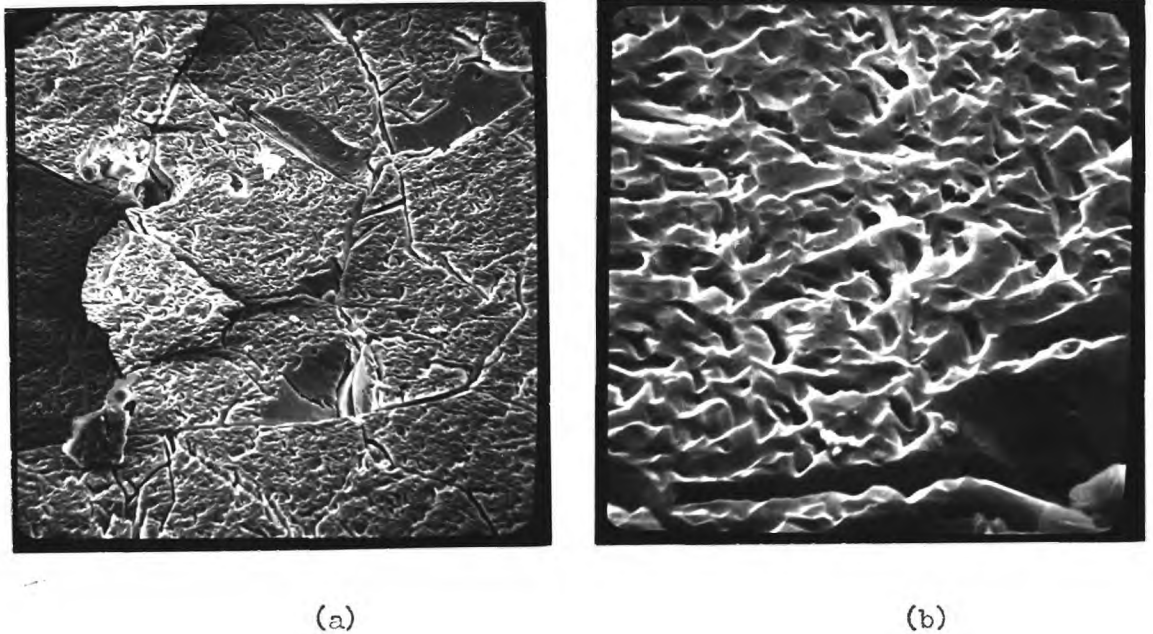
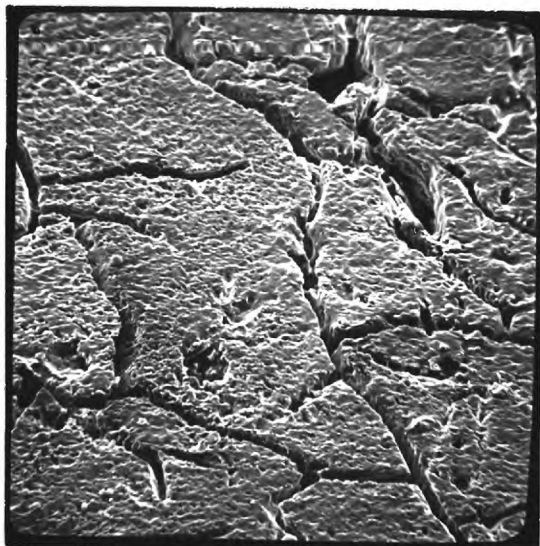


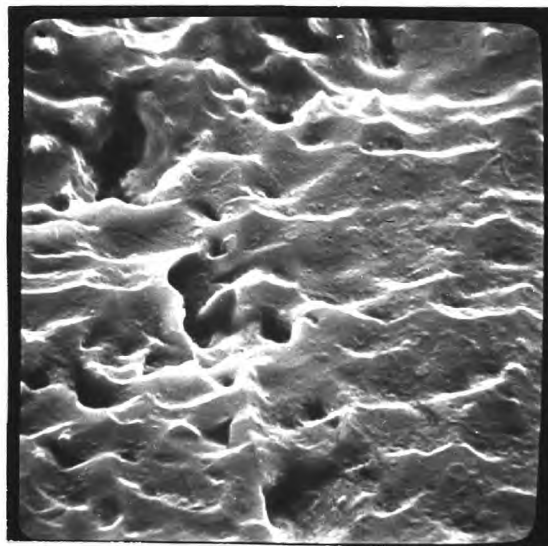
Figure 27. Scanning electron micrographs of quartz surface heated to 160°C in 500 g/l NaOH solution, (a) 907x; (b) Central area of micrograph (a), 4535x.

by the sodium hydroxide solution with the dissolution of the mineral. There was no evidence of any product formation on the mineral surface when treated at 160 or 190°C. The dissolution of quartz by pure sodium hydroxide solution, without the formation of a product layer on the surface, was similar to the dissolution of aluminosilicate minerals during the heating period in sodium hydroxide solutions in the presence of lime (section 5.1.1). As shown in section 5.1.3.4, the dissolution of the aluminosilicates was also found to take place in the absence of lime, with the formation of sodium hydroaluminosilicate as an inner layer on some aluminosilicate mineral surfaces.

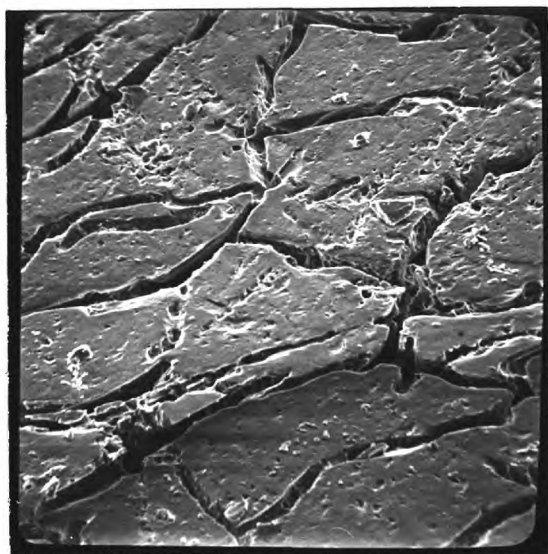
To elucidate the role of lime in the leaching process and to study



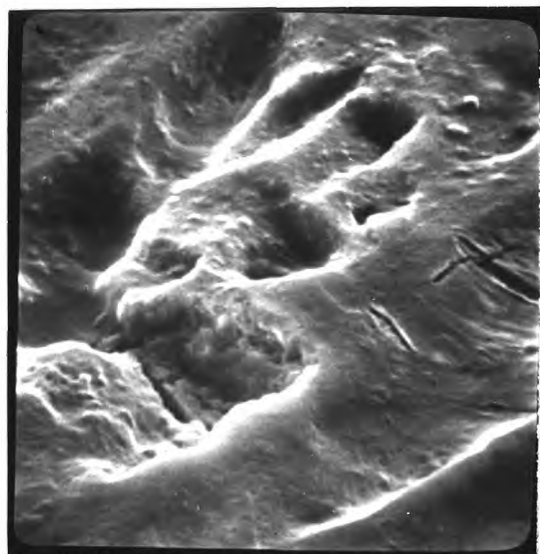
(a)



(b)



(c)



(d)

Figure 28. Scanning micrographs of quartz surface heated to  $190^{\circ}\text{C}$  in 500 g/l NaOH solution in the absence of lime (a & b) and in the presence of lime (c & d).

Magnification (a) 444x; (b) 4440x; (c) 383x; and (d) 7600x.

its effect on the reactivity of quartz, and on the attack of mineral surface by the solution during the heating step, a lump was heated to a temperature of  $190^{\circ}\text{C}$  in 500 g/l NaOH solution, in the presence of suspended lime. The surface was then examined. The results obtained were compared with those obtained in sodium hydroxide solution alone, heated to  $190^{\circ}\text{C}$ . Although the surface of the lump, heated in the presence of lime, looked smoother than that heated in its absence (Figure 28), both surfaces developed deep, large fissures and the weight losses were similar in both cases. No product layer was found on the mineral lump in either solution.

From the results it was evident that calcium hydroxide had no significant effect on the degree and the manner of the quartz dissolution in sodium hydroxide solutions during the heating period. In other words, calcium hydroxide did not seem to attack the mineral simultaneously with sodium hydroxide solutions during the dissolution of the mineral.

The quartz mineral was treated in sodium aluminate solutions in the presence of lime suspension at leaching temperatures of  $220^{\circ}\text{C}$  and  $280^{\circ}\text{C}$ . When treated at  $220^{\circ}\text{C}$  for one hour, the mineral was deeply attacked and a product layer of elongated prismatic crystals were formed on the surface (Figure 29.a). X-ray powder diffraction showed that the layer was composed of sodium calcium hydrosilicate crystals.

When the mineral was treated in a solution containing 500 g/l NaOH and about 16 g/l  $\text{Al}_2\text{O}_3$  with lime suspension at  $280^{\circ}\text{C}$  for two hours, the mineral was strongly attacked by the solution and developed

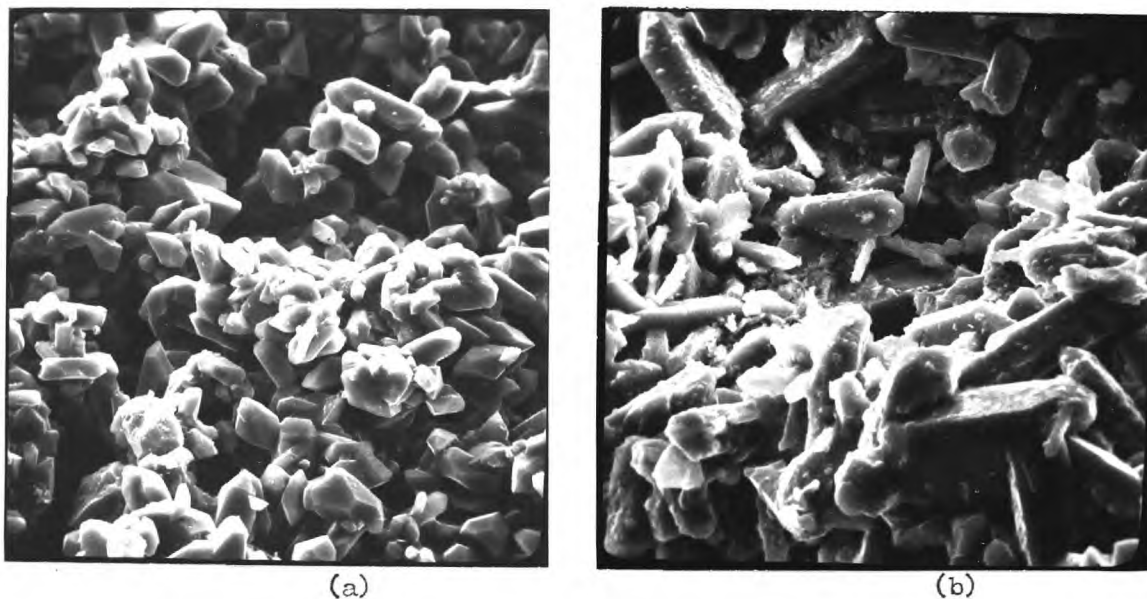


Figure 29. Scanning electronmicrographs of treated quartz surface in aluminate solutions; (a) Treated at 220°C for 1 hr., 400x; and (b) Treated at 280°C for 2 hrs., 477x.

a thick product layer on its surface. After scraping the product layer off the surface, the weight loss of the lump was found to be about 48%. The product layer on the mineral surface was found to consist of two parts; a) an outer layer of elongated prismatic crystals of sodium calcium hydrosilicate (Figure 29. b), and b) an inner layer of relatively smaller, rounded crystals of sodium hydroaluminosilicate with some sodium calcium hydrosilicate crystals. It should be noted that these results are similar to those obtained from treatment of reactive feldspar minerals under the same leaching conditions (section 5.1.3.4).

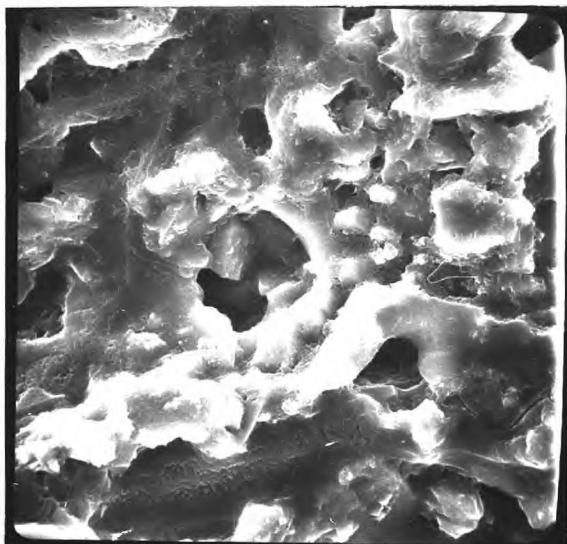
### 5.1.6 Treatment of Some Calcium Silicate Minerals

As shown in section 5.1.3.4, the treatment of quartz and some aluminosilicates, in sodium aluminate solutions at a constant temperature of 280°C for two hours, led to the formation of sodium hydroaluminosilicate crystals, as an 'inner' layer, on the mineral surface. The formation of these crystals was due to the deficiency of lime and the presence of alumina in the reaction zone. Some aluminium-free calcium silicate minerals were treated in the leaching solutions to find out whether a product layer could be produced on their surfaces and, if a thick product layer could be produced, what would be the composition of the 'inner' part of this product layer. For this purpose lumps of wollastonite ( $\beta\text{-CaO}\cdot\text{SiO}_2$ ) and pectolite ( $\text{Na}_2\text{O}\cdot 4\text{CaO}\cdot 6\text{SiO}_2\cdot \text{H}_2\text{O}$ ) were used.

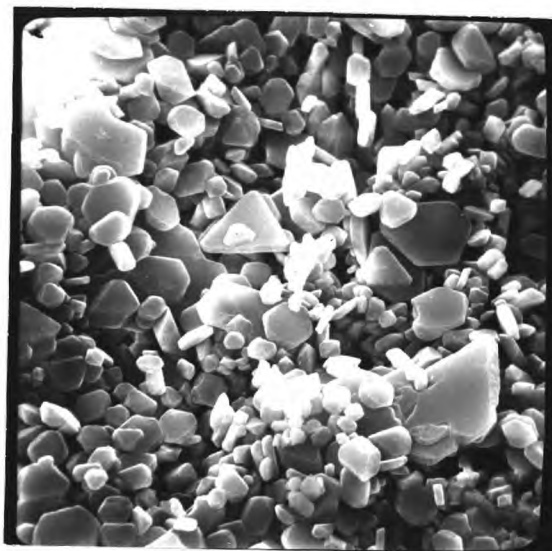
#### 5.1.6.1 Results of Treatment of Wollastonite

Wollastonite was chosen because of the fact that its dissolution would produce silicon and calcium in the ratio required for the production of sodium calcium hydrosilicate ( $\text{CaO}:\text{SiO}_2 = 1.0$ ). Polished lumps of a white crystalline wollastonite sample were treated in different concentrations of sodium hydroxide solutions, at leaching temperatures in the range 200 to 300°C. The mineral was slightly attacked under the different leaching conditions employed and no product layer was found on the mineral surface. When treated in a solution containing 646 g/l NaOH, at a constant leaching temperature for two hours, the mineral surface was attacked slightly and became rough (Figure 30. a), and the weight loss of the lump did not exceed 2%.

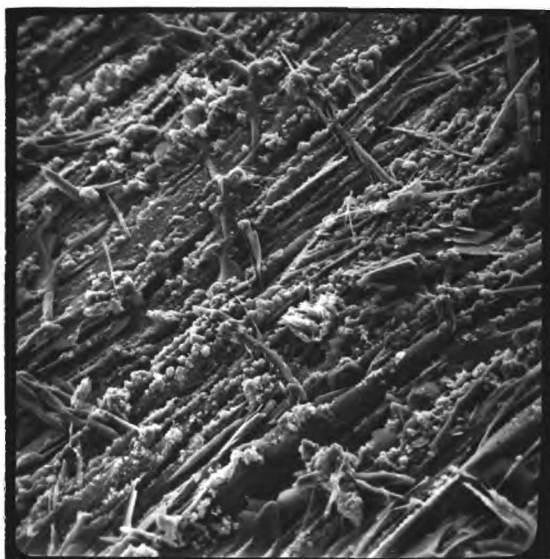




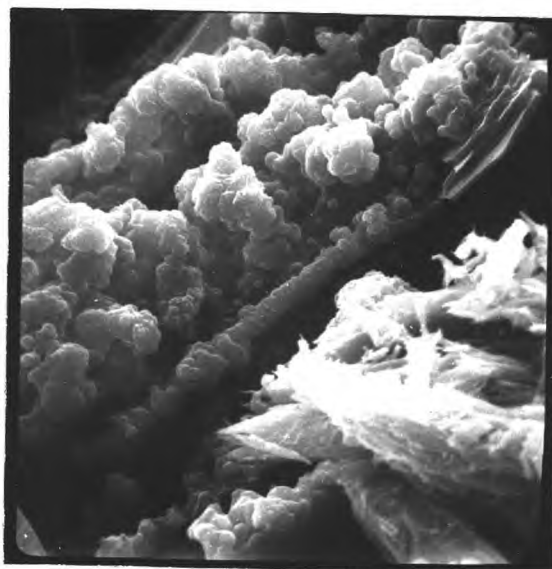
(a)



(b)



(c)



(d)

Figure 30. Scanning electronmicrographs of reacted surfaces of some aluminium-free minerals; (a) Wollastonite treated in 646 g/l NaOH at 300°C for 2 hrs., 854x; (b) Calcite treated in sodium aluminate solution at 280°C for 1 hr., 1470x; (c) Pectolite treated in 500 g/l NaOH solution at 280°C for 1 hr., 155x; and (d) Central area of micrograph (c) 1550x.

The presence of alumina or suspended lime in the leaching solution had no significant effect on the degree of attack of the mineral surface by the solution.

The results showed that the wollastonite mineral had a very low reactivity in the sodium hydroxide solutions. This was in agreement with the thermodynamic calculations given in section 1.2.

#### 5.1.6.2 Results of Treatment of Pectolite

Polished lumps of a crystalline pectolite sample were treated in both sodium hydroxide and sodium aluminate solutions at a constant leaching temperature of 280°C for one hour. The mineral surface was viturally unattacked in both solutions. No product layer was found on the surface, except the hexagonal crystals of calcium hydroxide, which deposited on the mineral surface from the leaching solution (Figure 30. c & d). This was confirmed by X-ray powder diffraction examination of the film scraped off the treated surface. It should be noted that the rough appearance of the treated mineral surface shown in Figure 30 c & d was not due to the attack of the surface by the leaching solution. Because of the fibrous nature of the mineral, it was not possible to obtain smooth surfaces by polishing.

It is interesting to note that calcite mineral lumps were strongly attacked in sodium hydroxide and in sodium aluminate solutions, and a thick product layer of hexagonal platy crystals of calcium hydroxide was formed in both solutions (Figure 30 .b).

#### 5.1.7 Treatment of Coarsely Ground Mineral Samples

To find out whether or not ground mineral samples would form a

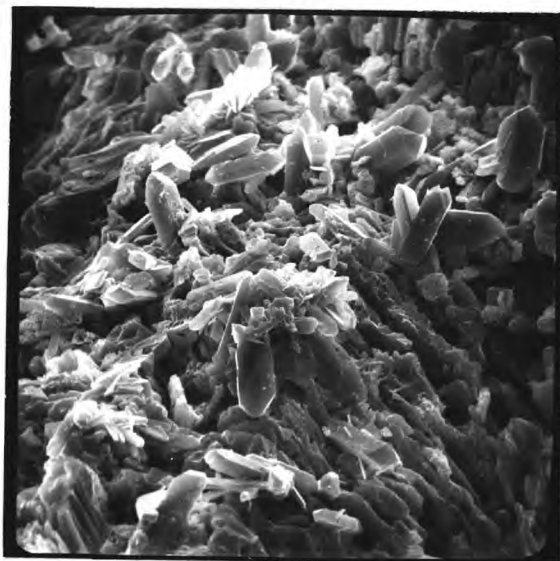
product layer on their surface during the leaching process, leaching experiments were carried out on coarsely ground feldspar samples. A -36 + 52 mesh size fraction of the ground samples of anorthosite and oligoclase were treated separately in a solution containing 500 g/l NaOH with a calculated caustic ratio of 30, and a molar ratio of CaO/SiO<sub>2</sub> of 1.1, at the leaching temperature of 220°C for 30 min. At the end of the experiment the precipitate was examined by optical microscopy, scanning electron microscopy and by X-ray powder diffraction. A polished section was prepared from the precipitate which was then examined by electron-probe micro-analysis.

The precipitates in both cases were found to be composed of sodium calcium hydrosilicate crystals, partially decomposed mineral grains and free calcium hydroxide. The surfaces of the mineral grains became very rough and had a layer of elongated prismatic crystals of sodium calcium hydrosilicate on them (Figure 31). The product layer was more continuous on the oligoclase particles than on the anorthosite one. The unreacted particles of anorthosite, and in particular their outer surfaces, were found to be mainly calcium feldspar, the sodium feldspar and quartz grains being preferentially attacked and dissolved from the original mineral sample. In the case of oligoclase mineral, the unreacted grains were almost pure feldspar, the quartz inclusions in the original mineral sample having been leached out.

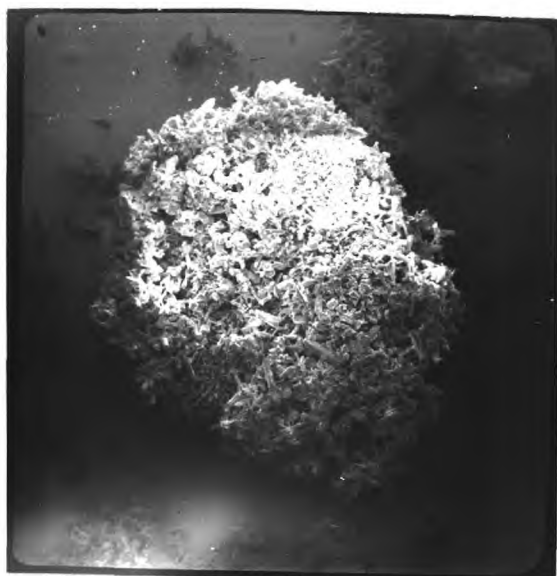
These results, on the coarsely ground mineral samples, showed



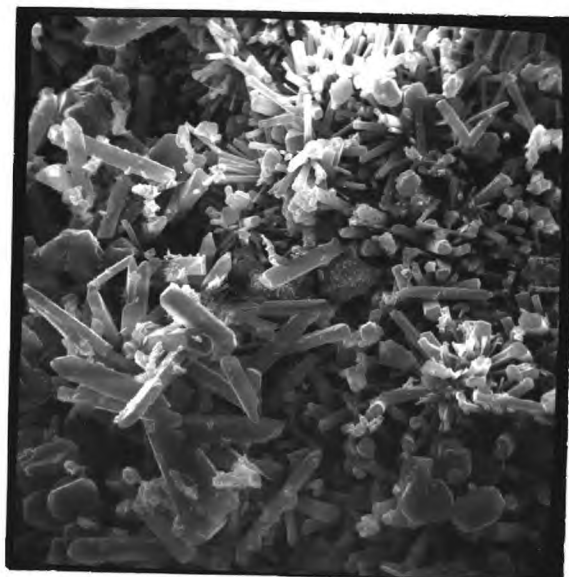
(a)



(b)



(c)



(d)

Figure 31. Scanning electronmicrographs of partially decomposed particles of Anorthosite (a & b) and Oligoclase (c & d) after treatment in 500 g/l NaOH solution at 220<sup>0</sup>C for 30 min. Magnification: (a) 120x; (b) 650x; (c) 122x; and (d) 627x.

that the formation of a product layer on the mineral surface during leaching was applicable to large mineral lumps as well as to ground mineral samples.

## 5.2 Discussion and Conclusions

The reactivities of the different aluminosilicate minerals obtained by the treatment of the mineral lumps were in agreement with the results described in the Chapter 4 using ground mineral samples. Kyanite was found to be the most refractory aluminosilicate mineral examined in both cases. Alkali feldspars were generally more reactive in sodium hydroxide solutions than the plagioclases. In the alkali feldspar series, potassium feldspar was more readily attacked by the solution than the sodium member. The calcium feldspar, anorthosite, had the lowest reactivity in sodium hydroxide solutions among the different feldspars.

The results also showed that:

a) The dissolution of the aluminosilicate minerals into different soluble species was the first main step in the leaching process. This step was followed by other steps such as the interaction between the dissolved, ionic species to form the solid phases.

b) Calcium hydroxide did not seem to attack the mineral simultaneously with the sodium hydroxide solution. It would react with the dissolved species to form the solid products in the system.

c) No product layer would form on the mineral surfaces in the early stages of heating in the leaching process. A product layer of sodium calcium hydrosilicate started to form on the surface of the

more reactive minerals when they became very rough and cracked. If this layer grew to a certain thickness, there would be a possibility for the formation of an 'inner' layer between the mineral surface and the outer layer.

By considering the formation of a product layer on the mineral surface when treated in aluminate solutions at a leaching temperature of 280°C, the different minerals examined could be divided into three main groups. These groups were

1) Minerals which formed a relatively thick product layer on the surface. This group represented the most reactive minerals and included microcline, albite, oligoclase, labradorite, andesine and quartz. The layer formed on these minerals was composed of two distinct parts: an outer layer of elongated prismatic crystals of sodium calcium hydrosilicate and an inner layer composed of sodium hydroaluminosilicate crystals.

The reactivity of muscovite was of the same order as these minerals, but the absence of a thick product layer could be attributed to the sheet structure of the mineral with its perfect cleavage along the (001) plane.

2) Minerals which formed a thinner product layer on the surface. The layer in this case was of sodium calcium hydrosilicate crystals only. Anorthosite, the least reactive feldspar, was the only member of this group.

3) Minerals which did not form a product layer, other than calcium hydroxide crystals, on the mineral surface. This group

represented the least reactive minerals in the leaching solutions and included kyanite, wollastonite and pectolite minerals.

#### 5.2.1 Role of Calcium Hydroxide in the Leaching Process

The presence of certain amounts of lime is an essential condition for the treatment of aluminosilicate minerals by the hydrochemical alkaline method. It has a favourable action on both the degree of alumina extraction and on the rate of decomposition of the original mineral. The effect of lime on alumina extraction has already been discussed in sections 1.1.3 and 3.1.5 where it was shown that the high alumina extraction in the presence of lime can be attributed to the formation of sodium calcium hydrosilicate which leaves the liberated alumina from the mineral in solution. On the other hand, the effect of calcium hydroxide on the rate of the dissolution of aluminosilicates has been noticed by many investigators (27,43,60), but no satisfactory explanation for this effect has been given.

Any explanation for the role of calcium hydroxide in the process must account for its favourable effect on the dissolution rate and for the following observations:

a) Calcium hydroxide did not seem to attack the mineral simultaneously with sodium hydroxide solution to dissolve the mineral. Its presence had no significant effect on the rate of mineral dissolution in the early stages of the leaching process.

b) Aluminosilicate minerals could be attacked and dissolved in the absence of lime, but a sodium hydroaluminosilicate crystallized

out instead of sodium calcium hydrosilicate. Similar results are reported in the literature<sup>(72,73,129,130)</sup> for the dissolution of nepheline-synite and other native aluminosilicates by sodium hydroxide solutions only.

c) The formation of the small crystals of sodium hydroaluminosilicate on the surface of some aluminosilicate minerals greatly reduced the rate of their dissolution by the sodium hydroxide solution.

Butt and Rashkovich<sup>(131)</sup> found that calcium hydrosilicates were formed in aqueous solutions heated at 170-200°C as a result of dissolution of both lime and silica and their subsequent interaction in the liquid phase. The interaction of lime and silica in the hydrochemical alkaline process could be considered, which is most likely the case, to take place by the same mechanism, i.e. the dissolved silica from the mineral dissolution step reacts with calcium hydroxide in solution to produce sodium calcium hydrosilicate. According to this mechanism calcium hydroxide would have no direct effect on the rate of the dissolution of the aluminosilicate minerals which is in agreement with what was pointed out in (a) and (b) above. Its presence would, however, prevent the formation of the coating layer of sodium hydroaluminosilicate crystals and instead forms the relatively large crystals of sodium calcium hydrosilicate. These crystals, if deposit on the mineral surface, would form a loose porous layer which allows free movements of the different soluble species and, therefore, have no harmful effect on the rate of the mineral dissolution. In other works, calcium hydroxide would favour a rapid



and more complete dissolution of the mineral not by attacking the mineral together with sodium hydroxide solutions, but by an indirect effect, i.e. by preventing the formation of a coating film on the mineral surface.

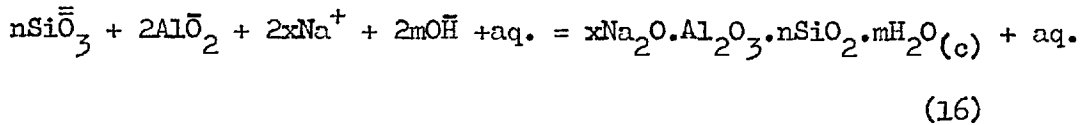
### 5.2.2 Mechanism of Solid Formation during the Leaching Process

From the different experimental results obtained and using the available data on the  $\text{Na}_2\text{O}-\text{CaO}-\text{Al}_2\text{O}_3-\text{SiO}_2-\text{H}_2\text{O}$  system, the process of aluminosilicate leaching by the hydrochemical alkaline method in its different stages could be as follows:

When aluminosilicate minerals are treated in concentrated sodium hydroxide solutions at high temperatures, the solution dissolves the mineral, forming mainly sodium aluminate and sodium silicate in solution. This step could be represented by the equations 1-7 in section 1.2 for the different types of aluminosilicate minerals. The rate of mineral dissolution would be a function of such factors as; sodium hydroxide concentration, temperature, surface area and the reactivity of the mineral itself.

When the solution concentration reaches saturation with respect to silica, a desilication step, i.e. the formation of insoluble silicate phases, would take place. This desilication step may follow one of two paths, depending on the availability of calcium hydroxide in the reaction zone:

a) In the absence of calcium hydroxide, desilication takes place by the interaction between sodium aluminate and sodium silicate forming a hydrated sodium aluminosilicate compound. This step may be represented by the equation:



The composition of the compound produced would largely depend on the sodium hydroxide concentration and temperature. If desilication takes place via this path, very little or no alumina would be transferred from the mineral into solution.

b) In the presence of calcium hydroxide, the sodium silicate formed by the mineral dissolution step will react with calcium hydroxide in solution producing the sparingly soluble compound sodium calcium hydrosilicate according to equation (10) in section 1.2. The alumina which enters the solution by the mineral dissolution step would, in this case, be retained in solution as long as its solubility limit is not exceeded.

It should be noted that the concentration of silica in equilibrium with sodium calcium hydrosilicate is much lower than the equilibrium concentration in contact with hydrated sodium aluminosilicates. The silica concentrations in solutions containing 500 g/l NaOH at 280°C are about 3-4 g/l SiO<sub>2</sub> and 15-20 g/l SiO<sub>2</sub><sup>(132-136)</sup> in contact with these two phases respectively. Therefore, in the presence of calcium hydroxide desilication would take place through path (b) and no hydrated sodium hydrosilicate would be formed.

If there is a deficit of lime, i.e. the molar ratio of lime to silica is less than unity, sodium calcium hydrosilicate will be formed according to path (b) and the excess of silica will interact with sodium aluminate according to equation (16).

It has already been shown (section 4.1.3.2) that if the calculated final caustic ratio,  $\alpha_f$ , is 12 or above, the dissolved alumina from the mineral would be retained in solution. Below a caustic ratio of 12, some of the alumina will go into the solid phase even though sufficient lime is present in the reaction zone. The sodium aluminate in this case would attack the already formed sodium calcium hydrosilicate producing sodium calcium hydroaluminosilicate according to equation (11) section 1.2.

Sodium calcium hydrosilicate may be formed in the leaching process directly after the mineral dissolution step or indirectly after the formation of an "intermediate" solid product. The path followed for its formation is determined by the relative rates of the mineral dissolution step and the step of diffusion of the dissolved species in the system. If, under certain reaction conditions, the rate of the mineral dissolution step is slower or comparable with the rate of silica removal by lime according to equation (10), sodium calcium hydrosilicate will form directly and alumina enters the solution by the mineral dissolution step. In other words, when the mineral dissolution is the rate determining step of the leaching process, the crystallization of the final solid will follow a "direct" mechanism with the following main chemical step reactions:

- i) Dissolution of the original mineral followed by
- ii) Crystallization of sodium calcium hydrosilicate. No "intermediate" solid products will be formed in this case. This direct mechanism for sodium calcium hydrosilicate formation was

followed when treating the different aluminosilicate minerals at low temperatures and for the less reactive mineral, kyanite at all temperature used.

If, on the other hand, the rate of the mineral dissolution is faster than the rate of diffusion or transportation of the various species, and in particular silica and calcium hydroxide, concentration gradients will develop in certain regions in the system. The silica concentration in the vicinity of the mineral surface, where dissolution is taking place, would be higher than in the bulk solution. The calcium hydroxide concentration gradient will be opposite to that of silica: a relatively high concentration in the bulk solution and very low in the vicinity of the mineral surface. As the mineral dissolution step continues, the silica concentration builds up in the vicinity of the mineral surface till it reaches a certain level when a desilication step takes place. Due to the absence of lime in this zone, this step proceeds according to equation (16) and forms hydrated sodium aluminosilicate crystals which coat the mineral surface. When calcium hydroxide diffused and reaches this zone, it will react according to equation (10) with the silica in equilibrium with hydrated sodium aluminosilicate phase. This reaction disturbs the equilibrium conditions and leads to the dissolution of some of the latter phase. This process of dissolution will be repeated by the arrival of more calcium hydroxide to the reaction zone. Thus the process of leaching aluminosilicate minerals will follow under these conditions an "indirect mechanism" to produce

sodium calcium hydrosilicate. This mechanism has the following main steps:

- i) Dissolution of the original mineral.
- ii) Crystallization of an "intermediate" phase of hydrated sodium aluminosilicate.
- iii) Dissolution of the newly crystallized phase.
- iv) Crystallization of sodium calcium hydrosilicate.

The more reactive minerals in the leaching solution, e.g. as microcline and albite, at high temperatures and when a relatively thick product layer of sodium calcium hydrosilicate was formed on their surfaces followed this indirect mechanism and formed an "intermediate" layer of sodium hydroaluminosilicate crystals between the mineral surface and sodium calcium hydrosilicate crystals.

S U M M A R Y

The reactivities of a number of aluminosilicate minerals of different types and compositions and of quartz in the system  $\text{Na}_2\text{O}-\text{CaO}-\text{H}_2\text{O}$  have been investigated under the conditions of the hydrochemical alkaline process for the purpose of recovering alumina from these aluminosilicate minerals. The influence of some important factors on the alumina recovery has been examined and the optimum leaching conditions have been determined. The role of calcium hydroxide and the mechanism of the formation of solids in the leaching process have been investigated. The summary of conclusion drawn from the investigation is as follows:

#### Optimum Leaching Conditions

The optimum leaching conditions under which most of the aluminosilicate minerals are completely decomposed and their alumina is extracted into solution with the formation of sodium calcium hydrosilicate as the solid product in the system are as follows:

1. The concentration of sodium hydroxide in solution should be about 500 g/l NaOH.
2. The leaching temperature should be about  $280^\circ\text{C}$  and the leaching time about 20 min.
3. The mineral sample should be ground to -100 mesh.
4. The calculated final caustic ratio of  $\text{Na}_2\text{O}/\text{Al}_2\text{O}_3$  should be 12 or over.
5. The molar ratio of  $\text{CaO}/\text{SiO}_2$  in the pulp should be 1.1 or more.

#### The Reactivity of Minerals

1. No significant differences in the reactivities of most of the aluminosilicate minerals in the leaching system are noticed when

treated under the optimum conditions. Kyanite does not, however, decompose completely under these conditions and gives only 57% alumina recovery. The differences in reactivities of the different minerals become more pronounced at lower temperatures.

2. Clay minerals are very reactive in sodium hydroxide solutions and can be decomposed completely at temperatures as low as 160°C.

3. Kyanite mineral is very refractory in sodium hydroxide solutions and cannot be decomposed completely in 646 g/l NaOH solution at 300°C and at a leaching time of two hours.

4. Feldspars of different compositions, muscovite mica and quartz are quite reactive in sodium hydroxide solutions. Their reactivities are intermediate between those of clays and kyanite minerals.

5. The reactivities of alkali feldspars in the leaching system are generally higher than those of plagioclases.

6. Potassium feldspar and sodium feldspar are of comparable reactivities but the former is slightly more readily dissolved in the leaching solutions.

7. Sodium feldspar is more reactive than calcium feldspar, which is the most refractory of all plagioclase feldspars in sodium hydroxide solutions.

8. Some minerals form a product layer on the mineral surface when it becomes very rough and porous during the leaching process. The formation and composition of this layer depends on the reactivity of the mineral in the system.

a) The refractory minerals, e.g. kyanite, do not form a product



layer on the mineral surface under the optimum leaching conditions.

- b) The moderately reactive calcium feldspar forms a thin layer of sodium calcium hydrosilicate crystals on the surface.
- c) The reactive aluminosilicate minerals form a thick product layer which consists of sodium calcium hydrosilicate crystals as an outer part and sodium hydroaluminosilicate crystals as an inner part.

#### Role of Calcium Oxide During Leaching

1. Calcium oxide does not seem to attack the aluminosilicate mineral simultaneously with sodium hydroxide in the mineral dissolution step.
2. It combines with the dissolved silica from the mineral and produces sodium calcium hydrosilicate under the leaching conditions.
3. Calcium oxide favours a rapid and complete dissolution of the mineral and a high degree alumina recovery in the process. This is attributed to the fact that its presence in the system prevents the formation of aluminium-containing solids such as sodium hydroaluminosilicate which coat the mineral surface and inhibit further dissolution.

#### Mechanism of Solid Formation in the Leaching Process

The proposed mechanism for the formation of solids in the leaching process is as follows:

1. The dissolution of the aluminosilicate mineral by the sodium hydroxide solutions and the formation of silicates and aluminates in solutions is the first step in the process followed by desilication of solution.
2. In the absence of lime, desilication takes place in the system by the combination of the silicates and aluminates in solution and

the crystallization of sodium hydroaluminosilicates.

3. In the presence of lime, sodium calcium hydrosilicate crystallizes out by the combination of dissolved silica with calcium oxide in solution.

4. Depending on the relative rates of the mineral dissolution step and the diffusion step (mainly for silicate and calcium hydroxide), the formation of sodium calcium hydrosilicate takes place by a direct or indirect path:

a) If the rate of mineral dissolution is slower than the rate of diffusion or transportation of calcium oxide and soluble silicates, sodium calcium hydrosilicate crystallizes out directly as the next step after the mineral dissolution step.

b) If the rate of the mineral dissolution step is faster than the rate of diffusion or transportation of calcium oxide and soluble silicates, sodium calcium hydrosilicate will be formed by an indirect path with the following main steps:

i) dissolution of the mineral by sodium hydroxide, ii) formation of an intermediate solid compound such as sodium hydroaluminosilicates, iii) dissolution of the intermediate product, and iv) crystallization of sodium calcium hydrosilicate.

5. Above the solubility limit of alumina in the leaching system, the aluminate solution attacks sodium calcium hydrosilicate with the formation of sodium calcium hydroaluminosilicate.

ACKNOWLEDGMENTS

I should like to express my sincere gratitude to Dr. O. Mellgren and Dr. A.P. Prosser for their valuable guidance and suggestions throughout the course of this work.

I would also like to thank Mrs. M. Culpan of the Metallurgy Department for taking the scanning electron microscope pictures, Mr. J. Mills of the Analytical Services Laboratory for the X-ray diffraction patterns, and the members of the academic and technical staff of the Department of Mining and Mineral Technology for their frequent assistance and useful discussions.

The financial support during the period of this work was given by Warren Spring Laboratory, Ministry of Technology; to them I am especially grateful.

REFERENCES

1. Edwards, J.D., Frary, F.C. and Jeffries, Z. 'The aluminium industry' Vol. I, "Aluminium at its production" New York and London, (1930).
2. Dennis, W.H., "Metallurgy of the non-ferrous metals" Pitman, London, (1954). pp. 273-302.
3. Pearson, T.G. "The chemical background of the aluminium industry" Monograph No.3, Royal Institute of Chemistry, London, (1960).
4. Richards, J.W., "Aluminium", Philadelphia and London, (1887).
5. Gmelin, L., "Handbuch der Anorganischen Chemie", Aluminium, B, No. 35, Berlin, (1934), pp.12-78.
6. Tilley, G.S., Millar, R.W. and Ralston, O.C., U.S. Bur. Mines, Bull. No. 247, (1926).
7. Fulda, W. and Ginsberg, H., "Tonerde und Aluminium", vol. i, Berlin, (1951).
8. Show, M.L. and Conley, J.E., U.S. Bureau of Mines. Rept. of Inv. No. 4649, (1950).
9. Calhoun, W.A., and Powell, Jr. H.E., U.S. Bureau of Mines Rept. of Inv. No. 5042, (1954).
10. Holbrook, W.F., and Yerkes, L.A., U.S. Bureau of Mines Rept. of Inv. No. 6280, (1963).
11. Cservenyak, F.J., U.S. Bu Mines Rept. of Inv. No. 4069, (1947).
12. Brown, R.A., Cservenyak, F.J., Anderberg, R.C., Kandiner, H.J. and Frattali, F.J., U.S. Bu Mines Rept. Inv. No. 4132, (1947).
13. Conley, J.E., and Skow, M.L., U.S. Bu Mines Rept. of Inv. No. 4462, (1949).

14. Conley, J.E., Brown, R.A., Cservenyak, F.J. Anderberg, R.C., Kandiner, H.J., and Green, S.J., U.S. Bu Mines Bull. No. 465, (1947).
15. St. Clair, H.W., Elkins, D.A., Shibler, B.K., Mahan, W.M., Merritt, R.C., Howcroft, M.R. and Hayashi, M., U.S. Bu Mines Bull. No. 577, (1959).
16. Cservenyak, F.J., Ruppet, J., and Garen, D.E., U.S. Bu Mines Rept. of Inv. No. 4299, (1948).
17. Ampian, S.G., U.S. Bu Mines Rept. of Inv. No. 6933, (1967).
18. Shvartsman, B. Kh., and Volkova, N.S., Tsvetnye Metally (1960), 1, No. 4, 60-3.
19. Rumyantseva, V.P., and Bessonova, A.S., Syr'evye Resursy Legkikh Metal., Vost. Sibiri, Akad. Nauk S.S.R., Sibirsk, Otd., Vost. Sibirsk, Filial, 5, (1965), 78-80; C.A., 64 (1966), 7734b.
20. Copson, R.L., Walthall, J.H., and Hignett, T.P., Trans. AIME, (1944), 159, 241-54.
21. Zbigniew Szczygiel, Zeszyty Nauk. Akad. Gorniczo-Hutniczej No. 10, Met. Odlewnictwo No.2, 133-42, (1957); C.A. (1958), 52, 4940d.
22. Mazel, V.A., and Eliseeva, A.A., Trudy Vses. Nauch-Issledovatel. Alyumin-Magn. Inst., (1957), 39, 214-26; C.A. (1960), 54, 12512b.
23. Pedersen, H., U.S. Pat. 1,618,105, Feb. 15, 1927; British Pat. 232,930, 1926.
24. Stroup, P.T., Trans. AIME, (1964), 230, No. 3, 356-71.

25. Blake, H.E., Fursman, O.C., Fugate, A.D., and Banning, L.H., U.S. Bu Mines Rept. of Inv. No. 6939, (1967).
26. Ponomarev, V.D., and Sazhin, V.S., Tsvetrye Metally, (1957) 30, No 12, 45-51.
27. Ponomarev, V.D., and Sazhin, V.S., J. Appl. Chem. USSR, (1958), 31, No. 8, 1134-9.
28. Ponomarev, V.D., Sazhin, V.S., and Ni, L.P., "The Hydrochemical Alkaline Method of Processing Aluminosilicates", (in Russian), Izd. Metallurgiya, Moscow, (1964).
29. Smirnov, M.N., and Vydrevich, E.Z., Tsvetnye Metally, (1959), 32, No. 8, 39-44.
30. Goldman, M.M., and Ni, L.P., Izvs. Akad. Nauk Kazakh. S.S.R., Ser. Met., Obogashch. i Ogneuporov, (1960), No. 1, 47-55.
31. Manvelyan, M.G., Sayadyan, A.S., Abramyan, A.A., Mikaelyan, D.A., and Kapyatyan, E.E., Tsvetnye Metally, (1961), 34, No. 4, 56-61.
32. Manvelyan, M.G., Sayadyan, A.G., Abramyan, A.A., Mikaelyan, D.A., Mosinyan, F.G., and Kapantsyan, E.E., Tsvetnye Metally, (1962), 35, No. 4, 46-9.
33. Ponomarev, V.D., Ni, L.P., Vydrevich, V.S., Montvid, A.E., Krym, A.I., Purits, M.F., and Agranovskii, A.A., U.S.S.R., 116, 775, Jan. 19, 1959; C.A. (1959), 53, 16905a.
34. Ponomarev, V.D., Trudy Inst. Geol. Nauk Akad. Kazakh. SSR, (1959) No. 2, 1960-70.
35. Ni, L.P., Ponomarev, V.D. Nurmagambetov, Kh. N., and Sazhin, V.S., U.S.S.R., 132, 20b, Oct. 5, 1960; C.A. (1961), 55, 1276f.

36. Ni, L.P., and Ponomarev, V.D., Izv. Akad. Nauk Kazakh., SSR, Ser. Met., Obogashch i Ogneuporov, (1959), No. 1, 16-20.
37. Rakhimov, A.R., Ponomarev, V.D., and Ni, L.P., Izv. Vys. Uch. Zav., Tsvetnye Metally, (1963), 6, No. 3, 111-15.
38. Ponomarev, V.D., Mal'tsev, V.S., Akhmetov, S.F., and Rakhimov, A.R., Vestn. Akad. Nauk Kazakh SSR, (1964), 20, No. 4, 47-53.
39. Ponomarev, V.D., and Sazhin, V.S., U.S.S.R., 108, 917, Nov. 25, 1957; C.A., (1958), 52, 10524b.
40. Ponomarev, V.D., and Sazhin, V.S., Izv. Vys. Uch. Zav. Tsvetnye Metally, (1958), No.2, 93-100.
41. Ponomarev, V.D. Nurmagambetov, Kh. N., Sazhin, V.S., Fateeva, Z.T., Putilin, Yu. M., and Taranenko, B.I., Sbornik Nauch. Trudov Kazakh. Gornomet Inst., (1959), No. 20, 348-64; C.A. (1961), 55, 19646i.
42. Ponomarev, V.D., Monich, V.K., Nurlybaev, A.N., Ni, L.P., Solenko, T.V., and Panchenko, A.G., Vestn. Akad. Nauk Kaz. SSR, (1961), 18, No.4, 23-31.
43. Ponomarev, V.D., Nurmagambetov, Kh.N., and Putilin, Yu. N., Tr. Inst. Met. i Obogashch., Akad. Nauk Kaz. SSR, (1962), 4, 62-73.
44. Ponomarev, V.D., Shcherban, S.A., Akhmetov, S.F., and Nurmagambetov, Kh.N., Tr. Inst. Met. i Obogashch., Akad. Nauk Kaz. SSR, (1964), 11, 31-7.



45. Ponomarev, V.D., Nurmagambetov, Kh.N., and Sazhin, V.S., Tret'ego Vses. Sov. po Khim. i Tekhnol. Glinozema, Erevan, (1964), 45-53; C.A. (1965), 63, 2654g.
46. Ni, L.P., Izv. Akad. Nauk Kazakh. SSR, Ser. Met. Obobshch i Ogneuporov, (1960), No.1, 21-6.
47. Ni, L.P., Materialy Vses. Soves. po Khim. i Tekhnol. Glinozema, Akad Nauk SSR, Sibir. Otdel., Novosibirsk, (1958), 149-52; C.A. 55, (1961), 20349e.
48. Rakhimov, A.R., Akhmetov, S.F., and Ponomarev, V.D., IVUZ, Tsvetnye Metally, (1965), 8, No.5, 71-6.
49. Isakov, U.I., Rakhimov, A.R., Nurmagambetov, Kh. N., Ponomarev, V.D., and Sadykov, Zh. S., Tsvetnye Metally, (1966), 7, No. 12, 61-3.
50. Ponomarev, V.D., Ni, L.P. and Sazhin, V.S., Tsvetnye Metally, (1960), 1, No.5, 44-8.
51. McCulloch, H.W., and Carter, A.L., South Africa, Government Metallurgical Lab., Project No. C20/62, Report No.11, Dec., 1963.
52. Hansen, K.R., Regester, W.V., and McCulloch, H.W., South Africa, Government Metallurgical Lab., Project No. C20/62, Report No. 18, Dec., 1965.
53. Hansen, K.R., von Rahden, H.V., Regester, W.V., and McCulloch, H.W., South Africa, Government Metallurgical Lab., Project No. C20/62, Report No. 19, Dec., 1966.
54. Hansen, K.R., Carter, A.L., Mihalik, P., and McCulloch, South Africa, Government Metallurgical Lab., Project No. 5/64, July, 1964.

55. Vydrevich, E.Z., and Gal'perin, E.L., J. Appl. Chem. U.S.S.R. (1961), 34, 9, 1875-81
56. Vydrevich, E.Z., J. Appl. Chem. U.S.S.R., (1962), 35, 2, 268-71.
57. Ibid, (1962), 35, 12, 2512-8.
58. Ibid, (1963), 36, 1, 50-6.
59. Sazhin, V.S., Shor, O.I., Golnik, V.F., Volkovskaya, A.I., Panchenko, R.G., and Polyakova, K.A., J. Appl. Chem. U.S.S.R. (1968), 41, No.8, 1581-6.
60. Sazhin, V.S., and Denisevich, V.E., J. Appl. Chem. U.S.S.R., (1966), 39, No.12, 2461-4.
61. Ni, L.P., Bunchuk, L.V., and Ponomarev, V.D., IVUZ, Tsvetnye Metally, (1963), 6, No.5, 64-8 .
62. Akhmetov, S.F., Akhmetova, G.L., and Ponomarev, V.D., J. Appl. Chem. U.S.S.R., (1967), 40, No.8, 1640-5.
63. Ponomarev, V.D., Tretego Vses. Soveshch po Khim. i Tekhnol. Glinozema, Erevan, (1964), 3-9, C.A. 63, (1965), 17533b.
64. Ni, L.P., Ponomarev, V.D., and Osipova, E.F., Tretego Vses Soveshch po Khim. i Tekhnol. Glinozema, Erevan, (1964), 145-55; C.A. 63, (1965), 2654f.
65. Ni, L.P., Bunchuk, L.V., Khalyapin, O.B., and Ponomarev, V.D., J. Appl. Chem. U.S.S.R., (1965), 38, No.2, 289-95.
66. Bernshtein, V.A., and Matsenok, E.A., Tsvetnye Metally, (1958) 12, 61-66.

67. Matyasi, J. and Nemeth, K., Kohaszati Lapok, (1959), 92, 313-16; C.A. (1959), 53, 20716c.
68. Kuznetsov, S.I., and Derevyankin, V.A., "Physical Chemistry of the Bayer Process for Alumina Production", (in Russian), Metallurgizdat, Moscow, (1964).
69. Ni, L.P., and Bunchuk, L.V., Tr. Inst. Met. i Obogashch., Akad. Nauk Kazakh. SSR, (1964), 9, 56-62.
70. Daulbaev, E.U., and Ni, L.P., Khim. i Tekhnol. Glinozema, Inst. Met. i Obogashch., Akad. Nauk Kazakh. SSR, Tr. Vses. Soveshch., Alma. Ata, (1959), 3-5; C.A. 57, (1962), 5580g.
71. Sazhin, V.S., and Shor, O.I., J. Appl. Chem. SSR, (1967), 40, No. 4, 717-20.
72. Manvelyan, M.G., Nadzharyan, A.K., Akopyan, Z.A., Babayan, S.A., and Arevshatyan, M.S., Izvest. Akad. Nauk Armyan SSR, Khim. Nauki, (1961), 14, 231-6; C.A. (1962), 56, 6946b.
73. Manvelyan, M.G., Nadzharyan, A.K., Babayan, S.A., and Arevshatyan, M.S., Tret'go Vses. Soveshch. po Khim i Tekhnol. Glinozema, Erevan, (1964), 163-75; C.A. (1965), 63, 7939h.
74. Ponomarev, V.D., and Sazhin, V.S., Izvest. Akad. Nauk SSR, Ser. Met., Obogashch. i Ogneuporov, (1960), No.1, 27-34.
75. Gol'dman, M.M. and Ponomarev, V.D., Izvest. Akad. Nauk Kazakh. SSR, Ser. Met., Obogashch. i Ogneuporov, (1961), No. 3, 50-8.
76. Gol'dman, M.M., Ponomarev, V.D., Galuzo, V.N., Polyakova, T.P., and Kairbaeva, Z.K., Tr. Inst. Met. i Obog. Akad. Nauk Kaz. SSR, (1963), 8, 72-6.

77. Ni, L.P., Zakharova, M.V., and Ponomarev, V.D., Tr. Inst. Met. i Obogashch. Akad. Nauk Kaz. SSR, (1964), 9, 76-84.
78. Sazhin, V.S., Bukhovets, K.G., Denisevich, V.E., and Obolonchick, N.V., Ukr. Khim. Zh., (1965), 31, No.9, 973-8.
79. Perekhrest, G.L., Khalyapina, O.B., Akhmetov, S.F., Ni, L.P., and Ponomarev, V.D., Izv. Akad. Nauk Kaz. SSR, Ser. Khim. Nauk., (1965), 15, No. 3, 55-61.
80. Perekhrest, G.L., Ni, L.P., and Ponomarev, V.D., Tr. Inst. Met. Obogashch., Akad. Nauk Kaz. SSR, (1966), 16, 18-23.
81. Arlyuk, B.I., J. Appl. Chem., USSR, (1967), 40, 729-33.
82. Criss, C.M., and Cobble, J.W., J. Am. Chem. Soc., (1964), 86, 5385-90.
83. "Selected Values of Chemical Thermodynamic Properties", National Bureau of Standards' Circular 500, U.S. Dept. of Comm., Washington, (1952).
84. Couture, A.M., and Laidler, K.J., Can. J. Chem., (1957), 35, 202.
85. Lewis, G.N., and Randall, M., "Thermodynamics", revised by Pitzer, K.S., and Brewer, L., 2nd ed., McGraw-Hill, New York, (1961).
86. Washburn, E.W., "International Critical Tables of Numerical Data for Physics, Chemistry and Technology", Vol. 5, 113, McGraw-Hill, London, (1929).
87. Kelley, K.K., U.S. Bu Mines Bull. No. 584, (1960).

88. Kelley, K.K., Todd, S.S., Orr, R.L., King, E.G., and Bonnicksen, K.R., U.S. Bu Mines Rept. of Inv. No. 4955, (1953).
89. Kelley, K.K., U.S. Bu Mines Rept. of Inv. No. 5901, (1962).
90. Barany, R., U.S. Bu Mines Rept. of Inv. No. 5900, (1962).
91. Wagman, D.D., Evans, W.H., Halow, I., Baily, S.M., and Schumm, R.H., "Selected Values of Chemical Thermodynamic Properties. Tables for the First Thirty Four Elements in the Standard Order of Arrangement". N.B.S. Tech. Note No. 270-3, 246 pp. (1968).
92. Pankraz, L.B., and Kelley, K.K., U.S. Bu Mines Rept. of Inv. No. 6370, (1964).
93. Wicks, C.E., and Block, F.E., U.S. Bu Mines Bull. No. 605, (1963).
94. King, E.G., and Weller, W.W., U.S. Bu Mines Rept. of Inv. No. 5810, (1961).
95. Kelley, K.K., and King, E.G., U.S. Bu Mines Bull. No. 692, (1961).
96. Barany, R., and Kelley, K.K., U.S. Bu Mines Rept. of Inv. No. 5825, (1961).
97. Weller, W.W., and King, E.G., U.S. Bu Mines Rept. of Inv. No. 6281, (1963).
98. Barany, R., U.S. Bu Mines Rept. of Inv. No. 6356, (1964).
99. Pankratz, L.B. U.S. Bu Mines Rept. of Inv. No. 6371, (1964).
100. Ibid, Rept. of Inv. No. 7201, (1968).
101. Cotrell, T.L. "Strength of Chemical Bonds", 2nd ed. Butterworths Scientific Publications, London, (1958).

102. Thilo, E., Funk, H., and Wichmann, E.M., Abh. Deutsche Akad. Wiss., (1950), 4, 5-55.
103. Arlyuk, B.I., J. Appl. Chem., USSR, (1966), 39, 1196.
104. Latimer, W.M., "The Oxidation States of the Elements and Their Potentials in Aqueous Solutions", 2nd ed., Prentice-Hall, Inc., New York, (1952), pp. 359-69.
105. Babushkin, V.I., Matveen, M.G., and Mchedlor-Petrosyan, O.P., "Thermodynamics of Silicates" (in Russian), Gosstroizdat, Moscow, (1962).
106. Wise, S.S., Margrave, J.L., Fedder, H.M., and Hubbard, W.N., J. Phys. Chem., (1963), 67, No. 4, 815-21.
107. Kubaschewski, O., Evans, E. Ll., and Alcock, C.B., "Metallurgical Thermochemistry", 4th ed., Pergamon Press, London, (1967), pp. 303-62.
108. Criss, G.M., and Cobble, J.W., J. Am. Chem. Soc., (1964), 86, 5390-3.
109. Robins, R.G., "The Application of Potential-pH Diagrams to the Prediction of Reactions in Pressure Hydrothermal Processes", Warren Spring Laboratory Report No. LR80 (MST), June, 1968.
110. Ibid, J. Inorg. Nucl. Chem., (1967), 29, 431.
111. Cobble, J.W. J. Am. Chem. Soc., (1964), 86, 5394-401.
112. Johnston, J., and Grove, C., J. Am. Chem. Soc., (1931), 53, 3976.
113. Peppler, R.B., and Wells, L.S., J. Res. Natl Bur. Std., (1954), 52, 75-92.
114. Bassett, H., J. Chem. Soc., (1934), 1270.

115. Bates, R.G., Bower, V.E., and Smith, E.R., J. Res. Natl. Std., (1956), 56, 305-12.
116. Barrer, R.M., and Villiger, H., Zeits. Krist., (1969), 128, 352-70.
117. Burkin, A.R., "The Chemistry of Hydrometallurgical Processes", Spon Ltd., London, (1966), pp. 9-21.
118. Seidell, A., and Linke, W.F., "Solubilities of Inorganic and Organic Compounds" Supplement to 3rd ed., Van Nostrand, New York, 1952, pp. 129-30.
119. Farrow, R.N.P., and Hill, A.G., Talanta (1961), 8, 116-128.
120. "Tables for Conversion of X-ray Diffraction Angles to Interplanar Spacing" National Bureau of Standards, Applied Mathematics Series No. 10, U.S. Dept. of Comm., (1950).
121. A.S.T.M. "Inorganic Index to the Powder Diffraction File", (1967), and also X-ray Powder Data File (Cards) (1960).
122. Deer, W.A., Howie, R.A., and Zussman, J., "Rock-Forming Minerals" Vol. 4, pp. 95-165, Longmans, London, (1963).
123. Barrer, R.M., and White, E.A.D., J. Chem. Soc. (1952), 1561.
124. Sazhin, V.S., Shor, O.I., Arakelyan, O.I., Volkovskaya, A.I., and Shebeko, L.G., Ukr. Khim. Zh., (1966), 32, No. 4, 393-400.
125. Sazhin, V.S., Shor, O.I., Arakelyan, O.I., Volkovskaya, A.I., and Kolesnikova, I.A., Ukr. Khim. Zh., (1963), 29, No. 11, 1123-8.
126. Sazhin, V.S., Shor, O.I., Arakelyan, O.I., and Volkovskaya, A.I., J. Appl. Chem. USSR, (1965), 38, No. 8, 1631-6.

127. Sazhin, V.S., Denisevich, V.E., Volkovskaya, A.I., and Obolonchik, N.V., J. Appl. Chem. USSR, (1967), 40, 4, 713-6.
128. Deer, W.A., Howie, R.A., and Zussman, J., "Rock-Forming Minerals" Vol. 1, pp.137-44, Longmans, London (1962).
129. Manvelyan, M.G., and Nadzharyan, A.K., Izv. Akad. Nauk Arm. SSR, Khim. Nauki, (1963), 16, No.6, 589-99.
130. Sazhin, V.S., Denisevich, V.E., Volkovskaya, A.I., Ukr. Khim. Zh., (1965), 31, No.4, 379-84.
131. Butt, Yu. M. and Bashkovich, L.N., J. Appl. Chem. USSR, (1959) 36, No.6, 1220-5.
132. Ni, L.P., "Alkali Hydrochemical Methods in Processing High-Silica Bauxites", Alma-Ata, Moscow, 1967.
133. Ni, L.P., Romanov, L.G., and Ponomarev, V.D., IVUZ, Tsvetnye Metally, (1964), 7, No.1, 95-101.
134. Ni, L.P., Romanov, L.G., Osipova, E.F., and Ponomarev, V.D., Tr. Inst. Met. i Obogashch., Akad. Nauk Kaz. SSR, (1964), 2, 90-6.
135. Ni, L.P., Romanov, L.G., Osipova, E.F., Isv. Akad. Nauk SSSR, Metal., (1966), No.6, 40-6.
136. Sazhin, V.S., and Pankeeva, N.E., Ukr. Khim. Zh., (1968), 34, No.3, 297-302.